SAND81-8023
Unlimited Release

Structural Analysis of Second Generation Heliostats

V. D. Dunder

Prepared by Sandia National Laboratories, Albuquerque, New Mexico 87185 and Livermore, California 94550 for the United States Department of Energy under Contract DE-AC04-76DP00789.

Printed December 1981

Sandia National Laboratories
energy report

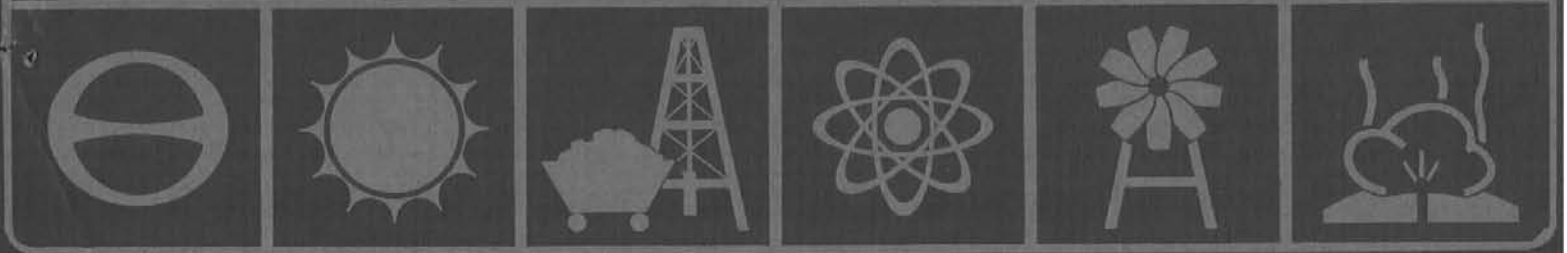

Issued by Sandia Laboratories, operated for the United States Department of Energy by Sandia Corporation.

NOTICE

Printed in the United States of America
Available from
National Technical Information Service
U. S. Department of Commerce
5285 Port Royal Road
Springfield, VA 22161
Price: Printed Copy $6.50 Microfiche $3.00

SAND81-8023
Unlimited Release
Printed December 1981

STRUCTURAL ANALYSIS OF SECOND GENERATION HELIOSTATS

V. D. Dunder
Applied Mechanics Division
Sandia National Laboratories, Livermore

ABSTRACT

As part of the overall evaluation of the four second-generation heliostats, a finite element analysis was performed to evaluate structure performance of the mirror modules subjected to gravity, operational wind loads and survival wind loads. All designs evaluated were found to be structurally adequate.

CONTENTS

ILLUSTRATIONS

TABLES

STRUCTURAL ANALYSIS OF SECOND GENERATION HELIOSTATS

1.0 Summary

A finite element model of each of the four completed 2nd generation heliostats was analyzed using the SAP4 computer code as part of the overall heliostat evaluation. The purpose of the anaysis was four fold:

1) Determine facet deflections due to operational wind velocities for the beam quality evaluation.
2) Determine individual facet deflections caused by gravity sag for the field performance evaluation to be done by the HELIOS computer code.
3) Calculate the natural frequencies and mode shapes to determine susceptibility to vortex shedding excitation.
4) Calculate stresses in the structural components due to loading by survival wind velocities and check for structural failure.

The analysis was performed with the aid of a Textronix Mesh Generator in creating the models, and the linear elastic SAP4 Finite Element program for the analysis.

The pedestal in each heliostat was modeled as a linear elastic beam fixed at ground level. Testing of the heliostats at the Central Receiver Test Facility (CRTF) verified that foundations did not substantially add to the structural deflections. Initially the drive mechanisms for all gravity and wind load (static) cases were modeled as rigid beams because the drive stiffnesses were not known. Once the drive stiffnesses were measured by testing at the CRTF their torsional and bending stiffnesses were incorporated into the model and the new frequencies determined. No structural deflections or stresses were determined with the measured drive stiffnesses.

2.0 Conclusions

The four primary analyses:

1) Operational Wind Pointing Error
2) Gravity Deflections of Individual Mirror Facets
3) Natural Frequencies and Mode Shapes
4) Stresses due to Survival Wind Velocities

performed on each heliostat found no inherent structural problem with any of the designs.

The operational wind pointing errors must be added to the drive mechanism errors before a comparison with the specification can be made. This information may be found in the Second Generation Heliostats - Evaluation Summary Report. The magnitude of the operational wind deflections is about the same or slightly less than the operational wind results of the 10-MWe pilot plant heliostats. The gravity induced mirror module deflections were used as input to the HELIOS optical performance code run at Sandia Albuquerque. The results of this analysis are presented in the Beam Quality and Tracking Evaluation of 2nd Generation Heliostats Report by D. King. These gravity deflections were also within the same order of magnitude as the 10-MWe pilot plant heliostat results. All heliostats produce RMS slope errors and pointing errors of the same order of magnitude.

The dynamic analyses found the heliostats' lowest natural frequencies to be greater than 1.75 Hz. This is well above the vortex shedding frequencies (0.3-0.7 Hz) in a 27 mph wind thus dynamic excitation is not a concern.

The largest stresses in the support structures were produced by the 90 mph, survival, wind loading while the heliostats are in stow position. The pedestals suffered the largest stresses in the case of a 50 mph wind heliostats in vertical position. All structural stresses were found to be below allowable values.

3.0 Introduction

3.1 Second Generation Heliostat Development Program

The Second Generation Heliostat Development Program is the second major heliostat development cycle in the Department of Energy's (DOE) Solar Thermal Central Receiver Program. During the first development cycle 222 heliostats were built for the Central Receiver Test Facility (CRTF); also, a design was developed and is presently being built for the central receiver pilot plant near Barstow, California.

The second heliostat development cycle started in 1978 with the DOE Prototype Heliostat Phase 1 contracts. These paper study contracts developed heliostat conceptual designs and mass-production cost estimates. Rather than continue these contracts into Phase 2, it was decided to initiate the Second Generation Heliostat contracts. Sandia National Laboratories placed these contracts in July 1979.

Technical management and evaluation of the Second Generation Heliostat contracts was performed by Sandia. Heliostat testing was performed at the CRTF in Albuquerque.

The objectives of the Second Generation Heliostat Program were to support the Solar Central Receiver research, development, and demonstration effort by:

- Establishing heliostat designs with associated manufacturing, assembly, installation, and maintenance approaches that, in quantity production, would yield low capital and operating costs over an assumed 30-year lifetime.
- Stimulating broader industry participation in the DOE solar energy program.
- Obtaining design data, manufacturing plans, and projected production costs for release to the solar community.
- Performing side-by-side testing and evaluation of prototype heliostats and evaluating production plans and cost estimates.

The Second Generation Heliostat development contracts are summarized below.

Second Generation Heliostat Contractors	Contract Dates Start	Complete	Contract Costs
ARCO Power Systems (Formerly Northrup Inc.)	July 79	February 81	$1.0M
Boeing Engineering and Construction	July 79	February 81	$1.7M
Martin Marietta Corp.	July 79	April 81	$1.4M
McDonnell Douglas Astronautics	July 79	February 81	$1.5M
Westinghouse	July 79	September 80	$1.7M

The program objectives have been met for all of the contractors except Westinghouse as they were not able to build prototype heliostats within the funding limits. Therefore, only limited information is available for the Westinghouse design.

Photographs of the ARCO, Boeing, Martin Marietta, and McDonnell Douglas heliostat designs are shown in Figure 3.1 and 3.2.

Each contractor except Westinghouse delivered two prototype heliostats and four spare mirror modules to Sandia for testing. Detailed design reports and final reports containing costs, manufacturing, installation, and maintenance data were also delivered. Westinghouse only delivered a detailed design report.

3.2 Second Generation Heliostat Evaluation

Sandia has evaluated the Second Generation Heliostat designs. The evaluation involved testing, design analysis, analysis of contractor production methods and cost estimates, and cost projections of bus bar energy costs for a power plant. Heliostat testing was performed at the CRTF to verify the ability to survive environmental requirements. Two prototype

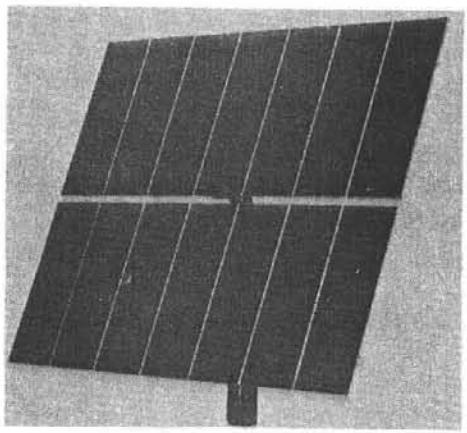

MC DONNELL DOULGAS

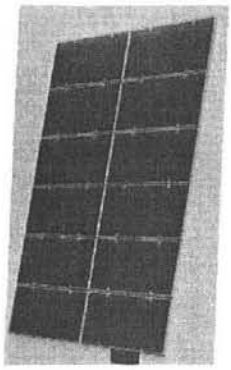

BOEING

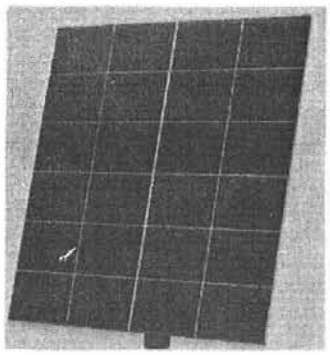

NORTHRUP

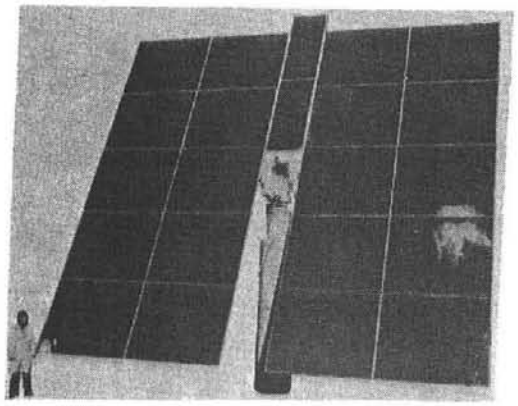

MARTIN MARIETTA

Figure 3.1. Second Generation Heliostats

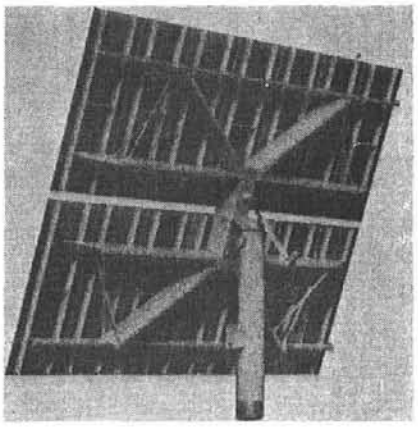

MC DONNELL DOUGLAS

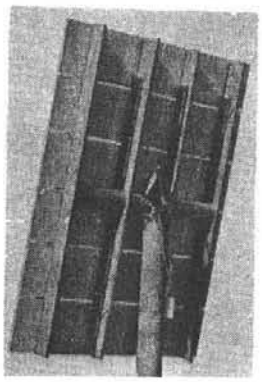

BOEING

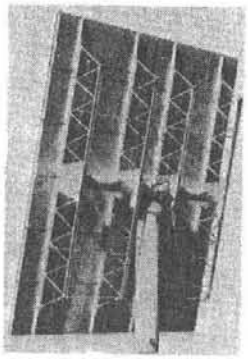

NORTHRUP

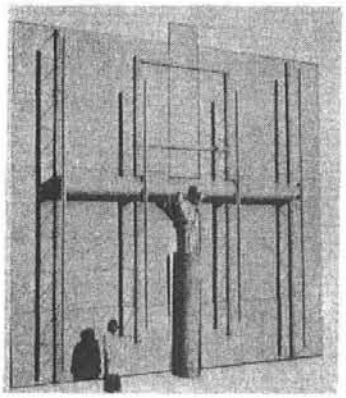

MARTIN MARIETTA

Figure 3.2. Second Generation Heliostats

heliostats from each contractor were tested. Similar performance and environmental testing of individual mirror modules was also performed in the laboratory at Sandia Livermore.

The objectives of the evaluation and test program were to:

- Compare design features
- Identify design strengths and weaknesses
- Estimate reliability and lifetimes of key components
- Determine performance capabilities
- Identify user concerns
- Estimate central receiver energy costs
- Identify further development requirements
- Disseminate information

Sandia was assisted in the evaluation by a Review Committee-advisors consisting of representatives from other solar programs and potential users as shown below.

User's Panel

- Public Service Company of New Mexico
- Arizona Public Service
- Southern California Edison
- Exxon
- U. S. Gypsum

Review Committee

- Department of Energy
- Electric Power Research Institute
- Solar Energy Research Institute
- Sandia's Solar Energy Projects Department
- Sandia's CRTF Division
- Sandia's Solar Programs Department
- Jet Propulsion Laboratory Solar Program

Information from the evaluation program is being disseminated in the form of published contractor and Sandia reports and a public seminar.

4.0 Purpose of Structural Modeling

The structural modeling of the Second-generation heliostats was done as part of the overall evaluation of these heliostats by SNLL at the culmination of the Second-generation heliostat contracts. The structural analysis provided information, not accessible by testing, on the structural performance and survivability of the heliostats, and identified potential problems with the structures. The analyses that met this need (shown below) are discussed in the following sections.

Required Values:	For Evaluation of:
Gravity deflections of the individual mirror facets	Field performance (by HELIOS)
Facet deflections due to operational wind	Compliance with performance specification
Natural frequencies and mode shapes	Potential excitation by vortex shedding
Stresses in structural components due to survival wind velocities	Survivability

5.0 Procedure and Tools

All heliostats were idealized as a mesh of finite element beam and plate elements from working drawings supplied by the heliostat contractors. The assumptions inherent in the idealization of each structure are described in Section 6.

Model components were created individually on the Textronix 4081 minicomputer using Textronix Finite Element Modeling (FEM) software.[3] The software allows nodes and elements to be created by copying and moving already existing nodes and elements, thus greatly simplifying the creation of symmetrical and repetative structures such as heliostats. It also allows rotation of the model on the viewing screen and displays "slices" through the model facilitating visual checking of the completed model or its parts. The majority of node and element properties may also be input at this stage.

The model components were created on separate data files for easier manipulation and verification. Once created and verified, the components were assembled into the complete models. These were input in a series of programs which created input card images for the SAP4 finite element analysis code. The card images were then transfered from the Textronix minicomputer to the CDC 6600 mainframe. After a final editing of the data files, the models were verified again using two interactive three-dimensional plotting routines (GRAPE[2] and DIS3D). The analyses were performed by the SAP4 finite element program on the CRAY computer. SAP4 is a finite element code for the static and dynamic analysis of linear elastic structures. It is based on the April 1974 version of the SAPIV code developed at U.C. Berkeley by J. Bathe, E. L. Wilson, and F. F. Peterson, but contains modifications made by S. Sackett at the Lawrence Livermore National Laboratory (May 1979).[1]

Each model was analyzed in seven different elevation angle orientations (15° increments from vertical to horizontal) with only gravity forces applied, three operational wind load conditions where gravity effects were not

included, and two load conditions of survival wind in addition to gravity forces. The five wind load cases (three operational, two survival) are listed in Table 5.1, with Table 5.2 showing the corresponding forces and moments. The moments in Cases 1, 2, and 5A were applied about a line parallel to the elevation axis and passed through the center of the reflective surface. For Cases 3 and 4, they were applied about a line parallel to the cross-elevation axis passing through the center of the reflective surface. For Case 5B the moment was again applied at the center of the reflective surface but about a line that is perpendicular to the elevation axis and is in the plane of the reflective area. The wind forces were applied as normal pressure on the plate elements representing the mirror module surface. The individual mirror module pressures for each case are shown in Appendix A.

TABLE 5.1

WIND LOAD CONDITIONS

	Wind Velocity	Heliostat Orientation	Wind Orientation To Heliostat
Operational:			
Case 1	27 mph	Vertical	Normal
Case 2	27 mph	70° from vertical	20° Angle of Attack to Elevation Axis
Case 3	27 mph	Vertical	20° Angle of Attack to Azimuth Axis
Survival:			
Case 4	50 mph	Vertical	20° Angle of Attack to Azimuth Axis
Case 5A	90 mph	Horizontal (stow)	10° Angle of Attack to Elevation Axis
Case 5B	90 mph	Horizontal (stow)	10° Angle of Attack to Cross Elevation Axis

Case 5B was run only on the McDonnell Douglas model because, due to the aspect ratio of the heliostat, larger forces are created on the heliostat when the wind is parallel to the elevation axis. The reverse is true for the other three heliostats. The heliostats were in stow position for Case 5 (A and B): mirror modules were facing downward for the Martin Marietta heliostat, but face-up for the other models. The choice of stow position was made by the contractor weighing the advantage of lessened mirror soiling when face-down versus the loss of reflective area, and thus produced energy, required for the cut-out to allow the pedestal to pass through the reflective surface.

TABLE 5.2

NET WIND LOADS

CASE	ARCO			BOEING			MARTIN MARIETTA			McDONNELL DOUGLAS		
	Force (lbs)	Moment (ft-lbs) Az.	Elev.	Force (lbs)	Moment (ft-lbs) Az.	Elev.	Force (lbs)	Moment (ft-lbs) Az.	Elev.	Force (lbs)	Moment (ft-lbs) Az.	Elev.
Operational:												
1	1044	0	0	767	0	0	1144	0	520	1116	0	0
2	808	0	3108	658	0	2426	849	0	3488	894	0	3095
3	754	2848	0	658	1983	0	815	3620	0	809	3546	0
Survival:												
4	2585	9767	0	2160	6800	0	2795	12414	0	2774	12160	0
5A	4072	0	24346	3476	0	19889	4116	0	26802	4506	0	24197
5B										4469	30541	0

The loads and moments on each heliostat are governed by the reflective area. The larger the mirror surface the more wind it catches. The moments are also affected by the aspect ratio of the heliostat. The 520 ft-lb moment in Case 1 of the Martin Marietta heliostat was created by the load on the extra center mirror.

The postprocessing of the SAP4 output, done on the CDC 6600, included ploting of deflected shapes and frequency mode shapes, and the computation of the individual, average, and RMS value of facet deflections.

The mirror module deflections, measured by a normal vector to the deformed surface, were calculated for each case of gravity loading and operational wind loading. The support points for the mirror modules were used to define the facet plane thus local mirror warping is not included. For the two heliostats with four point mirror module support, an average was taken of the four possible planes that may pass through the permutation of those four points, three at a time.

6.0 Heliostat Models and Assumptions

The four models differed in problem size and complexity. An indication of the difference is given in Table 6.1.

TABLE 6.1

SIZE OF MODELS

	ARCO	BOEING	MARTIN MARIETTA	MCDONNELL DOUGLAS
# of Nodes	1272	789	612	2154
# of Plate Elements	1092	576	300	1686
# of Beam Elements	1617	114	300	513
# of Degrees of Freedom	7312	4062	3203	10988

The models are shown in Figures 6.1 through 6.5

For all heliostats, the pedestals were modeled as beams fully fixed at the base. The assumption that the foundation does not significantly add to structural deflections, and can therefore be neglected in modeling, was verified by measurements at the Central Receiver Test Facility (CRTF) in Albuquerque, New Mexico. The drive mechanisms were modeled as rigid beams in all the static load cases analyzed. The frequency analyses were done twice: the first time the drive mechanisms were assumed rigid, as in the static cases, and the second time torsional and flexural springs were substituted. The spring values were determined by testing at the CRTF on the installed drives mechanisms.

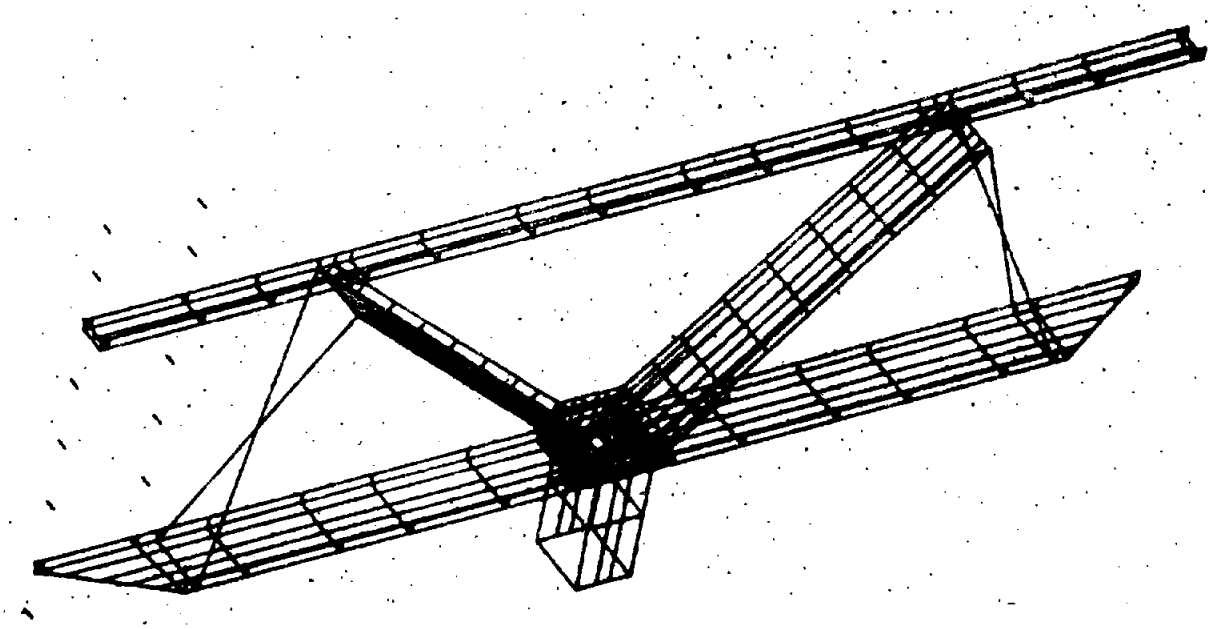

(Only top half of support structure is shown and mirror modules are omitted)

Figure 6.5. McDonnell Douglas Model

6.1 Arco Heliostat

The front and back facings of the mirror module box were modeled as thin plates, as were the webs of the C sections which reinforce the box. These components are the major contributors to the large number of plate elements in the model. The connectivity between the mirror module components is high, consequently so was the number of plate elements that were needed. The flanges of the C sections were modeled as beams running at top and bottom of the webs, and accounted for a large number of the beam elements. All the other components were also modeled with beam elements, with the exception of the gusset plates in the torque tube truss intersection.

6.2 Boeing Heliostat

The Z beams in Boeing's heliostat were modeled with plates in the true shape of the beam. The beams are connected to the mirror modules with clips that are specified by rigid beam elements. The beam element end releases allow the appropriate free movement between the mirror module and the clip, thus creating only one attachment per mirror module linked by all six degrees of freedom. The mirror modules are idealized as plates with stiffnesses computed by a sandwich structure theory.

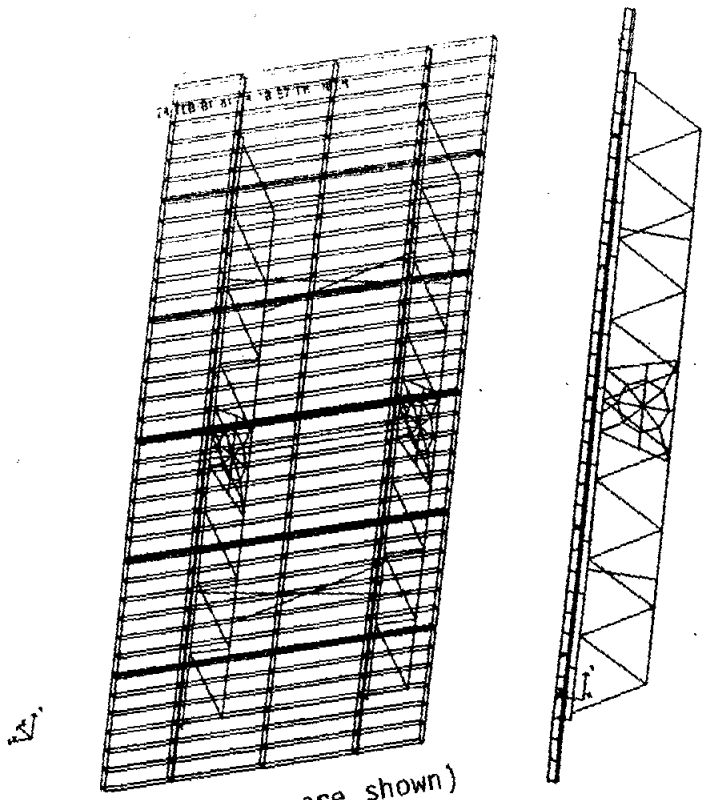

(Only half the mirror modules are shown)

Figure 6.1. ARCO Model

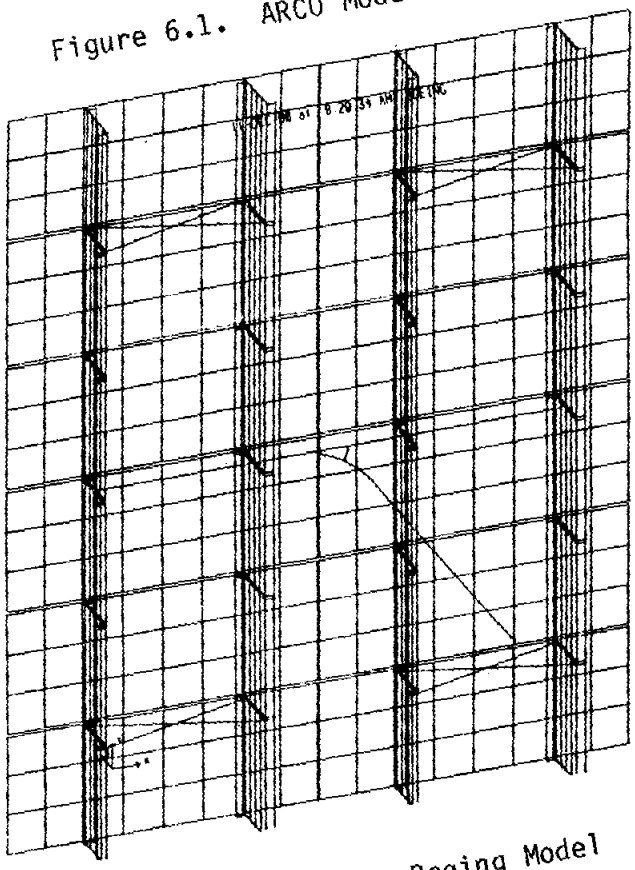

Figure 6.2. Boeing Model

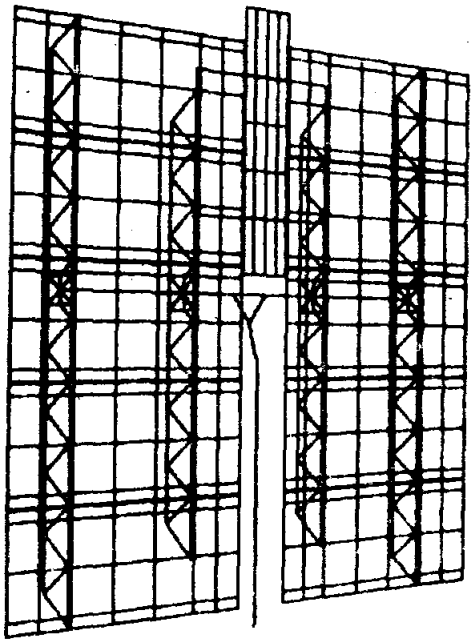

Figure 6.3. Martin Marietta Model

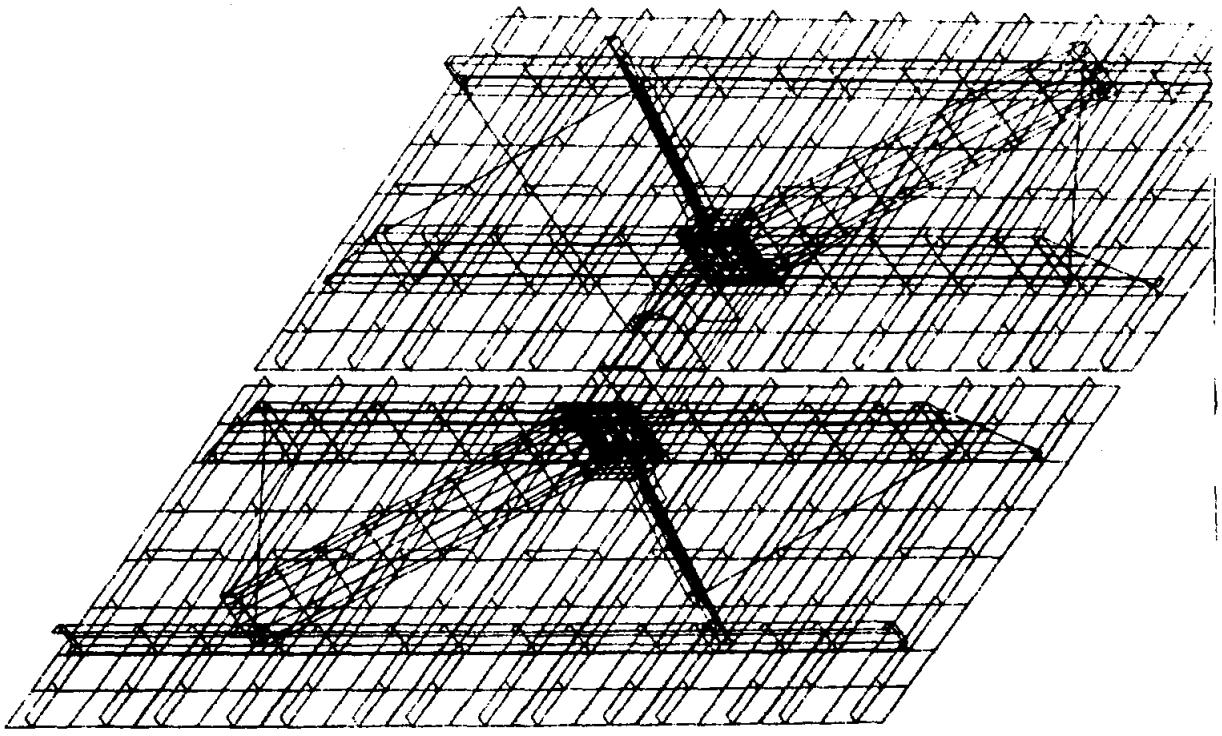

(Mirrors face down)

Figure 6.4. McDonnell Douglas Model

Sandwich Stiffness Formulation -- The bending stiffness for a sandwich structure (Figure 6.6) with thin facings and negligible bending stiffness of the core is calculated below.

For equal thickness facings:

$$D = \frac{Eth^2}{2(1-\mu^2)} \qquad \text{Eq. 1.1}$$

(μ = Poisson's Ratio)

Shear stiffness of the sandwich structure:

$$U \simeq hG_c \qquad \text{Eq. 1.2}$$

where G_c = Effective core shear modulus

$$\text{Axial stiffness } K = \sum \frac{E_i t_i}{1-\mu^2_i} \qquad \text{Eq. 1.3}$$

To find equivalent E and t:

$$D = \frac{Et^3}{12(1-\mu^2_{ave})} \qquad \text{Eq. 1.4}$$

$$K = \frac{Et}{1-\mu^2_{ave}} \qquad \text{Eq. 1.5}$$

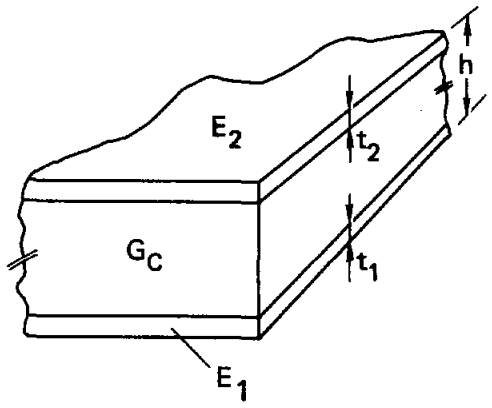

Figure 6.6. Sandwich Structure

$$\text{Equivalent Density} = \gamma = \frac{\sum \gamma_i t_i}{t} \qquad \text{Eq. 1.6}$$

Finding the properties of a homogenious plate equivalent to the sandwich structure requires the computation of the composite bending stiffness (Eq. 1.1 or 1.2) and axial stiffness (Eq. 1.3). Using these two quantities, and solving Eqs. 1.4 and 1.5 simultanously, yields the new thickness and modulus of elasticity. The shear stiffness of the new plate is taken as the shear stiffness of the core section and Eq. 1.6 provides the equivalent density.

6.3 Martin Marietta Heliostat

Martin Marietta's mirror modules were modeled in the same manner as Boeing's: plate elements with properties derived by sandwich structure theory. Since the glass was designed to be "free floating" it contributed only weight, not stiffness, to the module. The impregnated paper honeycomb also did not add to the bending stiffness. The remainder of the structure, with the exception of plates at the torque tube/truss connections, was comprised of beam elements.

6.4 McDonnell Douglas Heliostat

The model of the McDonnell Douglas heliostat had the highest degree of connectivity as a result of the inherent integration present in the structure. The majority of the structure was modeled with plate elements, including the inboard and outboard beams and cross-beams, rather than using equivalent beam models. All gusset plates, stiffners, and angles supporting the mirror modules were also individually modeled.

7.0 Results

7.1 Facet Deflections Due to Gravity

The average of the individual mirror facet pointing errors at each elevation angle affects beam pointing, and can be compensated for by the control software if this average error is known and remains constant in time. This is the precise case with gravity-induced pointing errors. However, since the control software orients the entire heliostat as a unit, only the average of the pointing errors of all facet can be compensated. The remaining error, the scatter of individual facet errors about the average (root-mean-square (RMS) value), affects beam quality and is used by the HELIOS computer code for the optical performance evaluation or field performance. For this reason, the deflections of each facet due to gravity loading were deterined at heliostat elevation angles from 0° to 90° in increments of 15°. The convention for the elevation angle is shown in Figure 7.1.

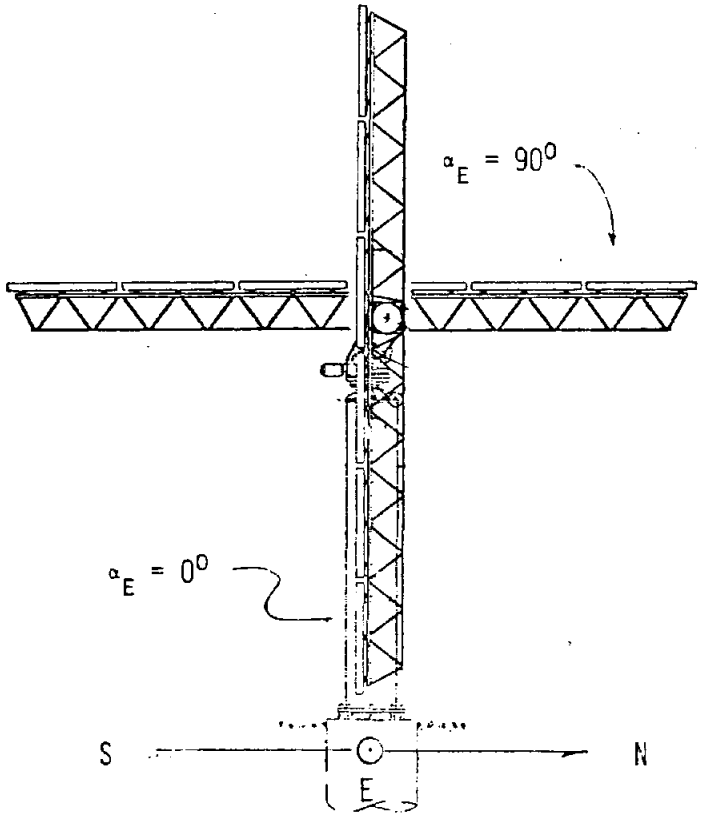

Figure 7.1. Heliostat Elevation Angle Convention

The pointing error of each facet was determined by calculating the vector normal to the facet plane. The plane of the facets was defined by the attachment points of the mirror module to the structure. The Arco and Martin Marietta heliostats have three attachment points per mirror module. Since three points define a plane, this computation was straight forward. For the two heliostats with four attachment points per module, McDonnell Douglas and Boeing, an average was taken of the four planes that could be passed through a permutation of those four points three at a time. This is the case for all mirror normal computations mentioned in the remainder of this report. It should be noted that this method of calculating pointing errors does not include local facet warping or curvature between these attachment points.

Figure 7.3 shows the pointing error about the elevation axis (mrad rotation), due to gravity, for each individual mirror module plotted versus the elevation angle of the heliostat. This information is also presented numerically in Appendix B. The mirror module numbering is shown in Figure 7.2. The difference in the pointing error among the facets at a given elevation angle is a characteristic of the beam quality degradation. The average of these pointing errors at each elevation angle is shown on Figure 7.4. These results were used as input to the HELIOS optical performance code. Sample deflected shapes resulting from this analysis are shown in Figures 7.5 to 7.14. Note that the displacements were amplified in these plots by the amount shown on each figure.

Table 7.1 lists the computed RMS values of the mirror module errors taken about the average of the individual errors. RMS values are listed for the elevation and cross-elevation axes at various elevation angles, a measure of the individual facet deflections effect the beam quality. All three torque tube/beam assembly heliostats (Arco, Boeing, and Martin Marietta)

TABLE 7.1

GRAVITY DEFLECTIONS - BEAM QUALITY DEGRADATION*
(MRAD)

	ARCO		BOEING		MARTIN MARIETTA		McDONNELL DOUGLAS	
HELIOSTAT ELEVATION ANGLE	C-ELEV.** AXIS	ELEV. AXIS	C-ELEV.** AXIS	ELEV. AXIS	C-ELEV.** AXIS	ELEV. AXIS	C-ELEV.** AXIS	ELEV. AXIS
0° (Vertical)	0.29	0.07	0.09	0.01	0.05	0.03	0.13	0.21
15°	0.34	0.12	0.16	0.04	0.23	0.08	0.15	0.28
30°	0.47	0.20	0.27	0.07	0.42	0.17	0.18	0.40
45°	0.60	0.28	0.35	0.10	0.58	0.24	0.22	0.53
60°	0.71	0.33	0.42	0.12	0.70	0.30	0.25	0.63
75°	0.77	0.37	0.47	0.13	0.78	0.34	0.27	0.69
90° (Horizontal)	0.80	0.39	0.49	0.14	0.81	0.36	0.28	0.71

*RMS About the Average of Individual Facet Slope Errors
**Cross Elevation Axis

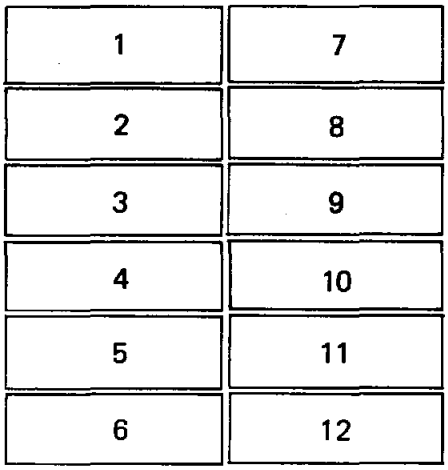

BOEING

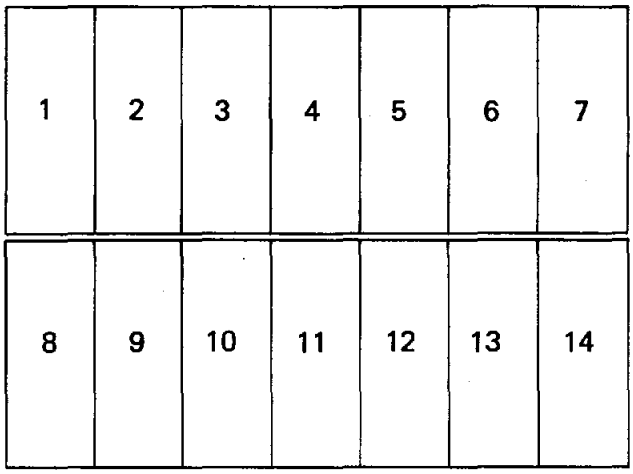

McDONNELL DOUGLAS

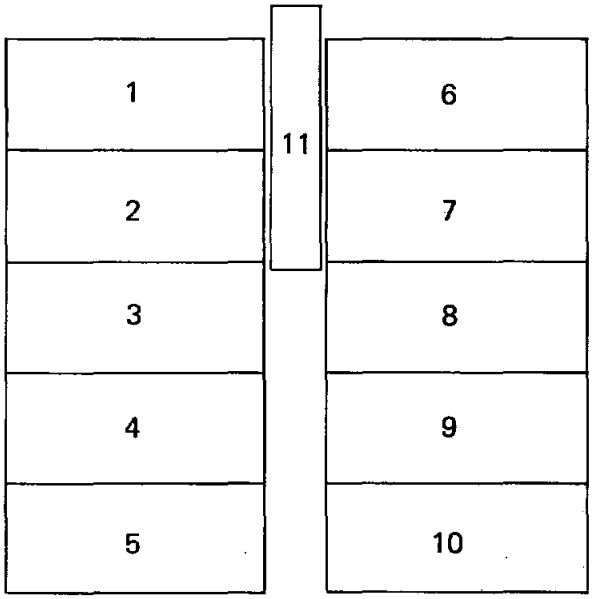

MARTIN MARIETTA

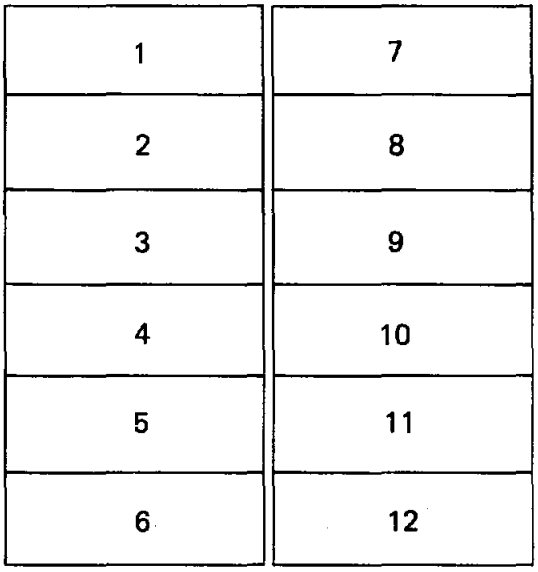

NORTHRUP

7.2. Mirror Module Numbering Convention

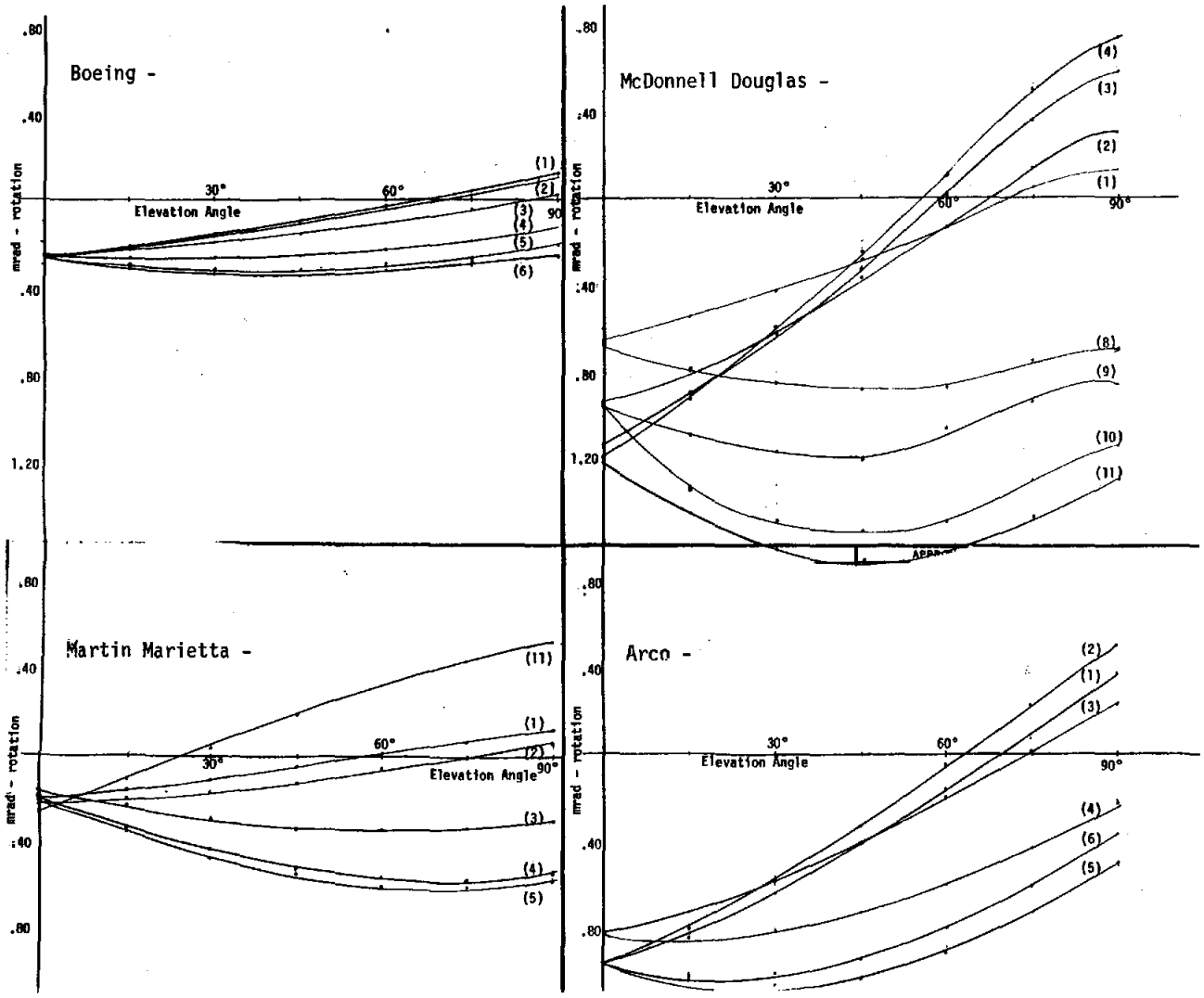

Individual Facet Slope Errors vs. Heliostat Orientation (about Elev. Axis)

Figure 7.3. Gravity Deflections

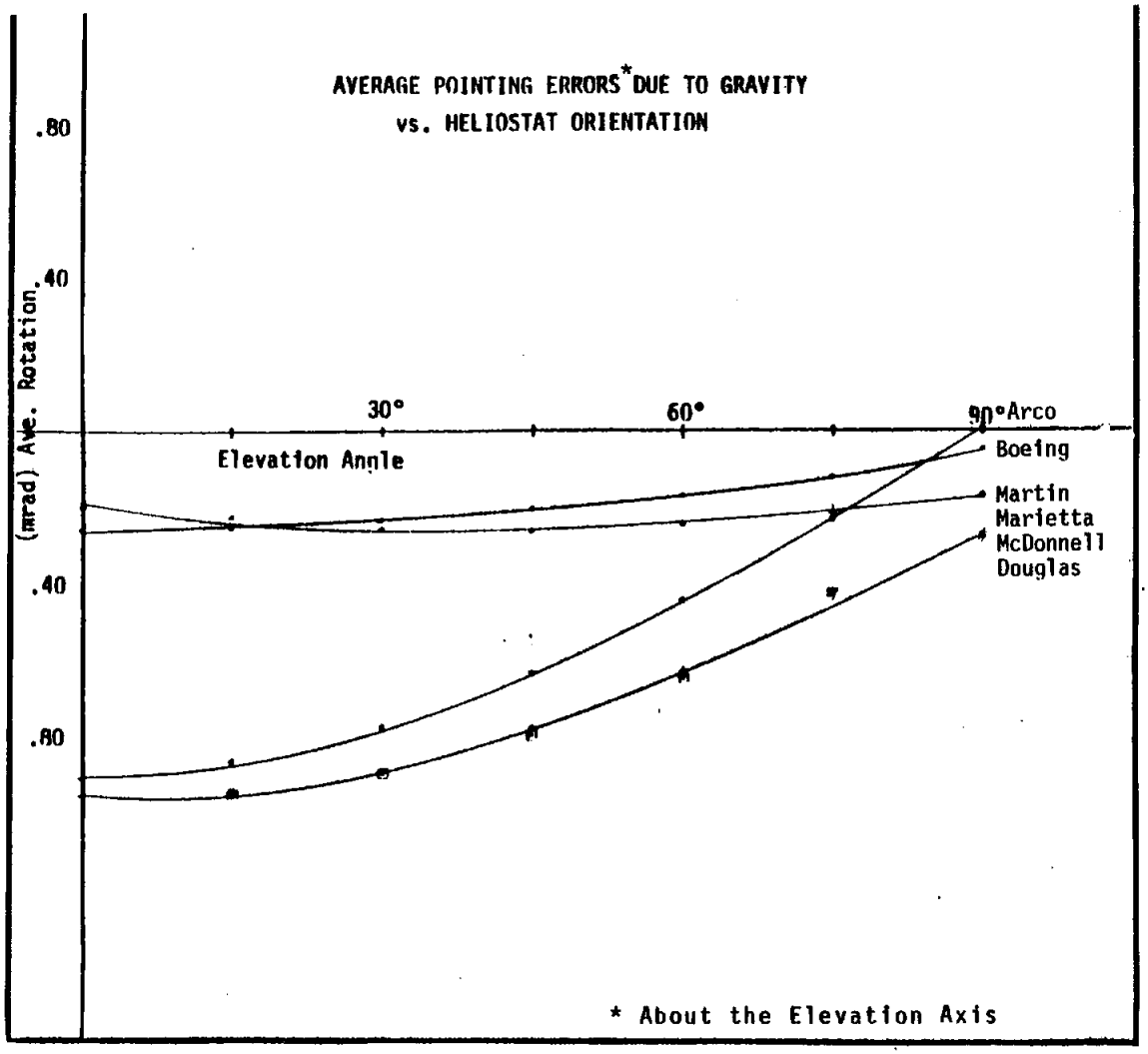

Figure 7.4. Gravity Deflections

Heliostat Vertical

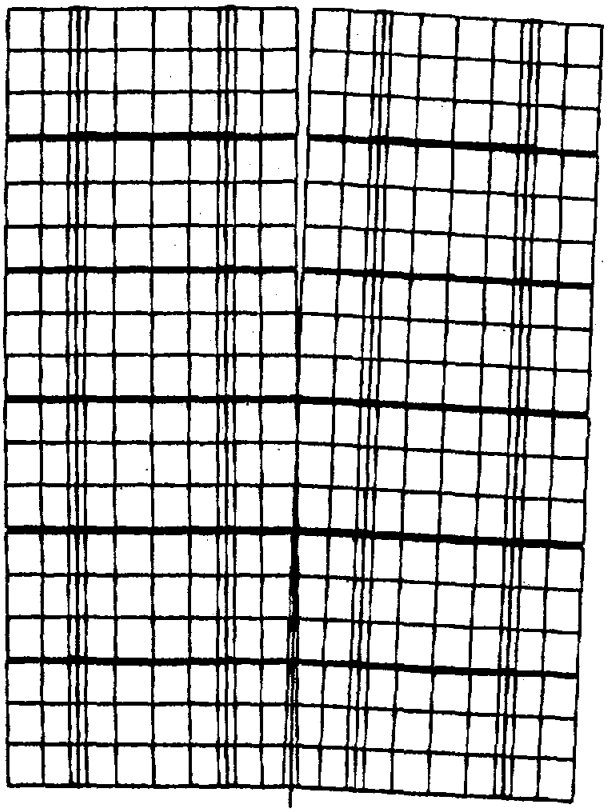

Displacement Amplification: 50

Figure 7.5 Boeing - Gravity Only

Heliostat Horizontal

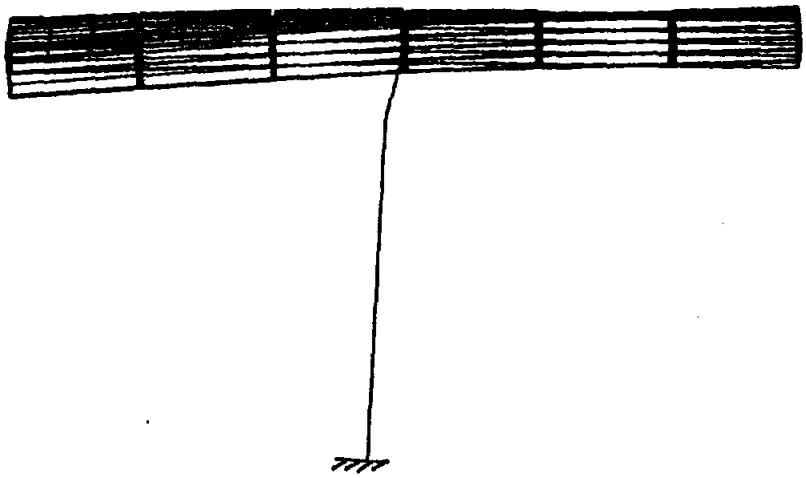

Displacement Amplification: 50

Figure 7.6. Boeing - Case 5

Displacement Amplification: 50

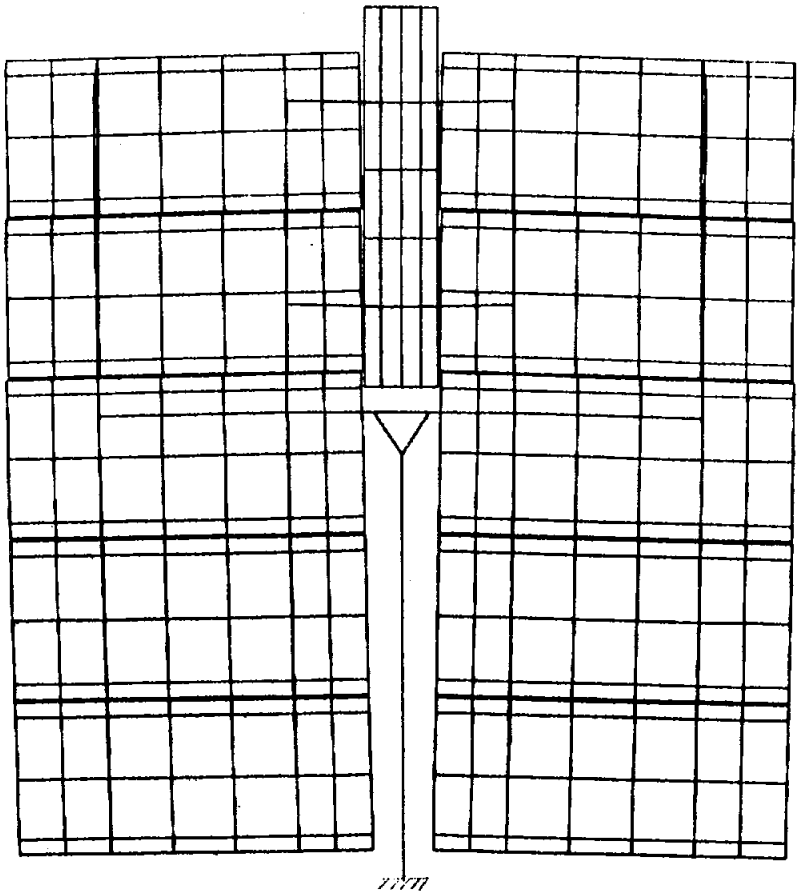

(Heliostat Vertical)

Figure 7.7. Martin Marietta - Gravity Only

(Heliostat Horizontal)

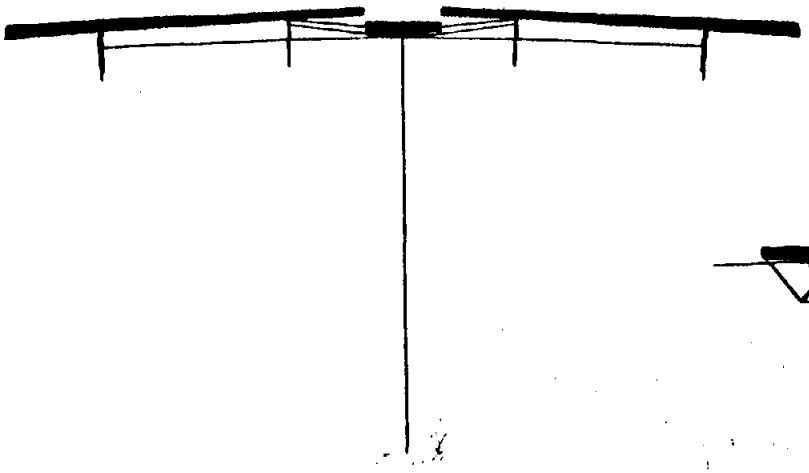

Displacement Amplification: 50

(Heliostat Horizontal)

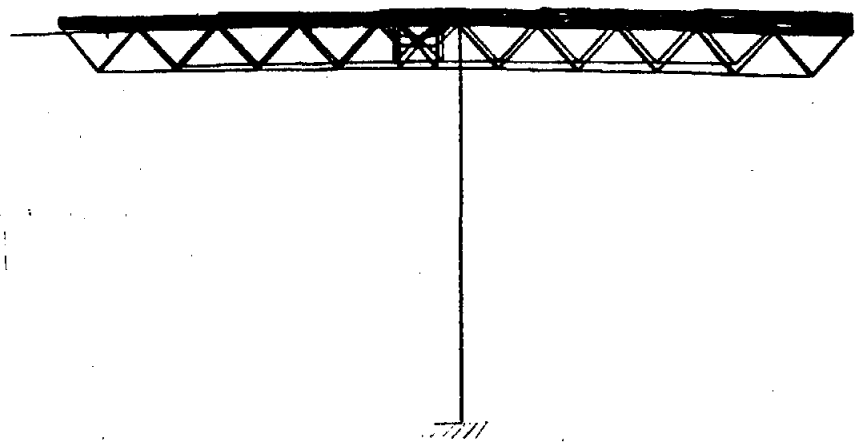

Displacement Amplification: 50

Figure 7.8. Martin Marietta - Gravity Only

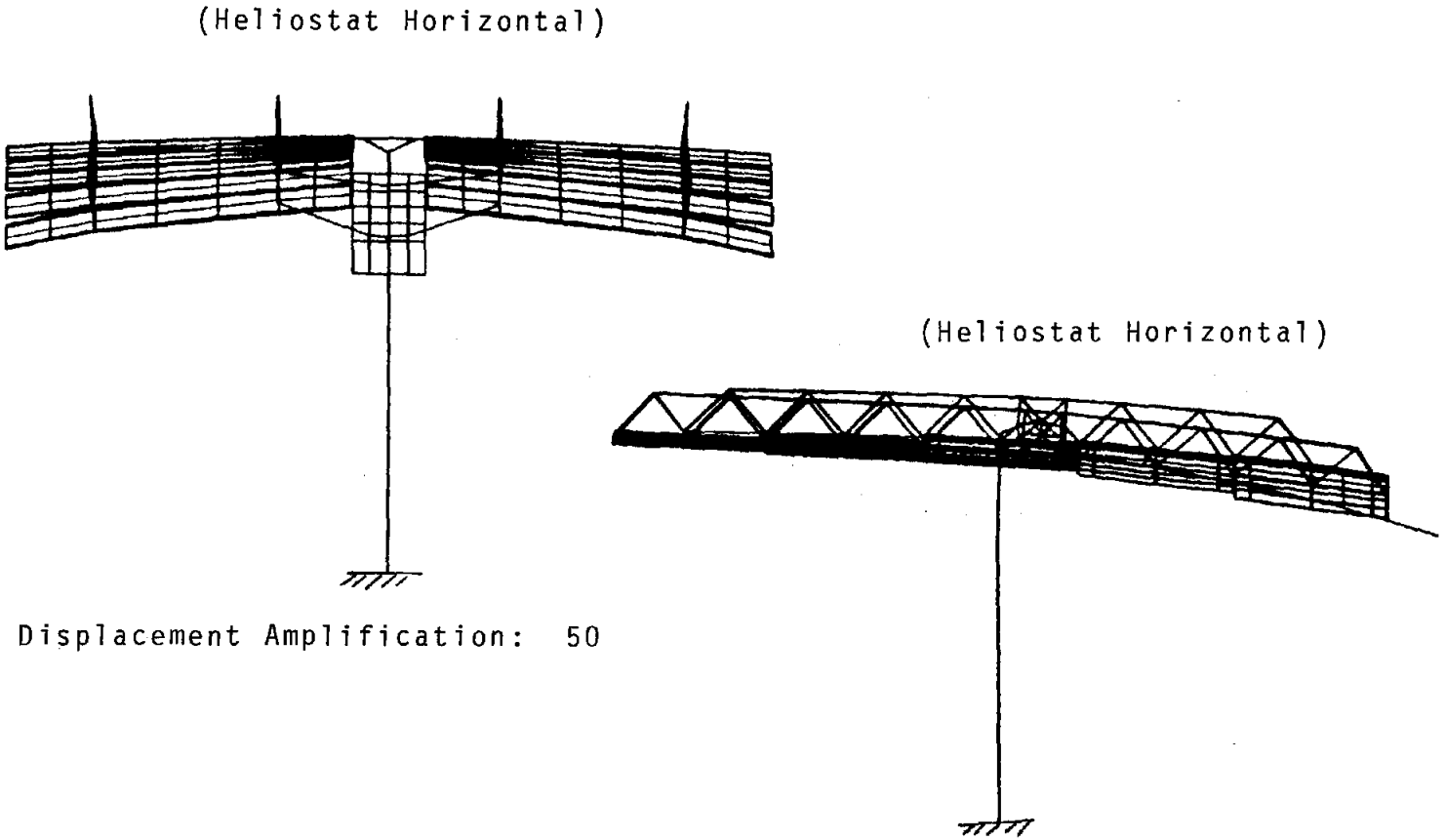

Figure 7.9. Martin Marietta - Case 5 Loading

(Heliostat Vertical)

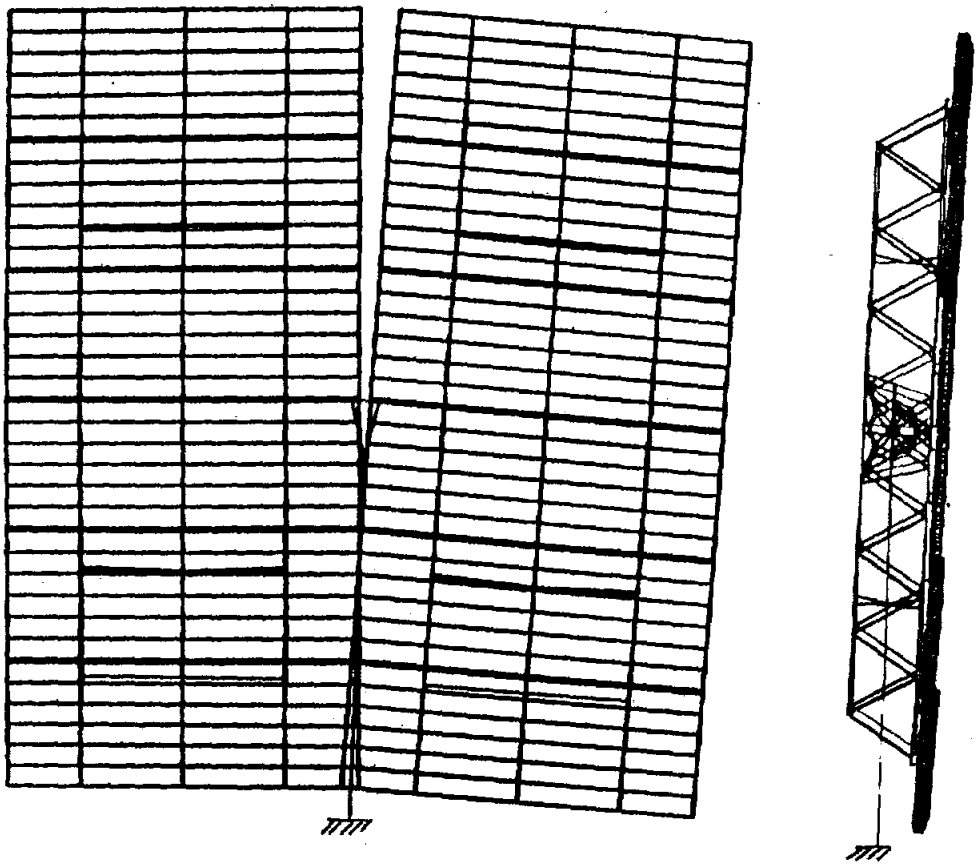

Displacement Amplification: 50

Figure 7.10. Arco - Gravity Only

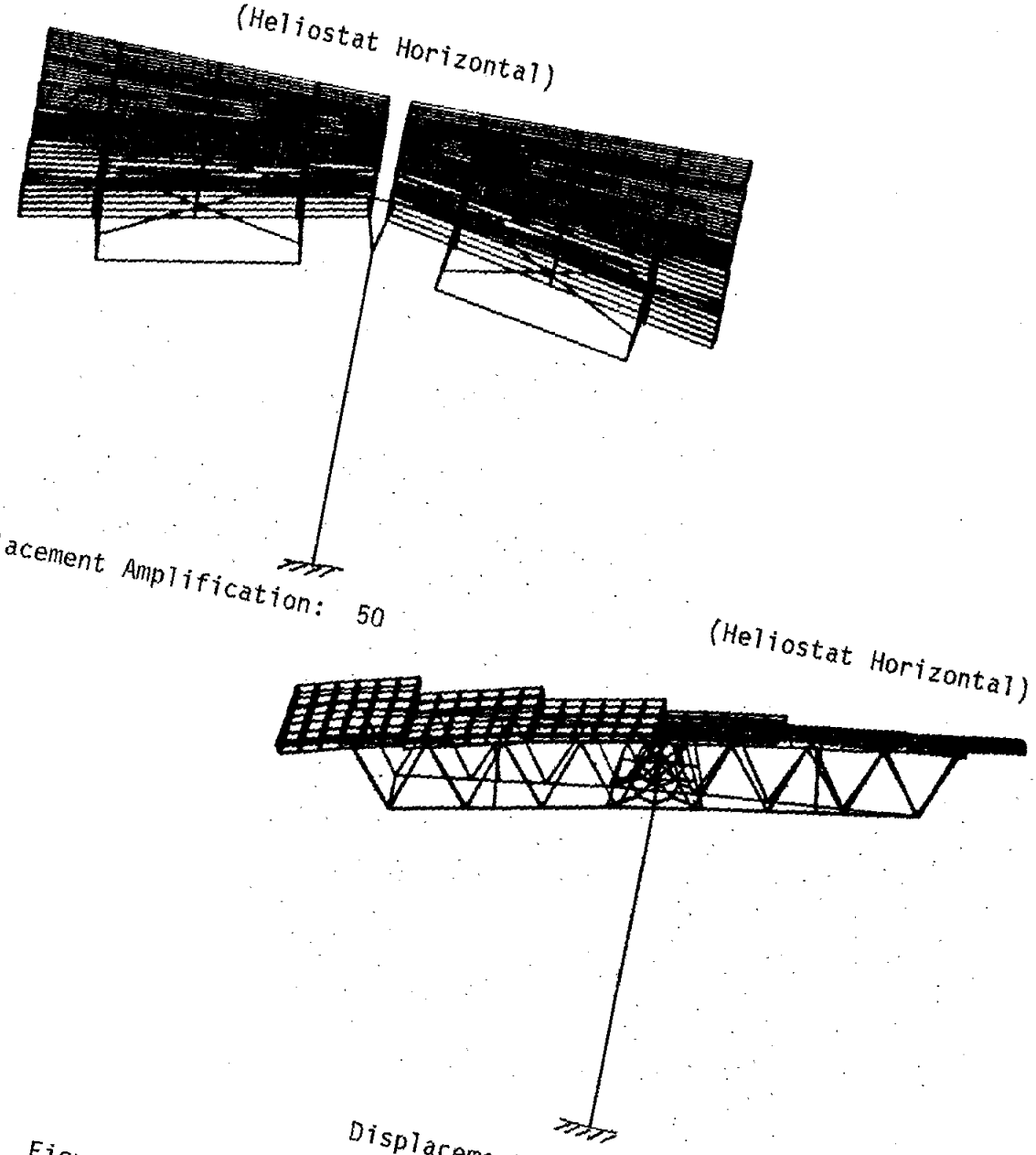

Figure 7.11. Arco Case 5 Loading

(Heliostat Vertical)

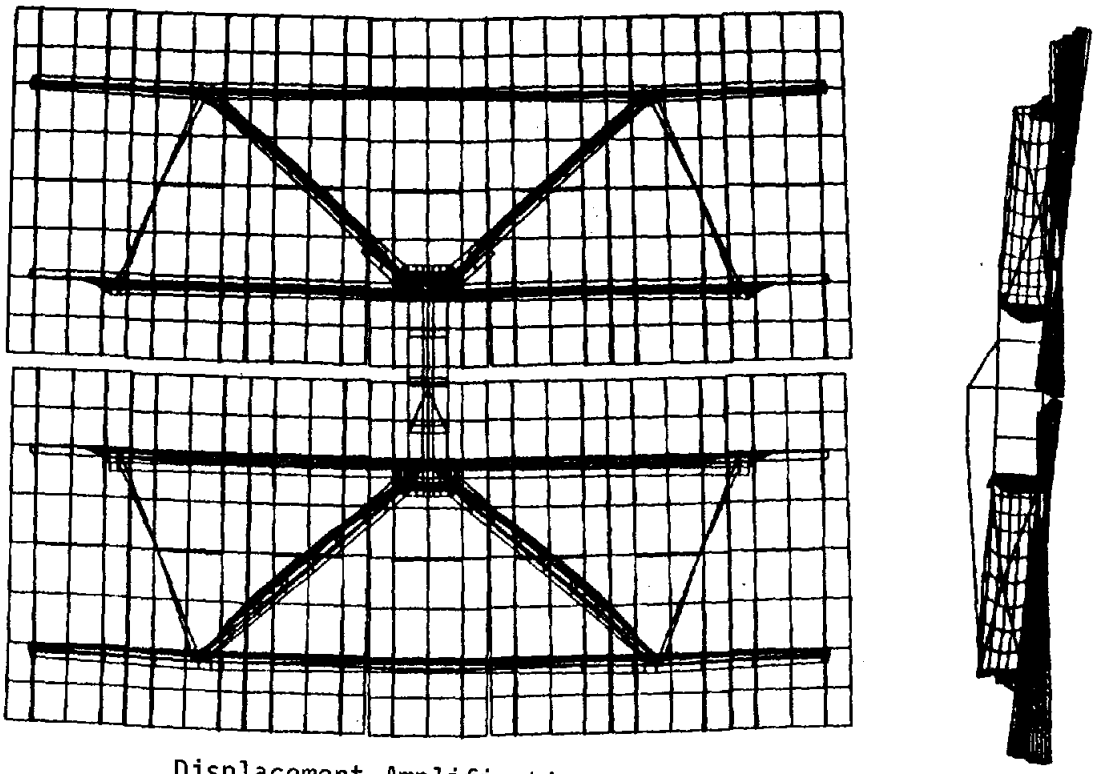

Displacement Amplification: 200

Figure 7.12. McDonnell Douglas - Gravity Only

(Heliostat Horizontal)

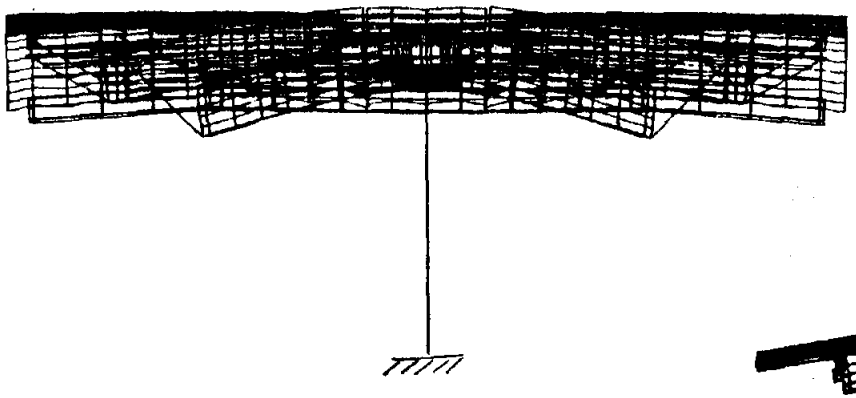

Displacement Amplification: 200

(Heliostat Horizontal)

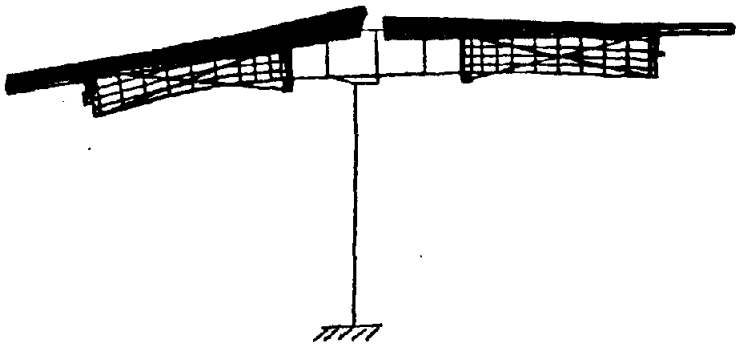

Displacement Amplification: 200

Figure 7.13. McDonnell Douglas - Case 5A Loading

(Heliostat Horizontal)

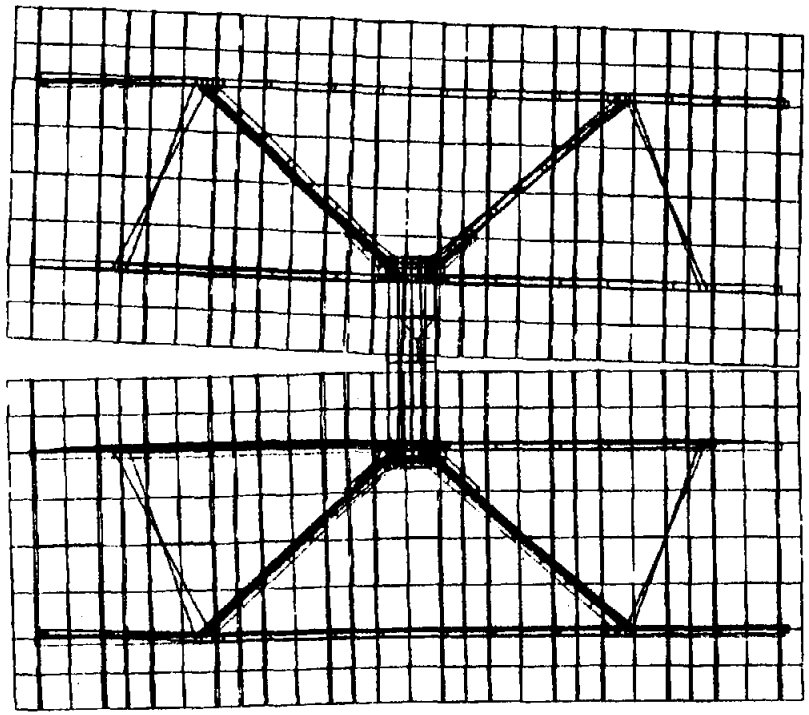

Displacement Amplification: 200

(Heliostat Horizontal)

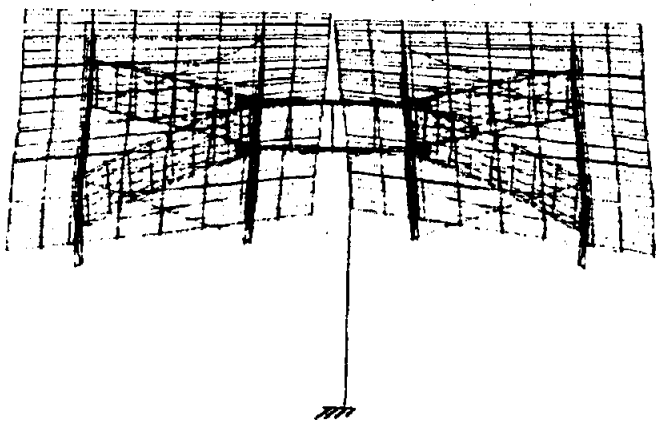

Displacement Amplification: 200

Figure 7.14. McDonnell Douglas - Case 5B Loading

show a larger beam degradation about the cross-elevation axis than the elevation axis. The opposite is true for the McDonnell Douglas heliostat whose main structural components are parallel to the elevation axis. Note also that the large spread of errors shown in Figure 7.3 for McDonnell Douglas is comparable to the cross-elevation rotations of the other three heliostats. If a similar graph was drawn for the individual cross-elevation axis errors, it would show McDonnell Douglas with the least spread between mirror module errors at any given elevation angle. On this hypothetical graph Arco and Martin Marietta would appear very similar to the McDonnell Douglas' elevation rotation, with Boeing approximately halfway in between.

Referring back to Table 7.2, Boeing shows the smallest RMS values about both axes of the three torque tube/beam assembly heliostats, but has higher RMS facet slope error than McDonnell Douglas about the cross elevation axes.

7.2 Facet Deflections Under Operation Wind Speeds

Facet deflections due to specified maximum operational wind loads were determined for three orientations of the heliostat to the wind (Table 5.1). The highest wind speed for which beam quality is specified under the contract is 27 mph.

The average pointing errors for each heliostat about the cross-elevation and elevation axes resulting from these load cases are listed in Table 7.2. Individual facet deflections are tabularized in Appendix B. Gravity loads were not included in these analyses so that gravity and wind load effects could clearly be separated. The drive mechanisms were assumed rigid in these analyses, so heliostat deflection due to drive flexibility must be added to the values in Table 7.2 before comparison with specifications can be made. Comparing Table 5.2 and Table 7.2 it may be noted that the differences in deflections are not due simply to the differences in loads. These wind load pointing errors are of the same order of magnitude as those produced by gravity although it is clear, from comparing Figure 7.4 with the elevation axis rotations in Table 7.2, that wind loads induce different types of deflections than gravity. Unlike the pointing errors induced by gravity, fluctuating wind load pointing errors cannot be compensated by the control software.

TABLE 7.2

OPERATIONAL WIND POINTING ERROR*
(MRAD)

	ARCO		BOEING		MARTIN MARIETTA		McDONNELL DOUGLAS	
	AZ. AXIS	ELEV. AXIS	AZ. AXIS	ELEV. AXIS	AZ. AXIS	ELEV. AXIS	AZ. AXIS	ELEV. AXIS
CASE 1: 27 mph Wind Elevation Angle: 0° Wind ⊥ to Hstat	0.0	0.54	0.0	0.14	0.0	0.19	0.0	0.29
CASE 2: 27 mph Wind Elevation Angle: 70° 20° A.ofA.~Elev. Axis	0.0	0.80	0.0	0.27	0.0	0.38	0.0	0.43
CASE 3: 27 mph Wind Elevation Angle: 0° 20° A.ofA.~Az. Axis	0.46	0.47	0.16	0.12	0.31	0.13	0.65	0.21

*Average of Individual Facet Slope Errors
-Note: Gravity Effects Not Included

As with gravity pointing errors, Boeing has the least error of the four heliostats about the elevation axis, followed closely by Martin Marietta. Arco has the largest elevation axis rotation whereas McDonnell Douglas had the largest gravity induced rotation.

A similar analysis was performed at SNLA on the two heliostats developed by Martin Marietta and McDonnell Douglas for the 10-MWe pilot plant at Barstow, California. The pilot plant heliostats and Second-generation heliostats showed gravity deflections on the same order of magnitude. Operational wind load deflections of the Second-generation heliostats were similar to those of the Martin Marietta design for Barstow but slightly less than McDonnell Douglas' Barstow heliostat. Although the two companies involved in the Barstow design were also participating in the Second-generation contracts, the Martin Marietta heliostat had undergone a significant redesign and McDonnell Douglas had a completely new design.

7.3 Structural Stresses Under Survival Wind Velocities

Structural stresses were computed for two combinations (three for McDonnell Douglas) of gravity and wind loads described as survival conditions in section 5 (Table 5.1).

The 50 mph criteria (Load Case 4) was taken from a study of thunderstorm gusts. The heliostat must survive a 50 mph gust at any elevation angle orientation. The 90 mph criteria covering a combination of wind and gusts (Load Case 5) was taken from the Uniform Building Code specification covering most sites in the Southwestern part of the U.S. The heliostats are in the stow position for such high winds: mirrors upward for Arco, Boeing, and McDonnell Douglas, and mirrors downward for Martin Marietta. The stow position was chosen by the heliostat contractor.

The largest stress values found in each heliostat are shown in Table 7.3. These stresses are not high since the designs were driven by deflection criteria rather than loading. Also shown in Table 7.3 are the theoretical wind speeds that would bring about the largest stress (up to the maximum stress allowable) and the theoretical wind speeds that would cause yielding. These wind speeds were calculated from the relationship between wind speed and induced pressure. The pressure or load varies with the square of the wind velocity.

The highest stresses, as a fraction of allowable, in the Arco and Boeing heliostats, occured in the torque tube near the connection to the drive mechanism. Arco also had relatively high stresses in the bolts connecting the mirror modules to the structure. Martin Marieta's highest stress occured in the chord of an exterior truss near the connection of the truss to the torque tube. For McDonnell Douglas, the highest stress was found in the deep cross-beam near the gusset plate reinforced area. The maximum "allowable" and "yield" winds listed in Table 7.3 are the wind velocities required to bring the location of highest stress to the AISC specified allowable and yield stress, respectively.

The heliostat structures experienced the highest stress in the Case 5 (90 mph-stowed) loading. However, the most severe condition for the pedestals was Case 4 (50 mph-heliostat vertical) because of the additional torsion and shear that are present when the heliostat is in a vertical position. All torque tubes showed the highest stresses in Case 5 loading at the connection to the drive mechanisms. The diagonal members in the trusses of the Martin Marietta and Arco heliostats were checked against buckling and were found to be satisfactory.

TABLE 7.3

LARGEST STRESSES IN SURVIVAL CONDITIONS

	Calculated Stress	Allowable Stress	Max "Allowable" Wind	Yield Stress	Max "Yield" Wind
Arco	8,497 psi	21,600 psi	143 mph	36,000	185 mph
Boeing	8,164 psi	21,600 psi	147 mph	36,000	189 mph
Martin Marietta	17,138 psi	21,600 psi	101 mph	36,000	130 mph
McDonnell Douglas	14,251 psi	21,600 psi	111 mph	36,000	143 mph

7.4 Natural Frequencies and Mode Shapes

For each heliostat, the lowest five natural frequencies were determined in order to evaluate the heliostats' susceptibility to excitation by vortex shedding. Excitation by vortex shedding is an oscillation caused by eddies of wind forming behind the heliostat. The frequencies at which this will occur are determined by the heliostat size and shape, and the wind velocity. The vortex shedding frequency is given by:

$$N_S = SU/D$$

where N_S = frequency of full cycles of vortex shedding
D = characteristic dimension of the body projected on a plane normal to the flow velocity
U = Velocity of incoming flow
S = Strouhal number

The Strouhal number is 0.156 for a flat plate with the direction of flow normal to the plate. In the case of flow parallel to the plate the Strouhal number is 0.145. Table 7.4 shows the vortex shedding frequencies resulting from the above calculation using these two cases with the worst case characteristic dimensions each heliostat (i.e. one side only), shown in Figure 7.15, at a wind velocity of 27 mph.

TABLE 7.4

VORTEX SHEDDING FREQUENCIES

	Arco	Boeing	Martin Marietta	McDonnell Douglas
for D =	144.23"	120.75"	144.00"	132.25"
With wind perpendicular to heliostat: N_S =	0.51 hz	0.61 hz	0.51 hz	0.56 hz
With wind parallel to heliostat: N_S =	0.48 hz	0.57 hz	0.48 hz	0.52 hz

It is worth noting that 90 percent of the wind energy is contained in frequencies below 0.5 Hz. Thus, the frequency range of concern is approximately 0.4- 0.6 Hz.

The frequency analysis of the models was first performed with rigid drive mechanisms. These results are presented in Table 7.5. The associated mode shapes are characterized in Figure 7.16 and the computer generated shapes are shown in Figures 7.17 through 7.36. The computer drawn mode shapes were done by a three-dimensional plotting routine, GRAPE, developed at the Lawrence Livermore National Laboratory.

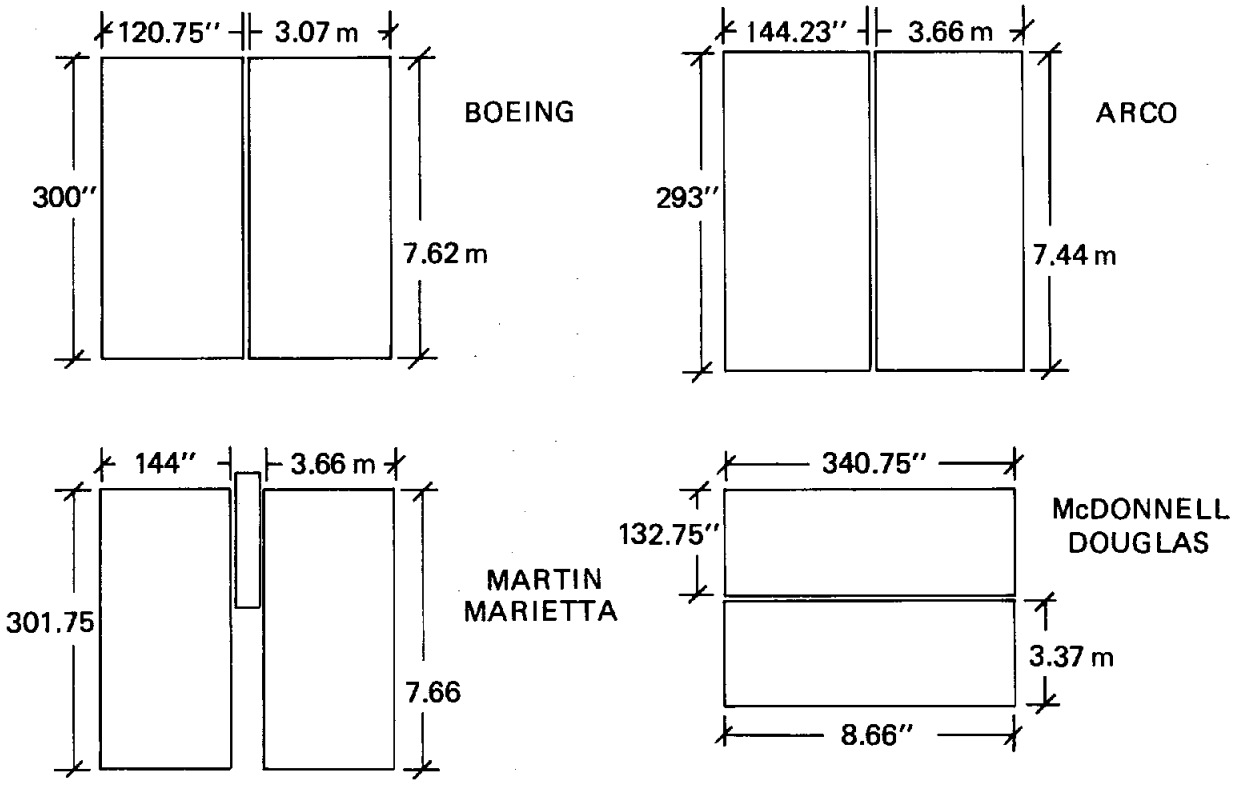

Figure 7.15. Characteristic Dimensions of Heliostats

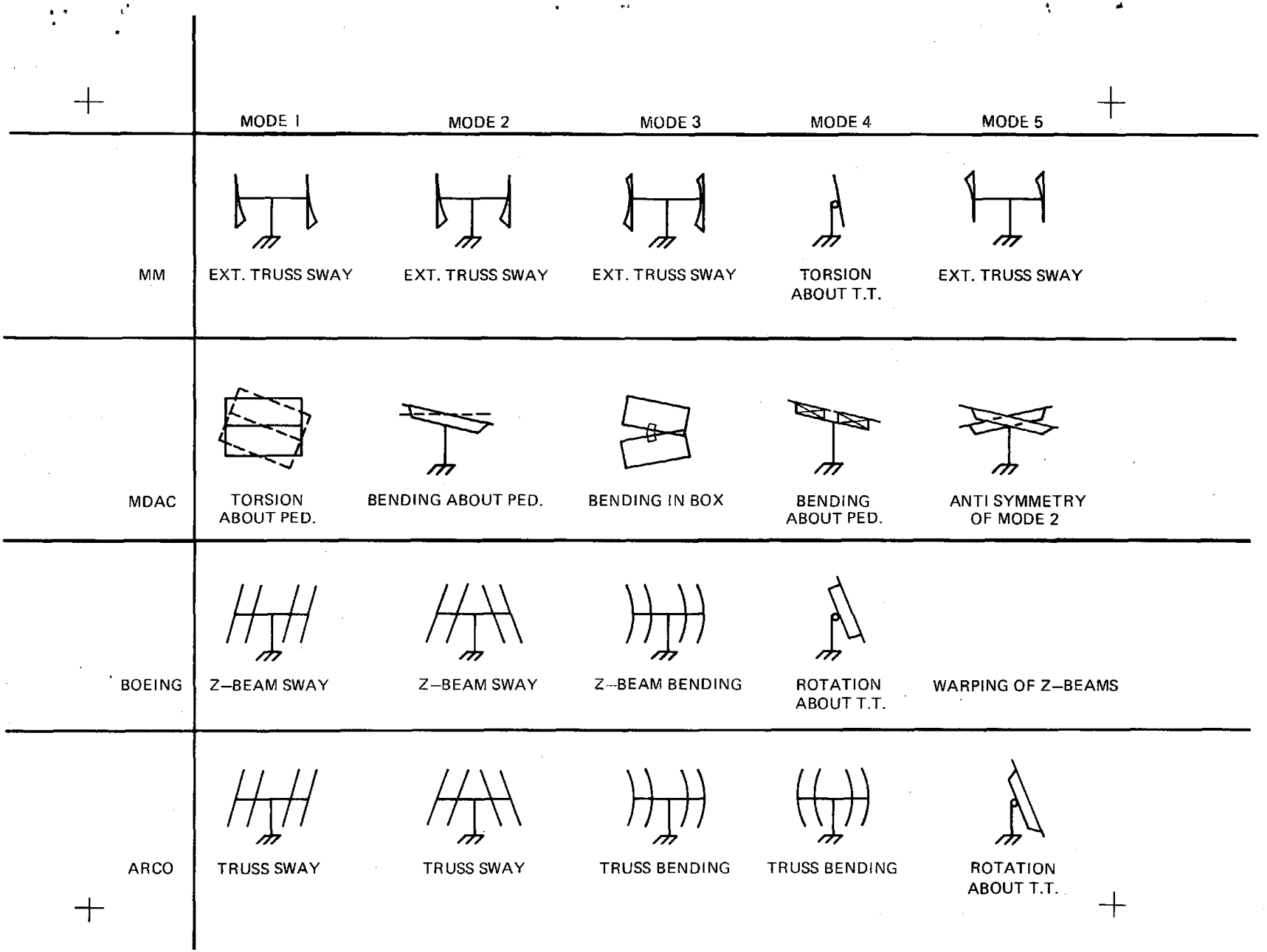

Figure 7.16. Mode Shapes With Rigid Drives

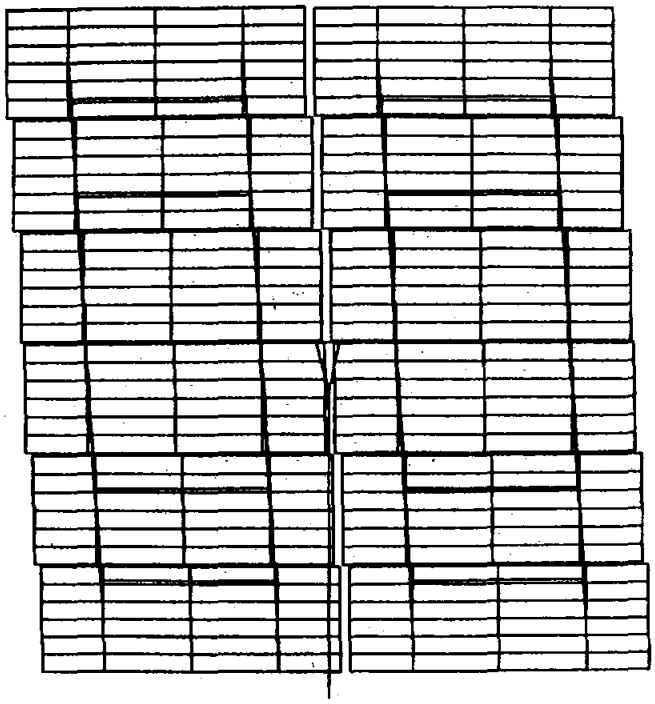

Figure 7.17. Arco Mode 1

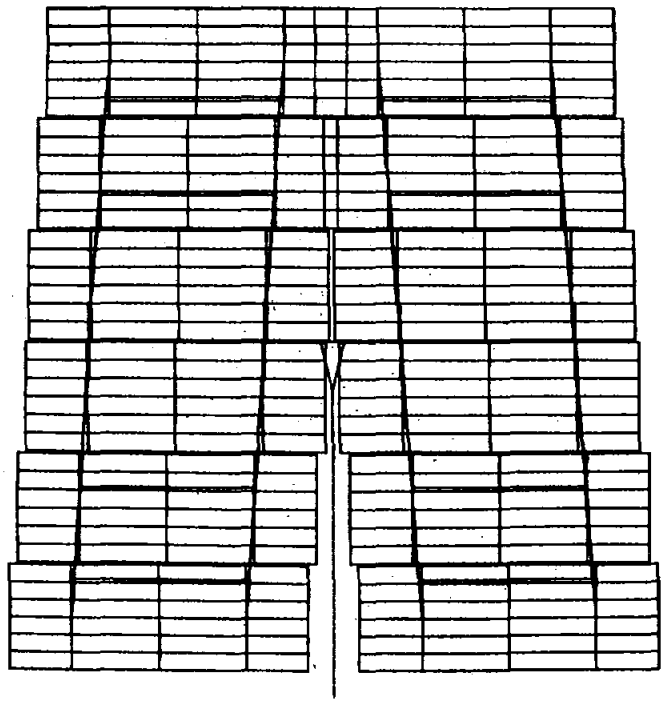

Figure 7.18. Arco Mode 2

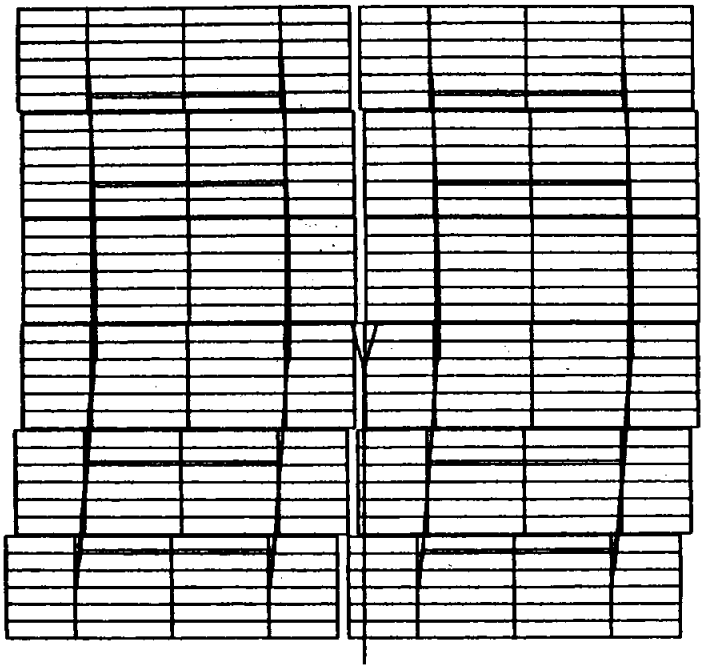

Figure 7.19. Arco Mode 3

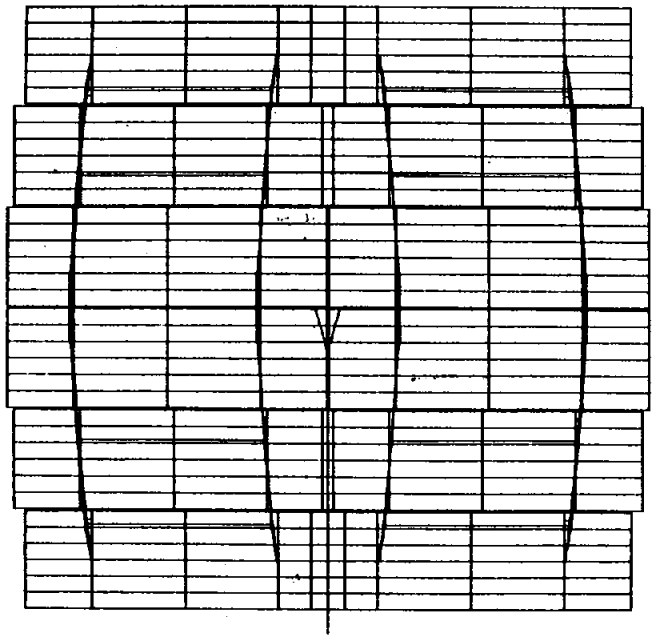

Figure 7.20. Arco Mode 4

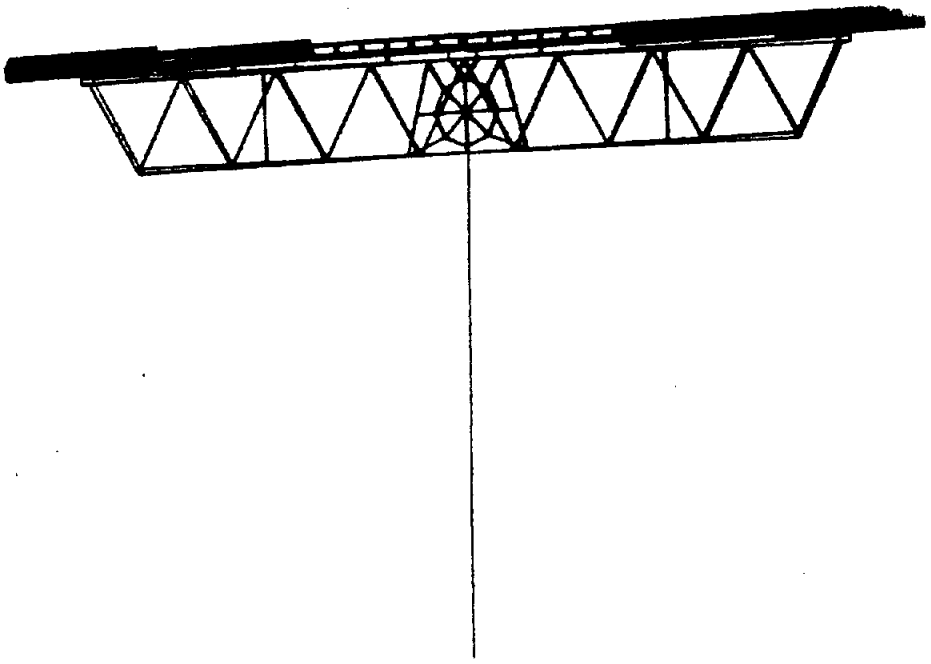

Figure 7.21. Arco Mode 5

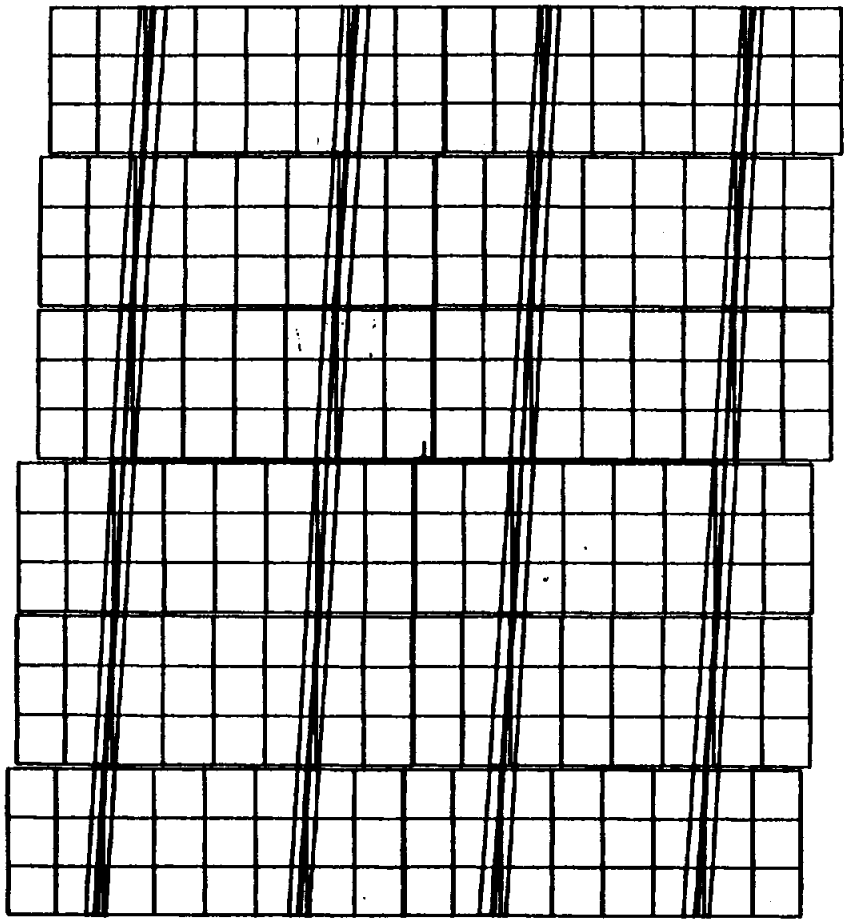

Figure 7.22. Boeing Mode 1

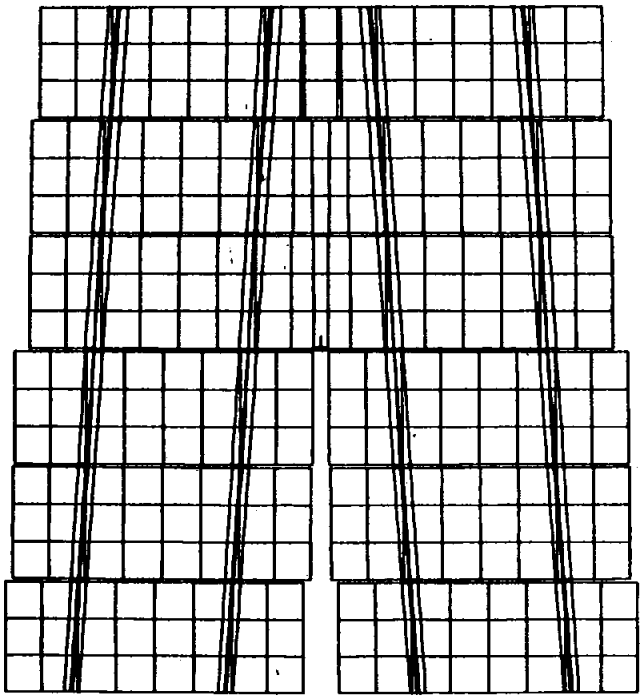

Figure 7.23. Boeing Mode 2

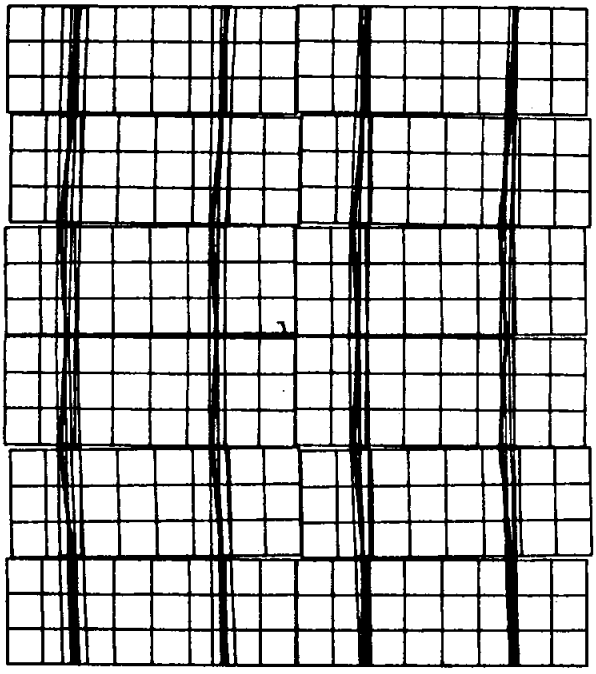

Figure 7.24. Boeing Mode 3

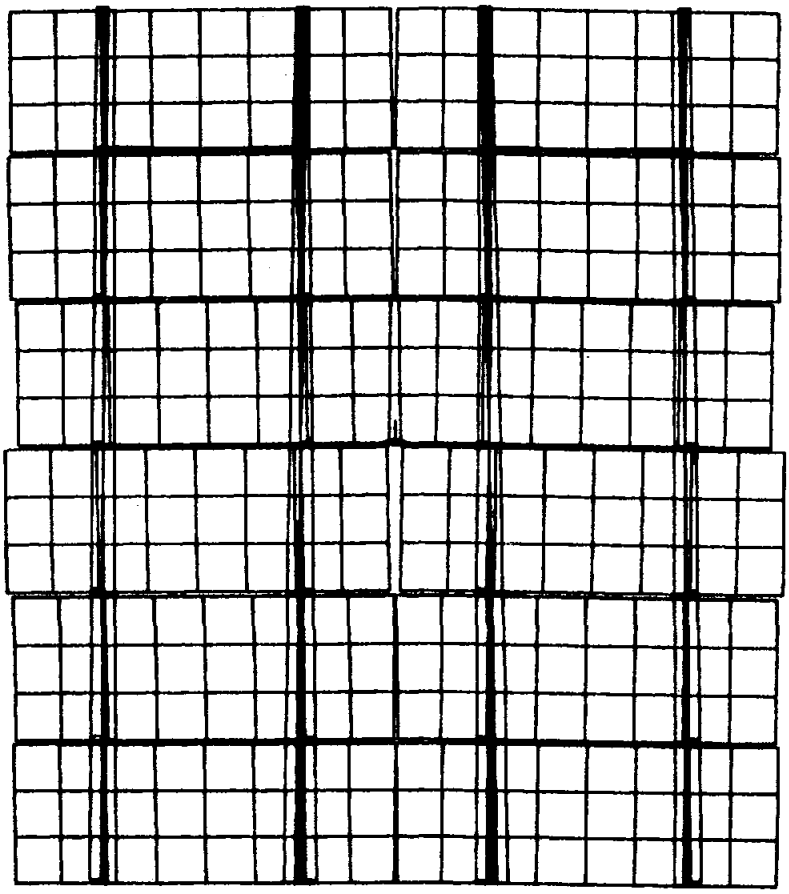

Figure 7.25. Boeing Mode 4

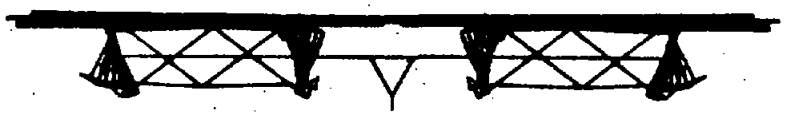

Figure 7.26. Boeing Mode 5

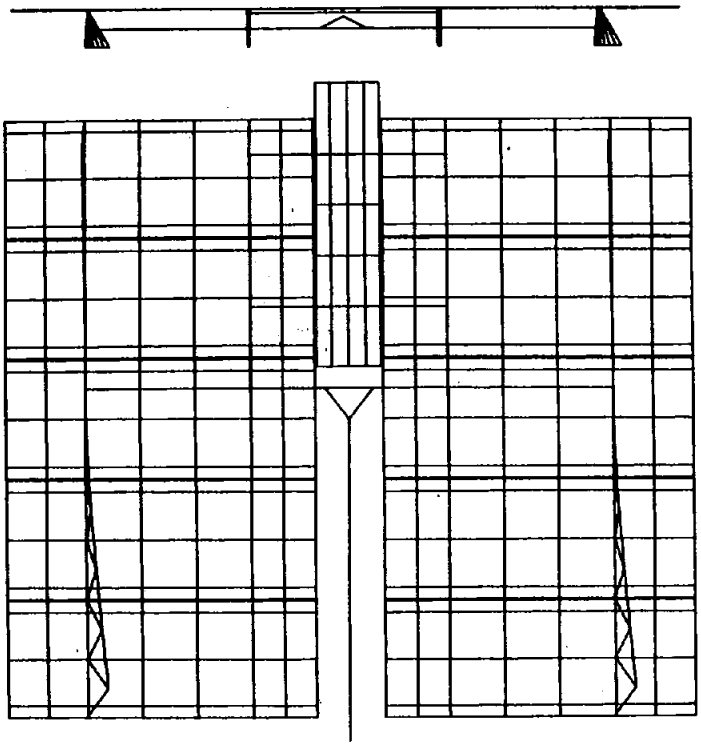

Figure 7.27. Martin Marietta Mode 1

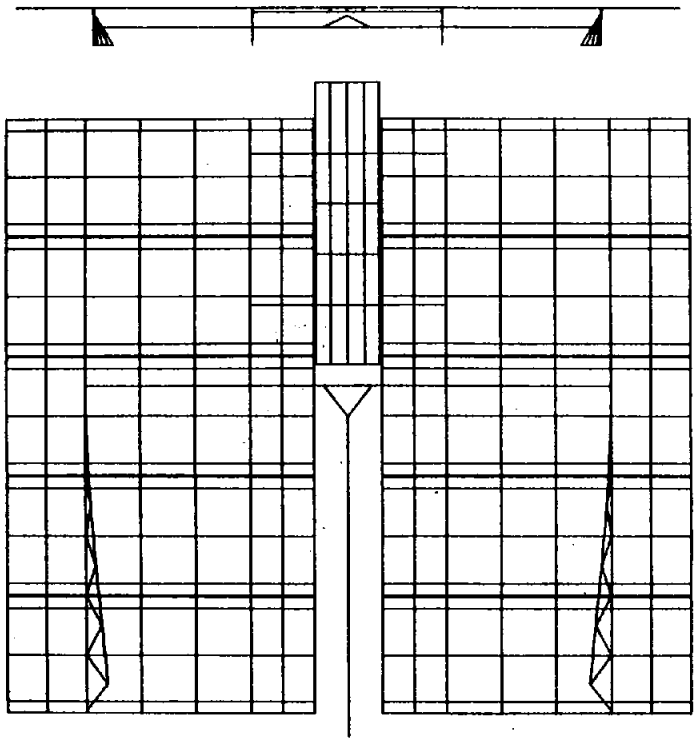

Figure 7.28. Martin Marietta Mode 2

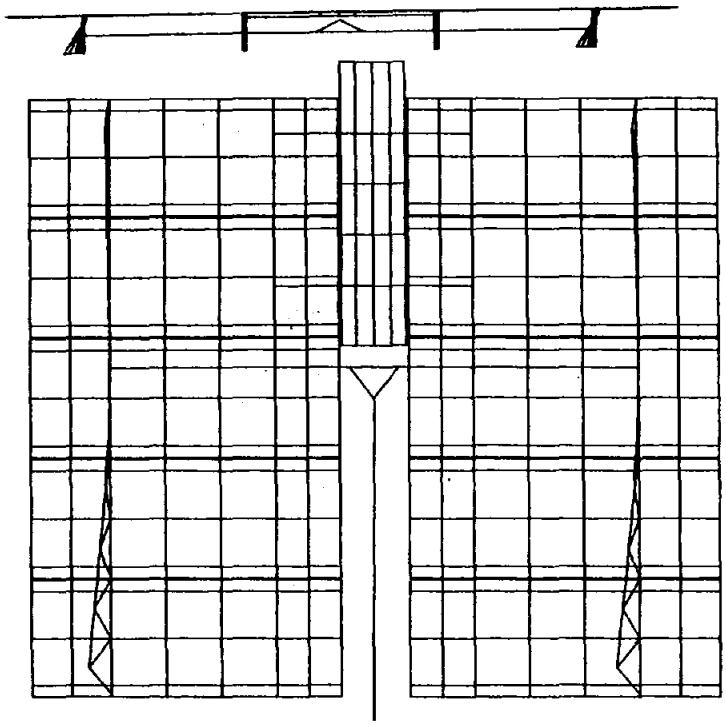

Figure 7.29. Martin Marietta Mode 3

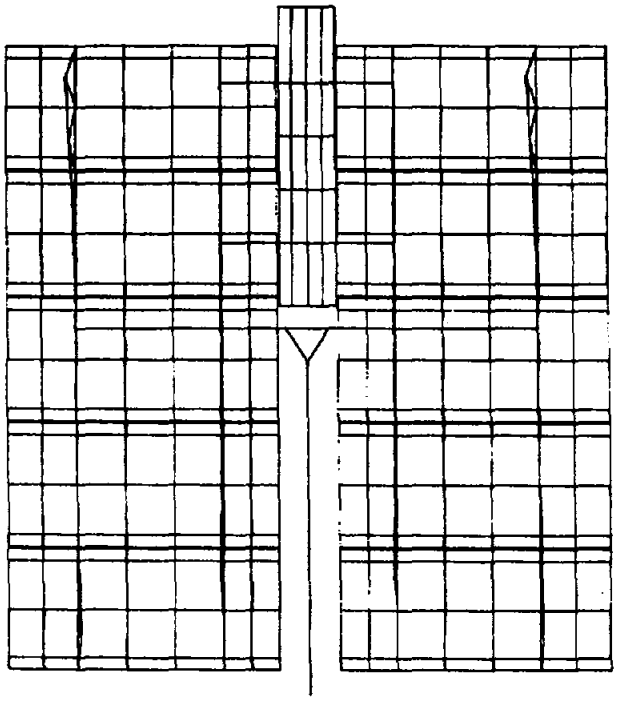

Figure 7.30. Martin Marietta Mode 4

Figure 7.31. Martin Marietta Mode 5

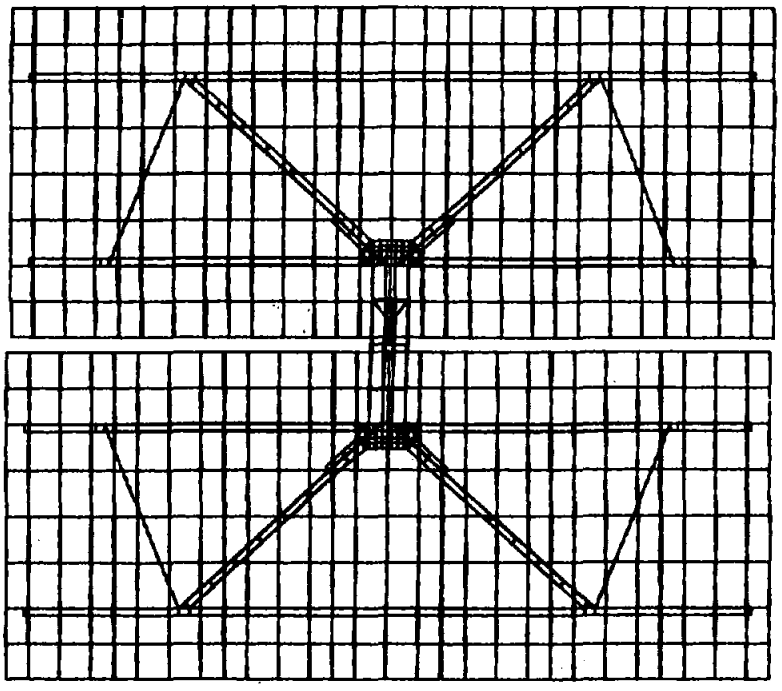

Figure 7.32. McDonnell Douglas Mode 1

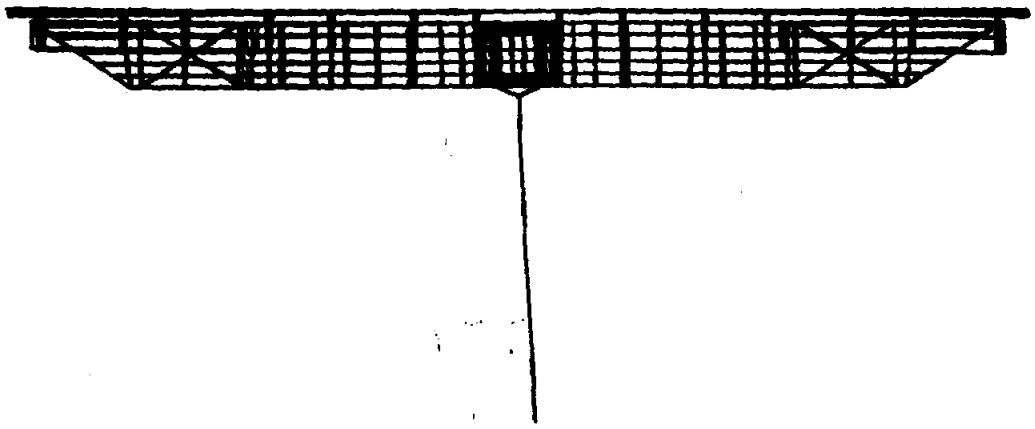

Figure 7.33. McDonnell Douglas Mode 2

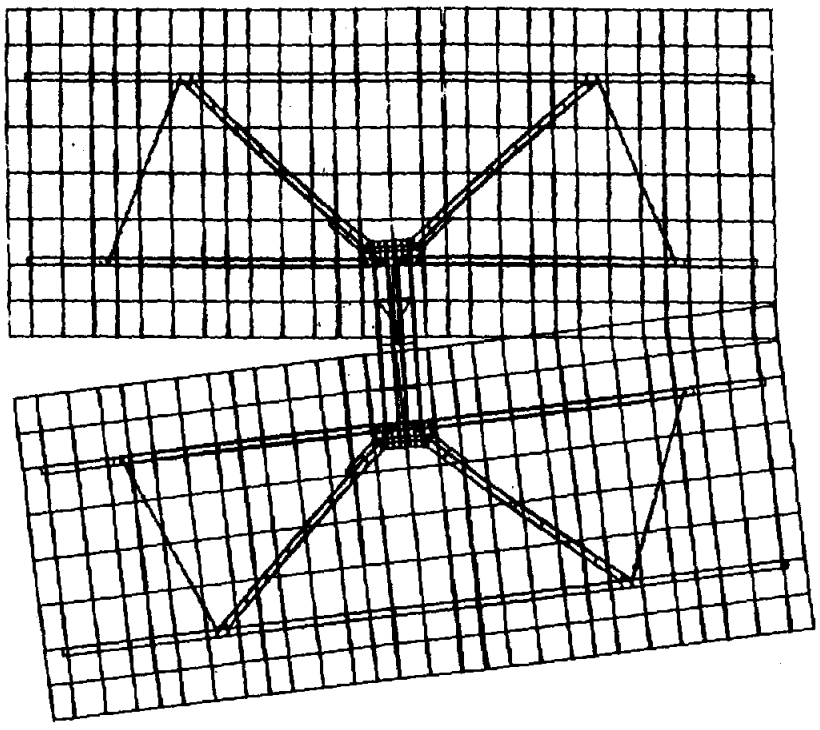

Figure 7.34. McDonnell Douglas Mode 3

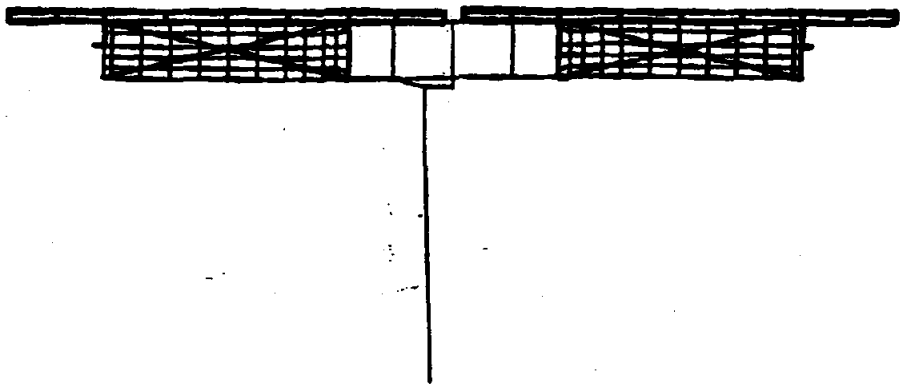

Figure 7.35. McDonnell Douglas Mode 4

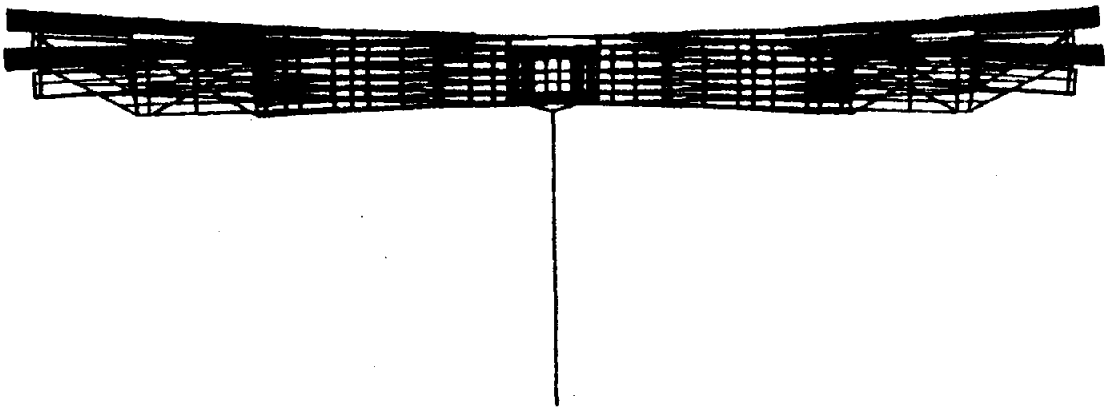

Figure 7.36. McDonnell Douglas Mode 5

Table 7.6 shows the frequencies of the heliostats where drive mechanisms were characterized by linear flexural and torsional springs (stiffness values were determined from testing data taken at the CRTF). The associated mode shapes are depicted in Figure 7.37 and again in the computer-drawn mode shapes in Figures 7.38 through 7. 57. Table 7.6 also shows the appropriate stiffnesses used in each case. The elevation stiffnesses varied with the elevation angles of the heliostats. The load deflection curves of the drive mechanisms generally did not follow a straight line, but rather diverged at two different slopes. The higher stiffness corresponded to the lower loads with a definite knee where the change in stiffness took place (see report on Structural Testing of Second-Generation Heliostats by W. Rorke for more information). The stiffness chosen was an average value. The effect of the drives was to soften the structure as a whole and to spread out the range of natural frequencies for each heliostat.

The lowest frequencies of the heliostats were still well above the vortex shedding frequencies for operational winds velocities and the entire range of concern.

The natural frequencies of the pilot plant heliostat were comparable with the second-generation results:

	Range of Lowest Five Frequencies	
	W/Rigid Drive	Drive W/Springs
Martin Marietta (Pilot Plant)	4.1 - 5.8 Hz	2.0 - 5.4 Hz
McDonnell Douglas (Pilot Plant)	3.1 - 6.2 Hz	1.8 - 5.6 Hz

TABLE 7.5

HELIOSTAT NATURAL FREQUENCIES-MODELS WITH RIGID DRIVES
HZ

Heliostat Elev. Angle	Arco		Boeing		Martin Marietta		McDonnell Douglas	
	0°	90°	0°	90°	0°	90°	0°	90°
Lowest Five Frequencies	2.29	2.28	2.48	2.47	4.56	4.45	3.59	3.43
	2.42	2.42	2.52	2.52	4.69	4.69	4.15	4.15
(Drives Assumed Rigid)	3.33	3.26	6.90	6.57	4.85	5.01	4.91	4.89
	3.96	3.96	6.94	6.60	5.62	5.57	5.67	5.30
	4.37	4.29	7.33	7.20	6.23	5.81	8.65	8.65

	MODE 1	MODE 2	MODE 3	MODE 4	MODE 5
MM	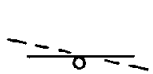 TORSION ABOUT PED.	 TORSION ABOUT T.T.	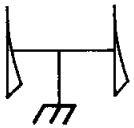 EXT. TRUSS SWAY	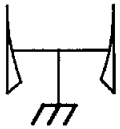 EXT. TRUSS SWAY	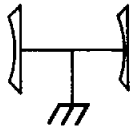 EXT. TRUSS SWAY
MDAC	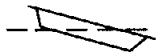 BENDING ABOUT PED.	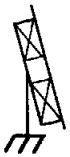 BENDING ABOUT ELEV. AXIS	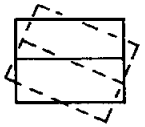 TORSION ABOUT PED.	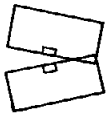 BENDING IN BOX	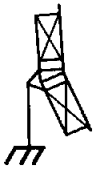 BENDING AT BOX
BOEING	 Z-BEAM SWAY	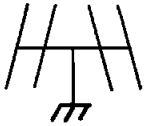 Z-BEAM SWAY	 ROTATION ABOUT T.T.	 Z-BEAM & T.T. SWAY	WARPING OF Z-BEAMS
ARCO	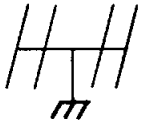 TRUSS SWAY	 ROTATION ABOUT T.T.	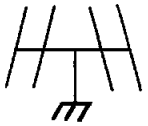 TRUSS SWAY	 ROTATION ABOUT T.T.	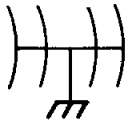 TRUSS BENDING

Figure 7.37. Mode Shapes With Flexible Drives

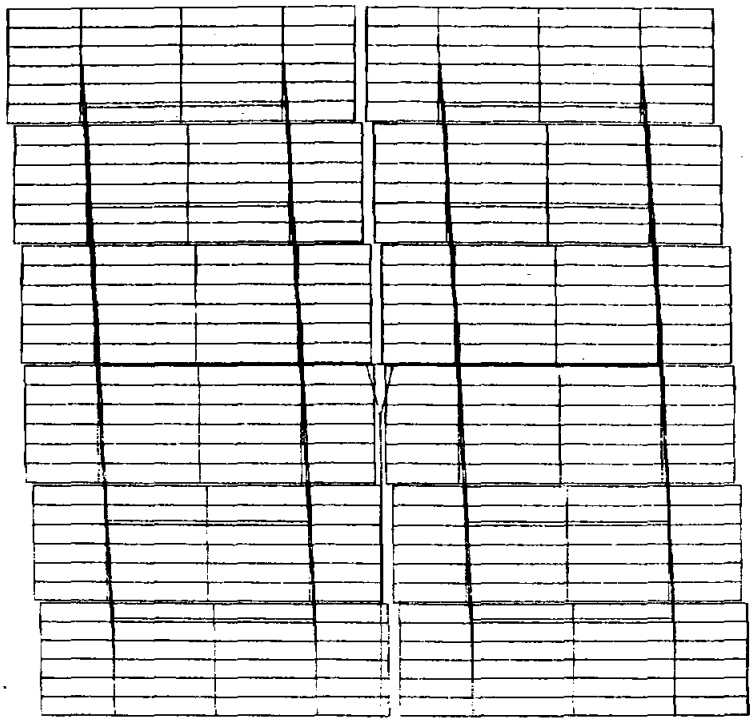

Figure 7.38. Arco With Flexible Drive - Mode 1

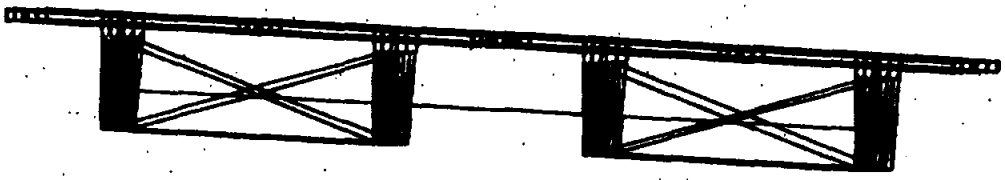

Figure 7.39. Arco With Flexible Drive - Mode 2

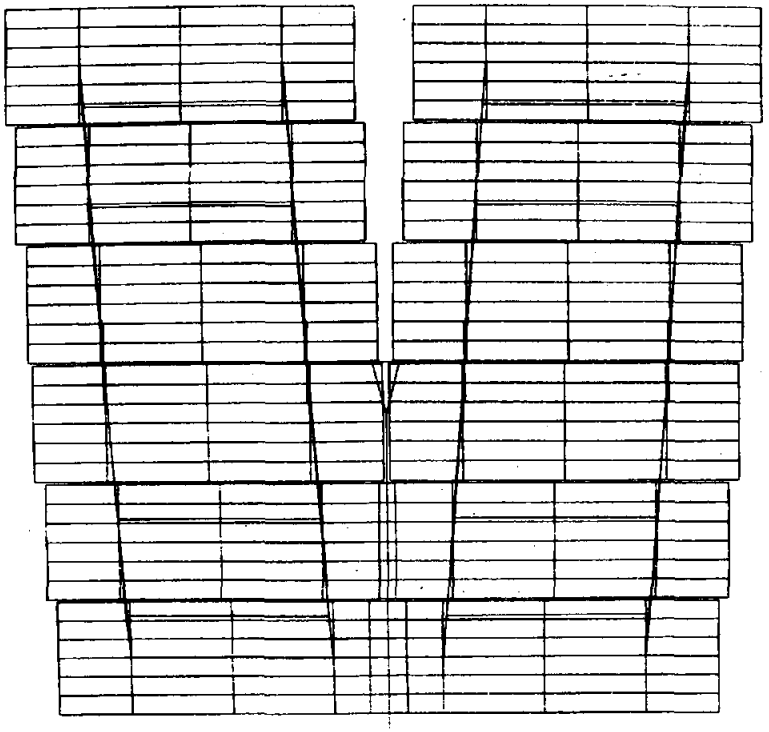

Figure 7.40. Arco With Flexible Drive - Mode 3

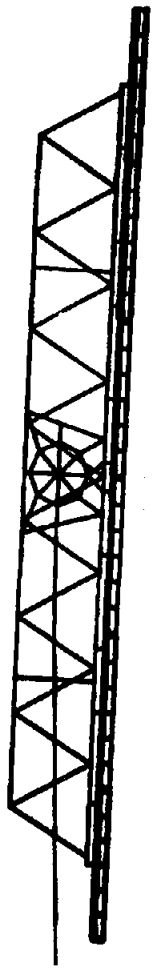

Figure 7.41. Arco With Flexible Drive - Mode 4

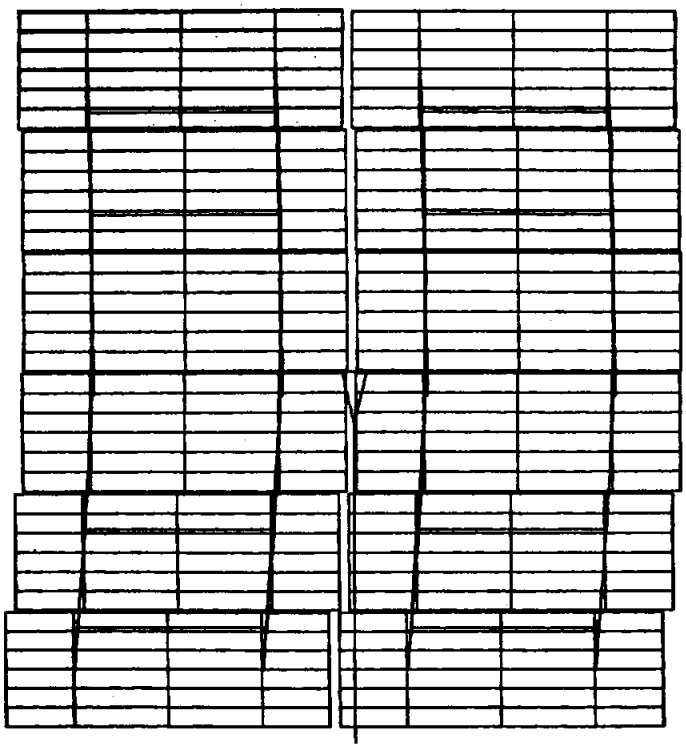

Figure 7.42. Arco With Flexible Drive - Mode 5

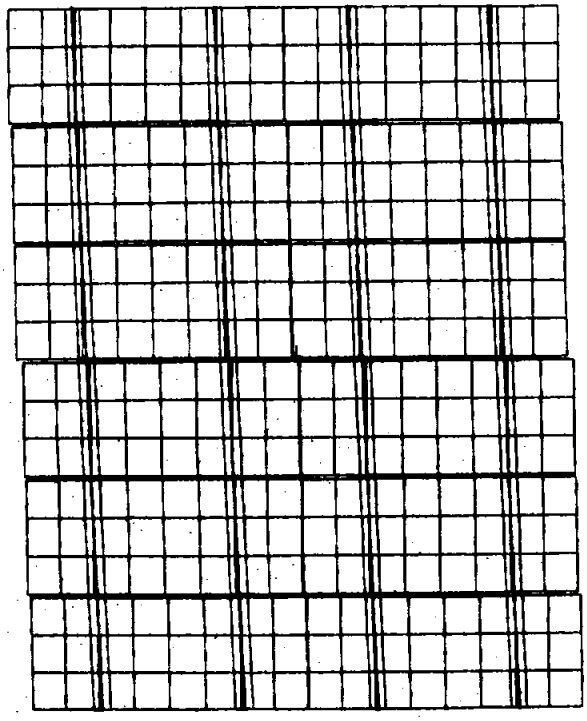

Figure 7.43. Boeing With Flexible Drive - Mode 1

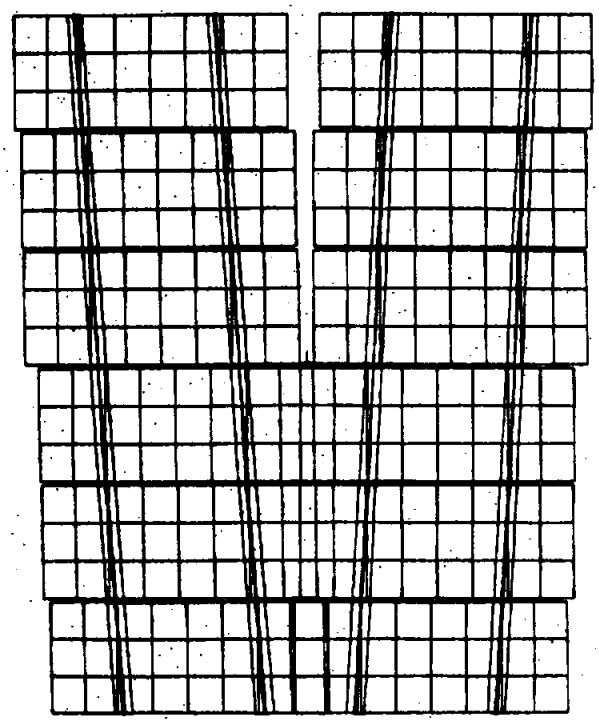

Figure 7.44. Boeing With Flexible Drive - Mode 2

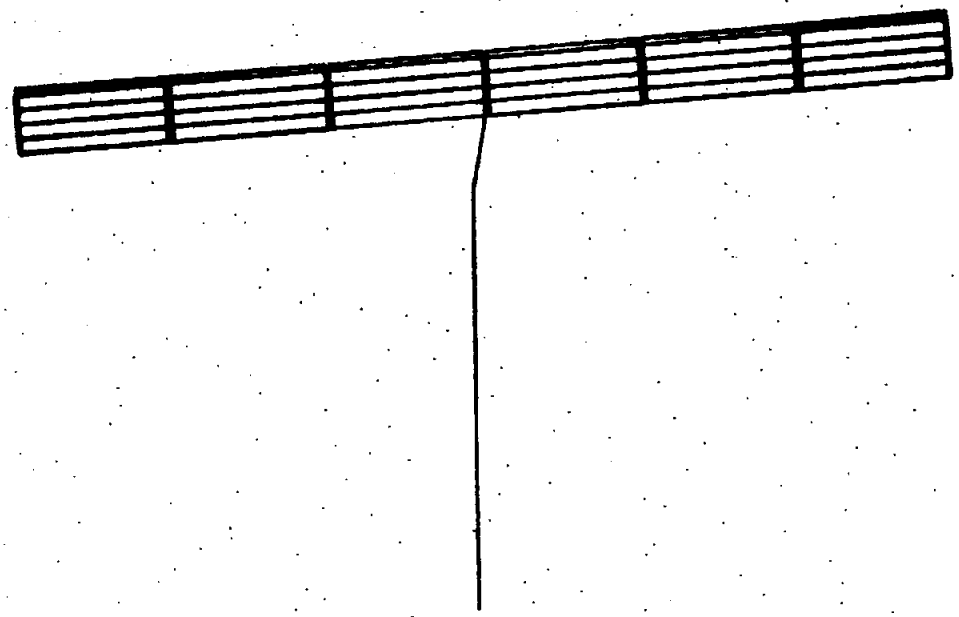

Figure 7.45. Boeing With Flexible Drive - Mode 3

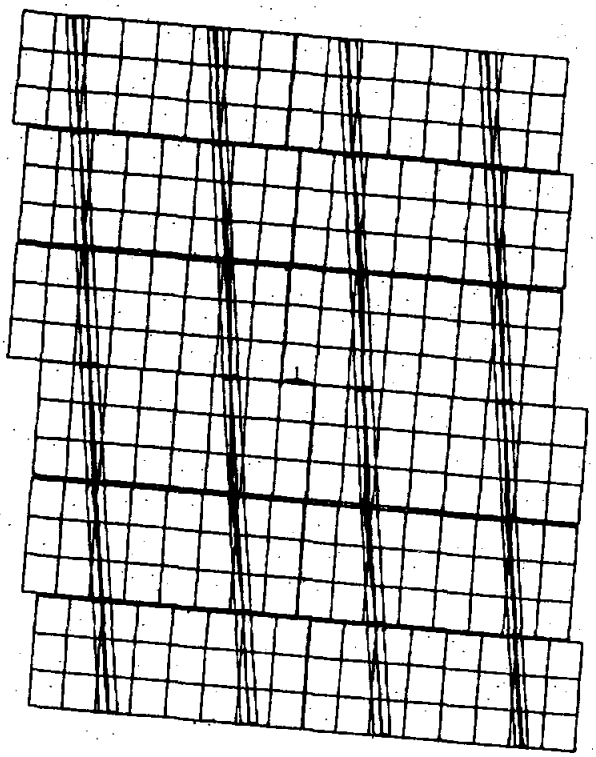

Figure 7.46. Boeing With Flexible Drive - Mode 4

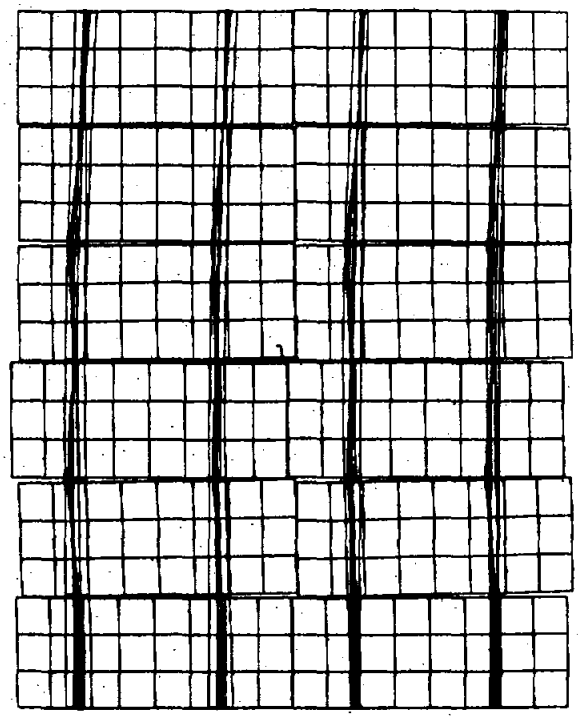

Figure 7.47. Boeing With Flexible Drive - Mode 5

Figure 7.48. McDonnell Douglas With Flexible Drive - Mode 1

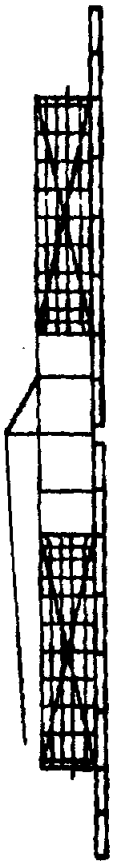

Figure 7.49. McDonnell Douglas With Flexible Drive - Mode 2

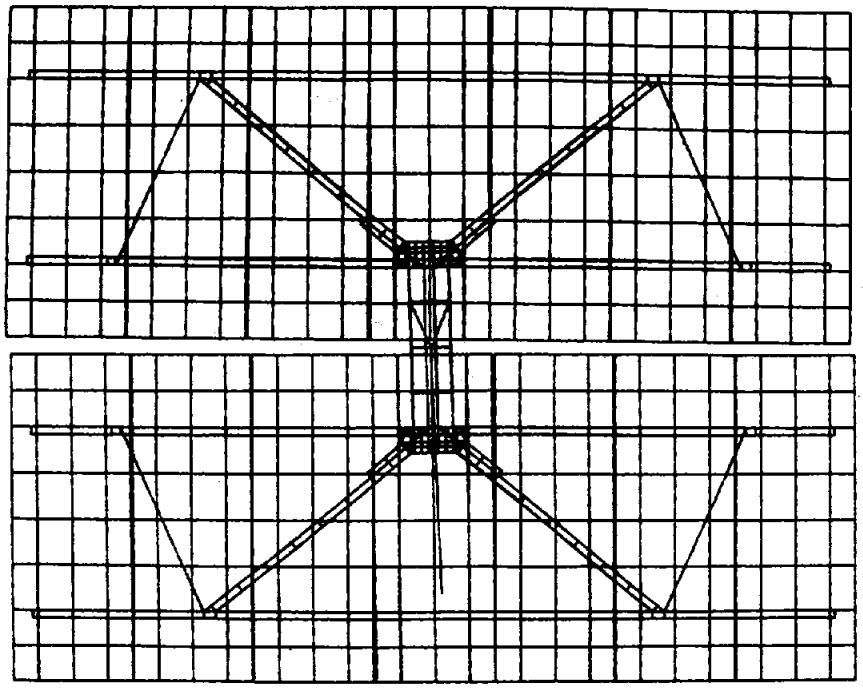

Figure 7.50. McDonnell Douglas With Flexible Drive - Mode 3

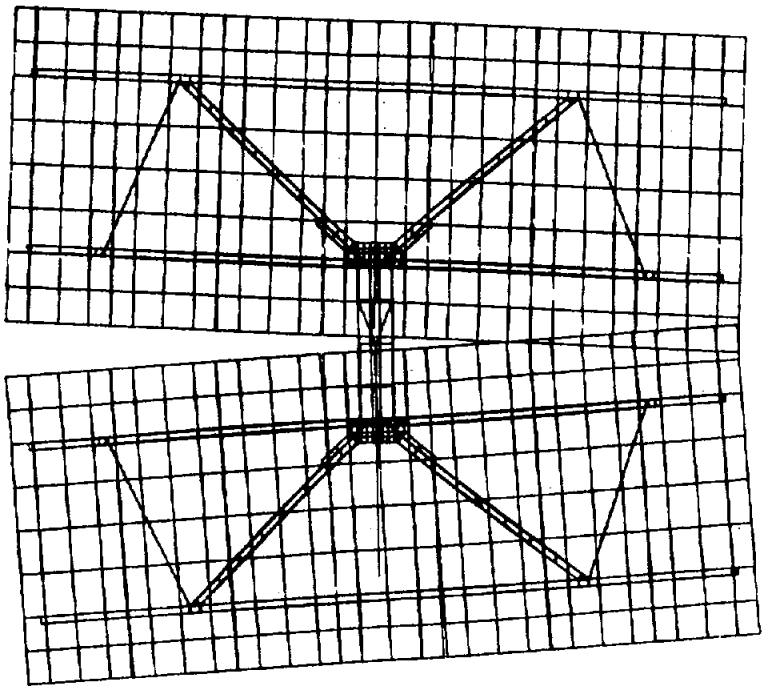

Figure 7.51. McDonnell Douglas With Flexible Drive - Mode 4

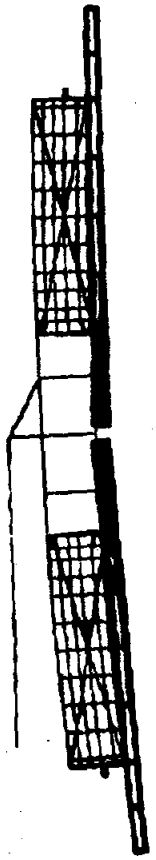

Figure 7.52. McDonnell Douglas With Flexible Drive - Mode 5

Figure 7.53. Martin Marietta With Flexible Drive - Mode 1

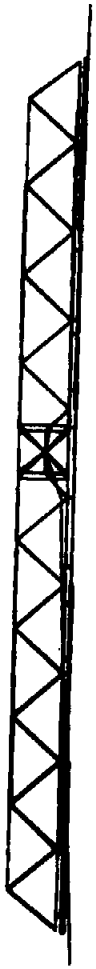

Figure 7.54. Martin Marietta With Flexible Drive - Mode 2

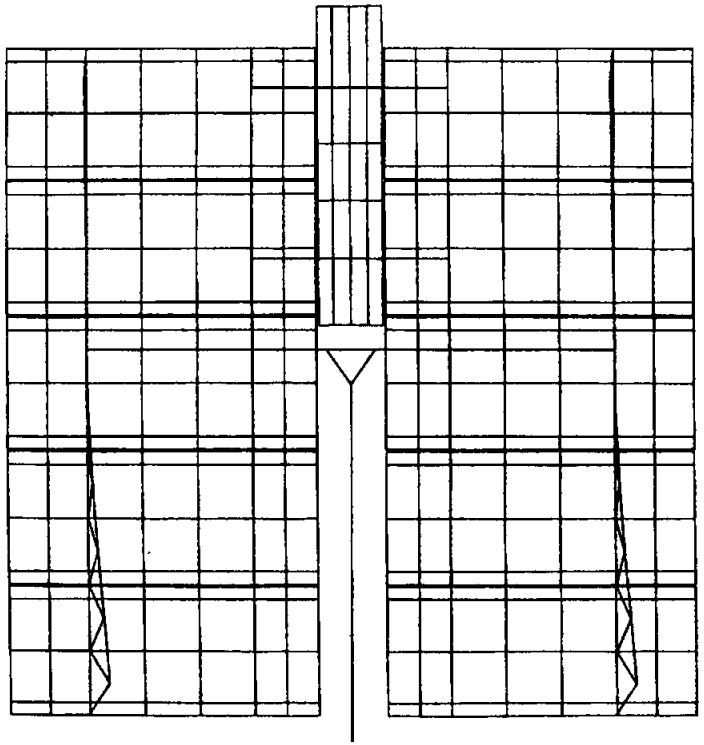

Figure 7.55. Martin Marietta With Flexible Drive - Mode 3

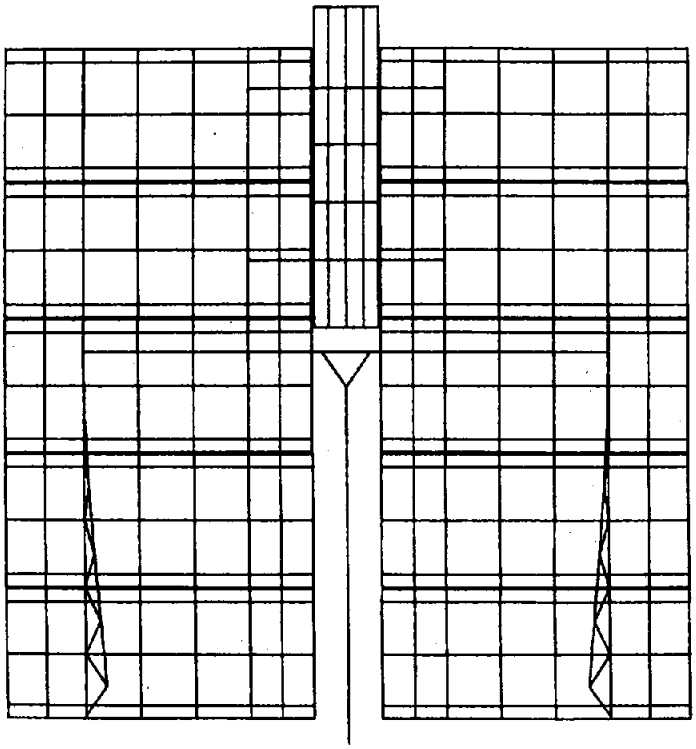

Figure 7.56. Martin Marietta With Flexible Drive - Mode 4

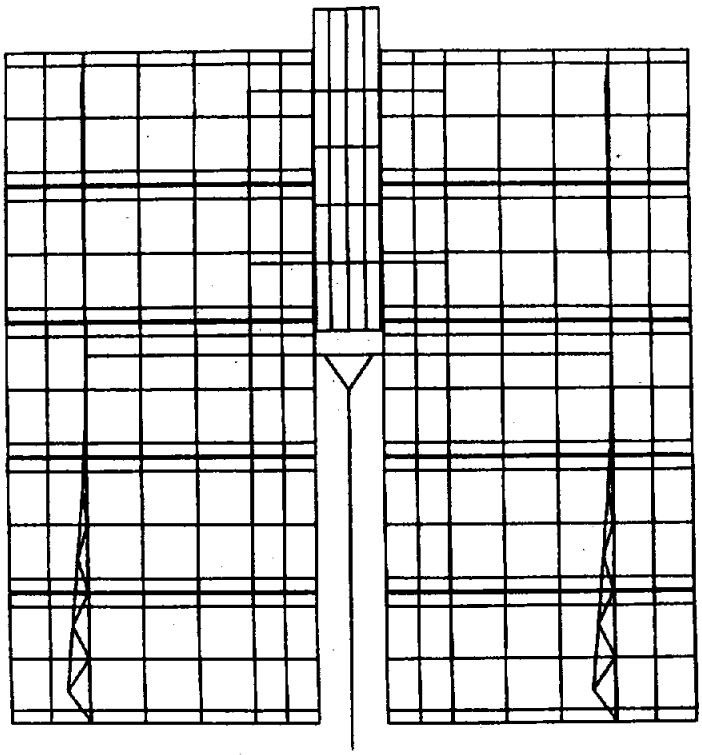

Figure 7.57. Martin Marietta With Flexible Drive - Mode 5

TABLE 7.6

HELIOSTAT NATURAL FREQUENCIES-MODELS WITH FLEXIBLE DRIVES
HZ

	Arco		Boeing		Martin Marietta		McDonnell Douglas	
	0°	90°	0°	90°	0°	90°	0°	90°
Elev. Stiff $\frac{\text{in-lb}}{\text{rad}}$	2.1x10		$1.8\text{x}10^7$	$2.2\text{x}10^7$	$5.4\text{x}10^7$		$4.9\text{x}10^7$	1.8x
Azim. Stiff $\frac{\text{in-lb}}{\text{rad}}$	$1.8\text{x}10^7$		$1.5\text{x}10^7$	$1.5\text{x}10^7$	$2.0\text{x}10^7$		$2.2\text{x}10^7$	2.2x
(Drives Modeled as Springs-CRTF Test Data)	2.28	1.59	2.39	1.75	2.15	1.62	2.03	1.65
	2.34	2.39	2.52	2.52	3.40	3.44	3.38	2.30
	2.41	2.45	2.67	2.81	4.55	4.69	3.58	4.13
	2.57	3.24	3.19	4.51	4.69	4.72	4.90	4.89
	3.56	3.70	6.94	6.49	4.81	5.67	8.53	8.64

8.0 Recommendations for Further Analysis

In the event these heliostats will be structurally refined, a review of the deflection results yielded by the current analysis would be very useful. Such a review could identify the percent deflection, individual components are contributing to the total. Consequently, each of the components could be redesigned to more cost effective.

Since it is anticipated that heliostat analyses will continue to be done at Sandia or in the private sector, a single coherent post-processing code to handle the data extraction, vector normal computation and averaging, coordinate convertion, optional gravity, out referencing, and various output options with regard to its further use (i.e. HELIOS, statistical information, reports) would be valuable.

The analysis using measured drive mechanism stiffnesses was limited. Reanalyzing all static load cases with this stiffness is not necessary since deflections due to the drive can be calculated separately and added to structural deflections. However, further work can be done to determine the effects of nonlinear behavior of the drives that may result in lower natural frequencies, possibly enough to slip near the range of concern.

APPENDIX A -- WINDLOAD PRESSURES

Windload pressures applied to mirror modules. The pressures were applied uniformely over the shown area and normal to the reflective surface.

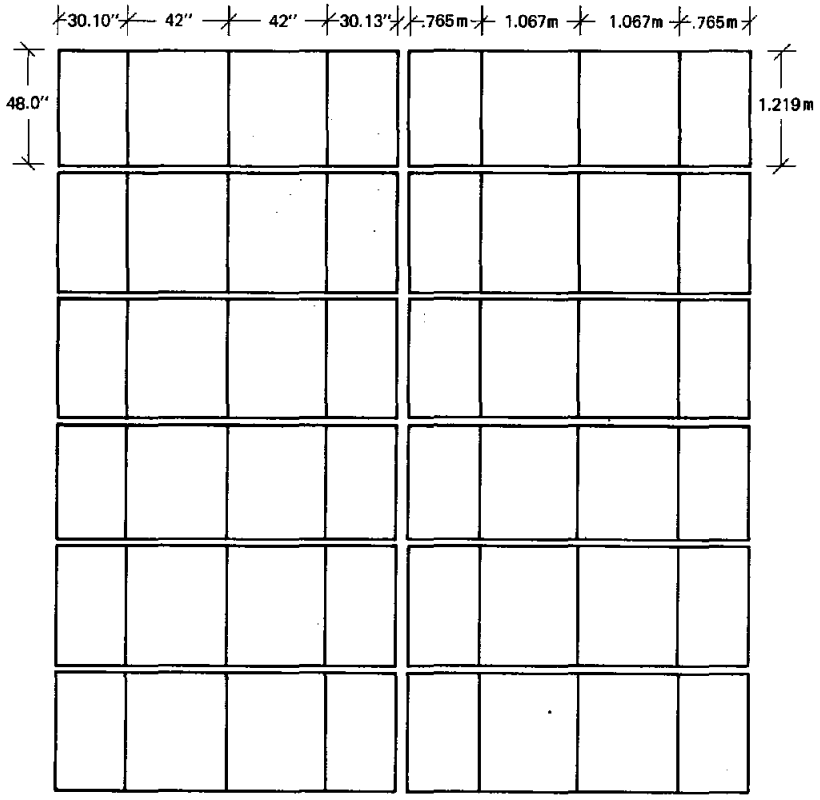

Figure A-1. Arco Heliostat Dimensions

28.73 (0.60)	45.97 (0.96)	63.20 (1.32)	69.43 (1.45)	69.43 (1.45)	63.20 (1.32)	45.97 (0.96)	28.73 (0.60)
52.67 (1.10)	69.91 (1.46)	87.62 (1.83)	93.37 (1.95)	93.37 (1.95)	87.62 (1.83)	69.91 (1.46)	52.67 (1.10)
64.64 (1.35)	82.32 (1.72)	99.59 (2.08)	105.34 (2.20)	105.34 (2.20)	99.59 (2.08)	82.32 (1.72)	64.64 (1.35)
64.64 (1.35)	82.32 (1.72)	99.59 (2.08)	105.34 (2.20)	105.34 (2.20)	99.59 (2.08)	82.32 (1.72)	64.64 (1.35)
52.67 (1.10)	69.91 (1.46)	87.62 (1.83)	93.37 (1.95)	93.37 (1.95)	87.62 (1.83)	69.91 (1.46)	52.67 (1.10)
28.73 (0.60)	45.97 (0.96)	63.20 (1.32)	69.43 (1.45)	69.43 (1.45)	63.20 (1.32)	45.97 (0.96)	28.73 (0.60)

NET FORCE = 464 N, (1044 lbs)
NET MOMENT = 0

Figure A-2. Arco Case 1 Wind Pressures, Pascals, (lbs/ft^2)

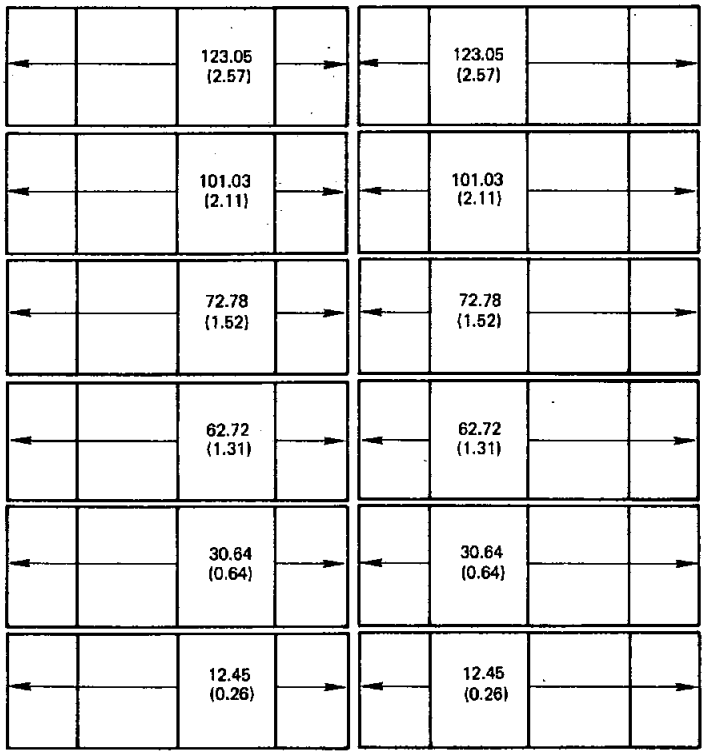

NET FORCE = 3594 N, (808 lbs)
NET MOMENT = 4214 N·m, (3108 ft-lbs)

Figure A-3. Arco Case 2 Wind Pressures, Pascals, (lbs/ft^2)

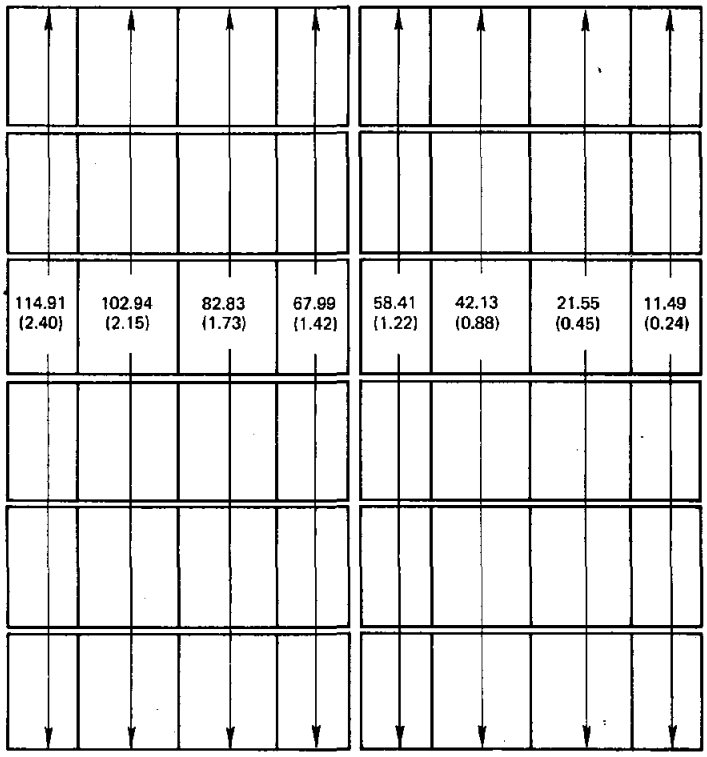

NET FORCE = 3354 N, (754 lbs)
NET MOMENT = 3861 N·m, (2848 ft-lbs)

Figure A-4. Arco Case 3 Wind Pressures, Pascals, (lbs/ft^2)

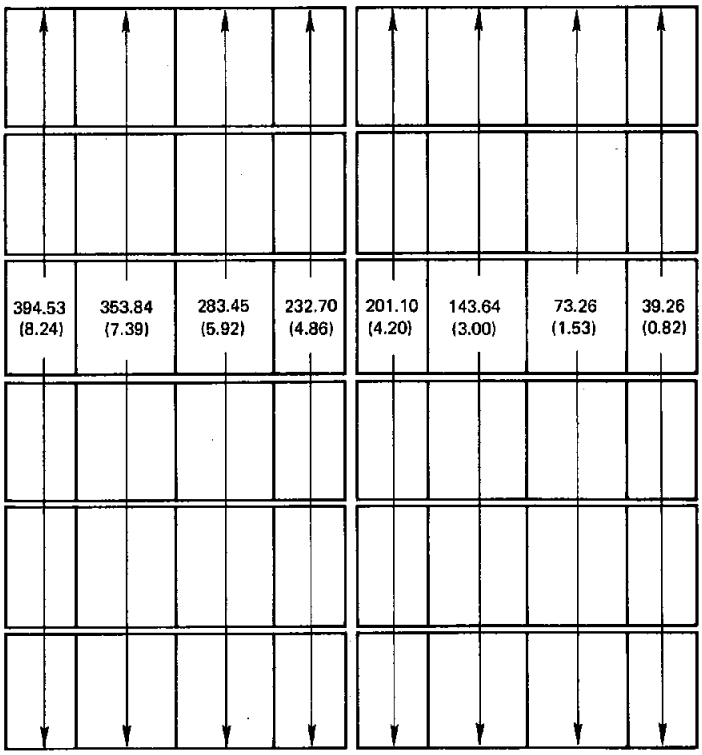

NET FORCE = 11499 N, (2585 lbs)
NET MOMENT = 13242 N·m, (9767 ft-lbs)

Figure A-5. Arco Case 4 Wind Pressures, Pascals, (lbs/ft^2)

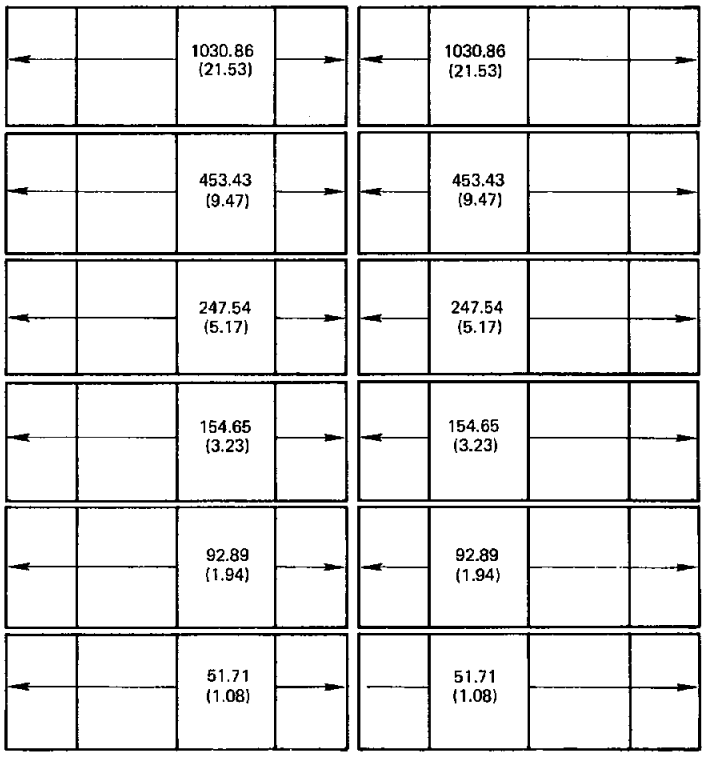

NET FORCE = 18,113 N, (4072)
NET MOMENT = 33,008 N·m, (24,346 ft-lbs)

Figure A-6. Arco Case 5 Wind Pressures, Pascals, (lbs/ft^2)

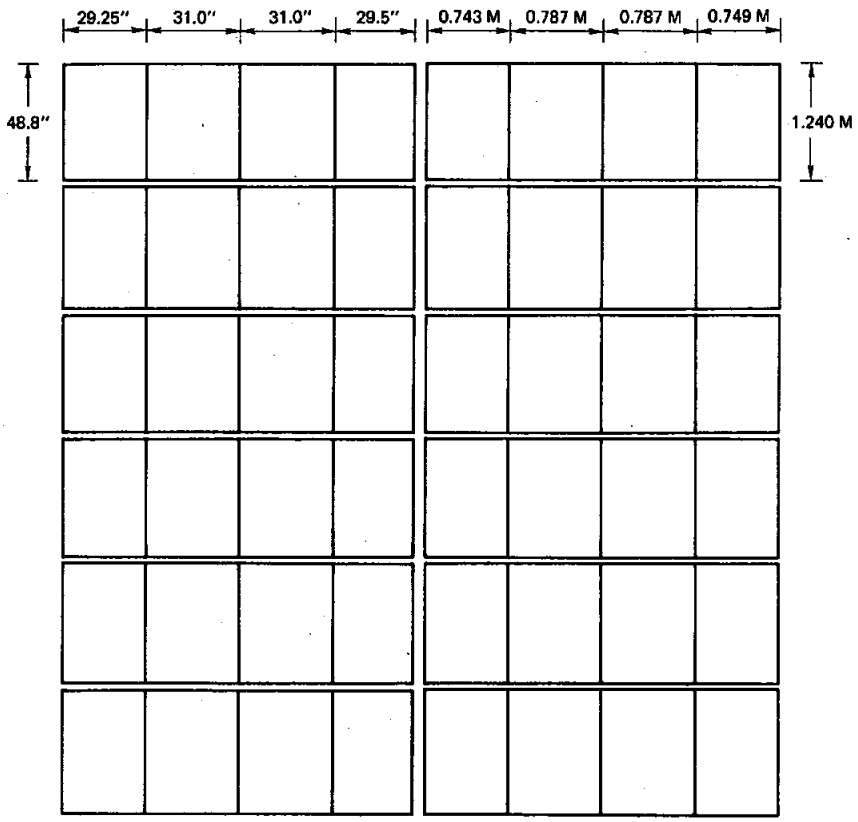

Figure A-7. Boeing Heliostat Dimensions

28.73 (0.60)	48.84 (1.02)	62.24 (1.30)	69.43 (1.45)	69.43 (1.45)	62.24 (1.30)	48.84 (1.02)	28.73 (0.60)
52.67 (1.10)	72.28 (1.52)	86.66 (1.81)	93.37 (1.95)	93.37 (1.95)	86.66 (1.81)	72.78 (1.52)	52.67 (1.10)
64.64 (1.35)	85.23 (1.78)	98.63 (2.06)	105.34 (2.20)	105.34 (2.20)	98.63 (2.06)	85.23 (1.78)	64.64 (1.35)
64.64 (1.35)	85.23 (1.78)	98.63 (2.06)	105.34 (2.20)	105.34 (2.20)	98.63 (2.06)	85.23 (1.78)	64.64 (1.35)
52.67 (1.10)	72.78 (1.52)	86.66 (1.81)	93.37 (1.95)	93.37 (1.95)	86.66 (1.81)	72.78 (1.52)	52.67 (1.10)
28.73 (0.60)	48.84 (1.02)	62.24 (1.30)	69.43 (1.45)	69.43 (1.45)	62.24 (1.30)	48.84 (1.02)	28.73 (0.60)

NET FORCE = 3870 N, (870 LBS)
NET MOMENT = 0

Figure A-8. Boeing Case 1 Wind Pressures, Pascals, (lbs/ft^2)

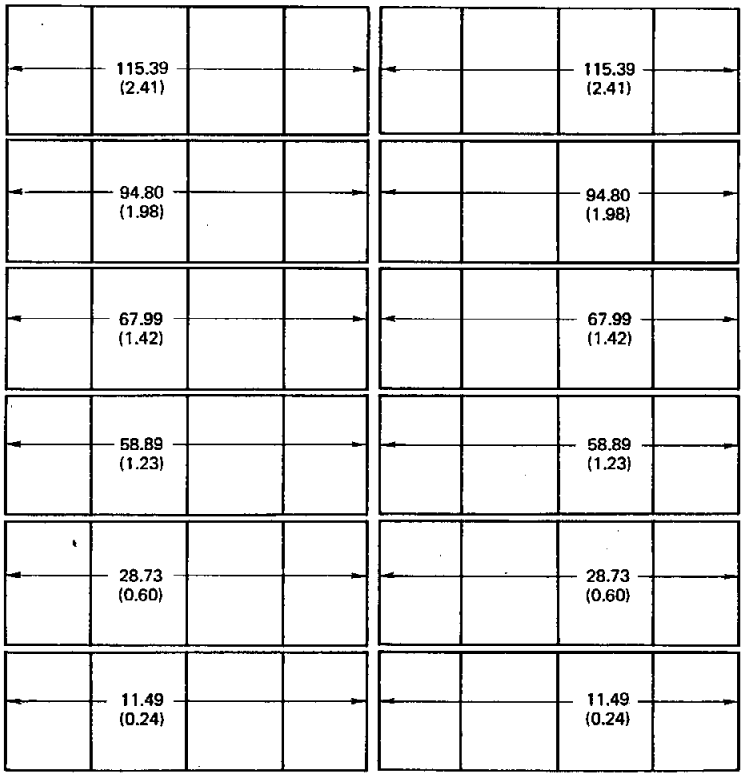

NET FORCE = 2807 N, (631 LBS)
NET MOMENT = 3289 N • M, (2426 FT-LBS)

Figure A-9. Boeing Case 2 Wind Pressures, Pascals, (lbs/ft^2)

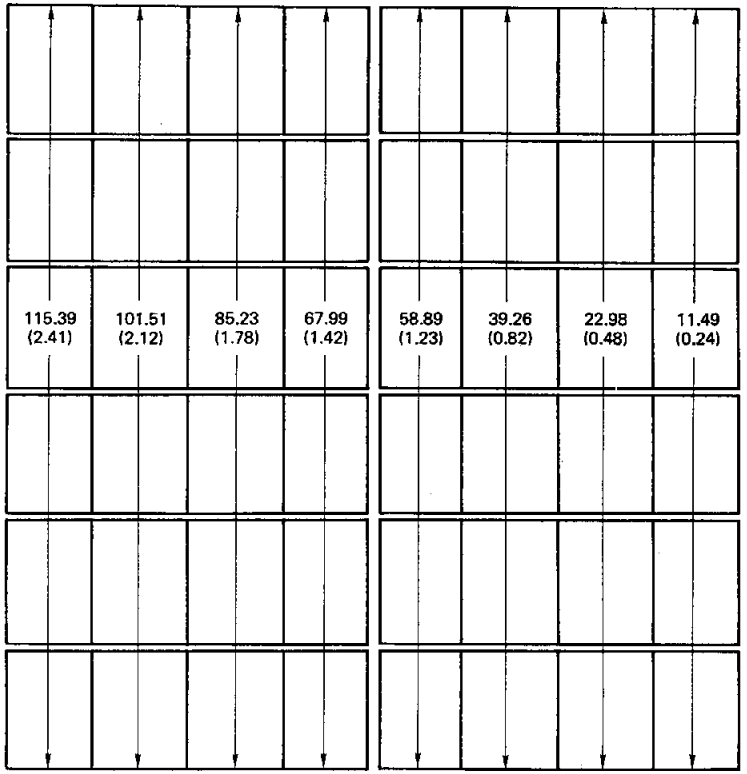

NET FORCE = 2802 N, (630 LBS)
NET MOMENT = 2689 N • M, (1983 FT-LBS)

Figure A-10. Boeing Case 3 Wind Pressures, Pascals, (lbs/ft^2)

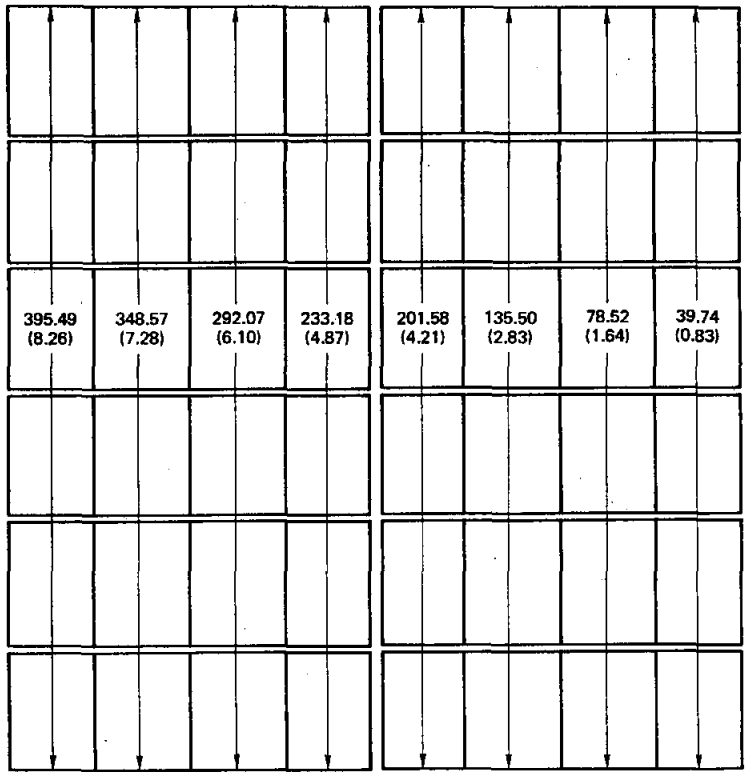

NET FORCE = 9608 N, (2160 LBS)
NET MOMENT = 9219 N • M, (6800 FT-LBS)

Figure A-11. Boeing Case 4 Wind Pressures, Pascals, (lbs/ft^2)

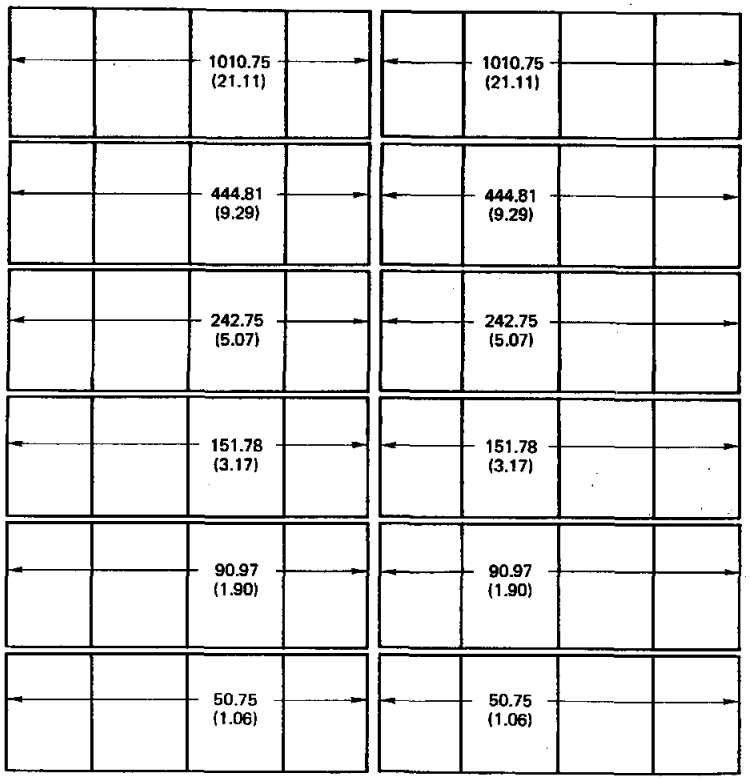

NET FORCE = 14,795 N, (3326 LBS)
NET MOMENT = 26,966 N • M, (19889 FT-LBS)

Figure A-12. Boeing Case 5 Wind Pressures, Pascals, (lbs/ft^2)

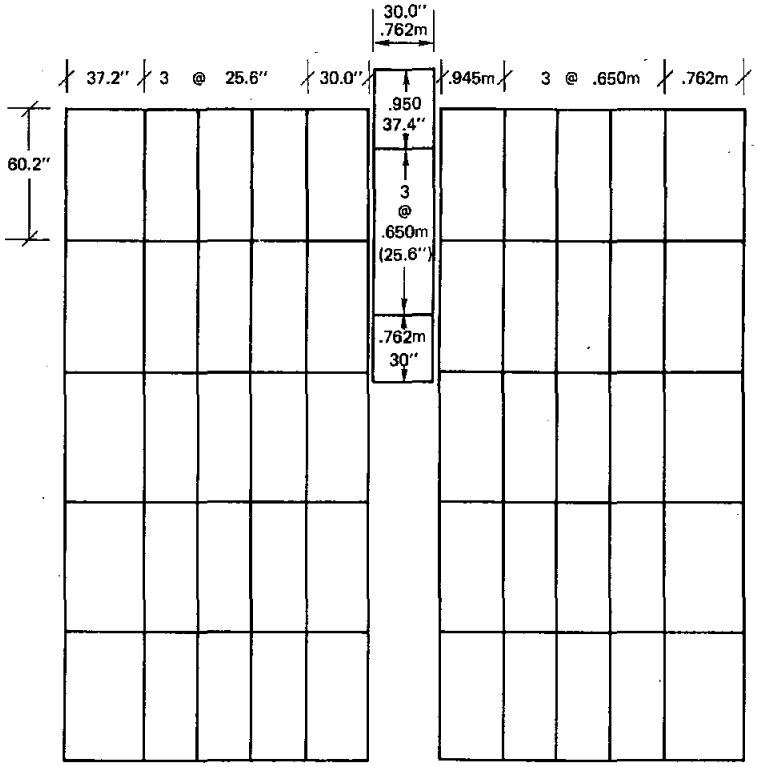

Figure A-13. Martin Marietta Heliostat Dimensions

40.22 (0.84)	56.50 (1.18)	65.12 (1.36)	84.27 (1.76)	93.85 (1.96)	98.06 (1.86)	93.85 (1.96)	84.27 (1.76)	65.12 (1.36)	56.50 (1.18)	40.22 (0.84)
					94.80 (1.98)					
					106.8 (2.23)					
69.91 (1.46)	86.66 (1.81)	95.76 (2.00)	106.29 (2.22)	126.40 (2.64)	124.5 (2.60)	126.40 (2.64)	106.40 (2.22)	95.76 (2.00)	86.66 (1.81)	69.91 (1.46)
					130.7 (2.73)					
79.96 (1.67)	96.72 (2.02)	105.35 (2.21)	116.35 (2.43)	124.49 (2.60)		124.49 (2.60)	116.35 (2.43)	105.35 (2.21)	96.72 (2.02)	79.96 (1.67)
69.91 (1.46)	86.66 (1.81)	95.76 (2.00)	106.29 (2.22)	126.40 (2.64)		126.40	106.40 (2.22)	95.76 (2.00)	86.66 (1.81)	69.91 (1.46)
40.22 (0.84)	56.50 (1.18)	65.12 (1.36)	84.27 (1.76)	93.85 (1.96)		93.85 (1.96)	84.27 (1.76)	65.12 (1.36)	56.50 (1.18)	40.22 (0.84)

NET FORCE = 5088 N, (1144 lbs)
NET MOMENT = 705 N·m, (520 ft-lbs)

Figure A-14. Martin Marietta Case 1 Wind Pressures, Pascals, (lbs/ft^2)

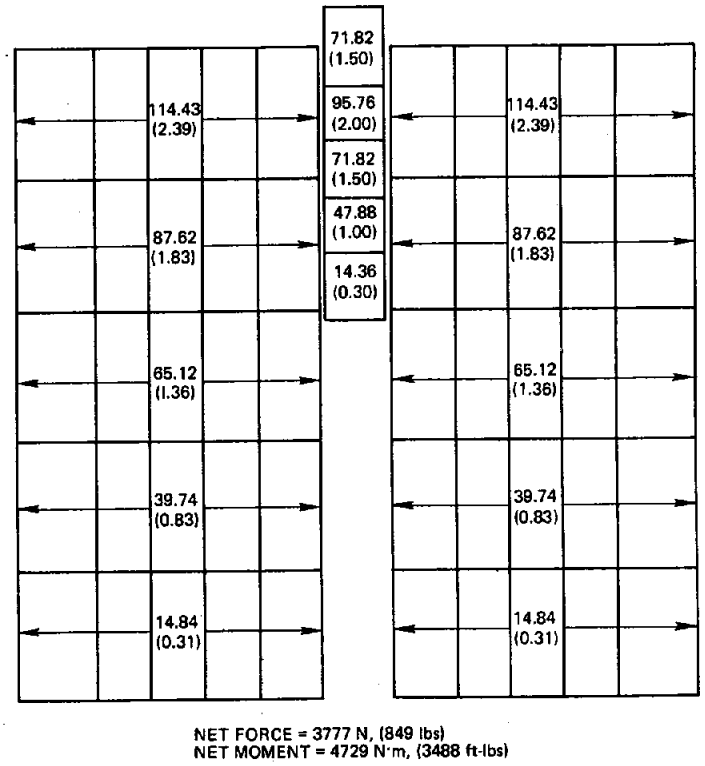

Figure A-15. Martin Marietta Case 2 Wind Pressures, Pascals, (lbs/ft^2)

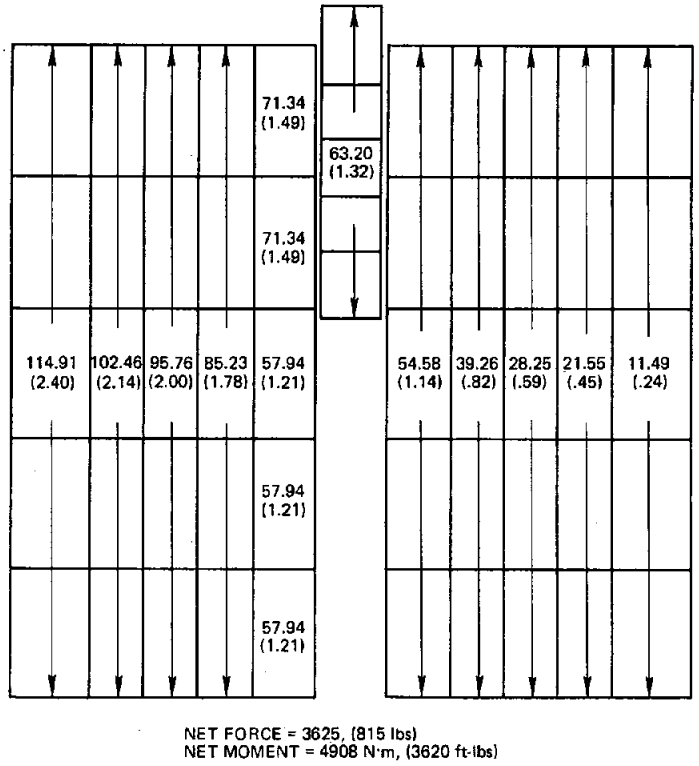

Figure A-16. Martin Marietta Case 3 Wind Pressures, Pascals, (lbs/ft^2)

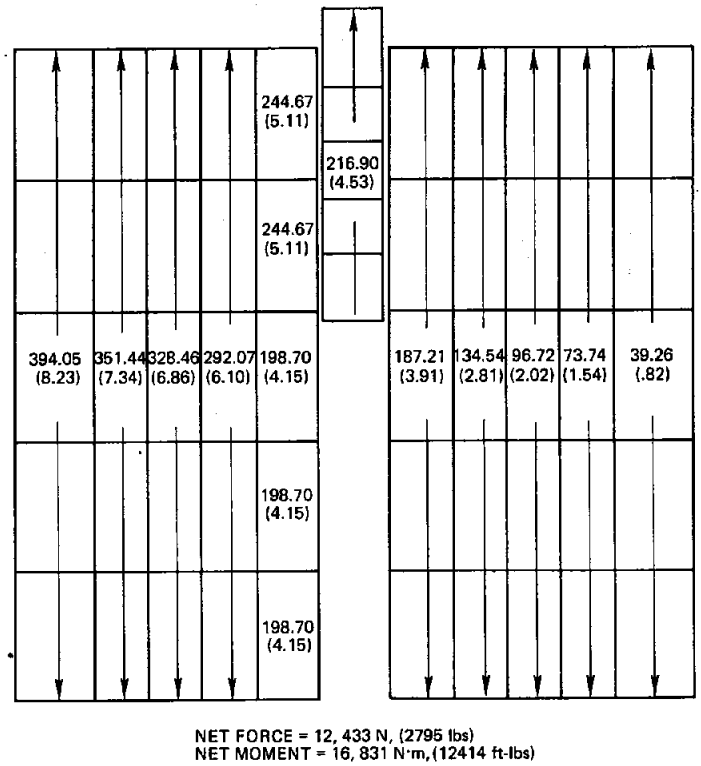

NET FORCE = 12, 433 N, (2795 lbs)
NET MOMENT = 16, 831 N·m, (12414 ft-lbs)

Figure A-17. Martin Marietta Case 4 Wind Pressures, Pascals, (lbs/ft^2)

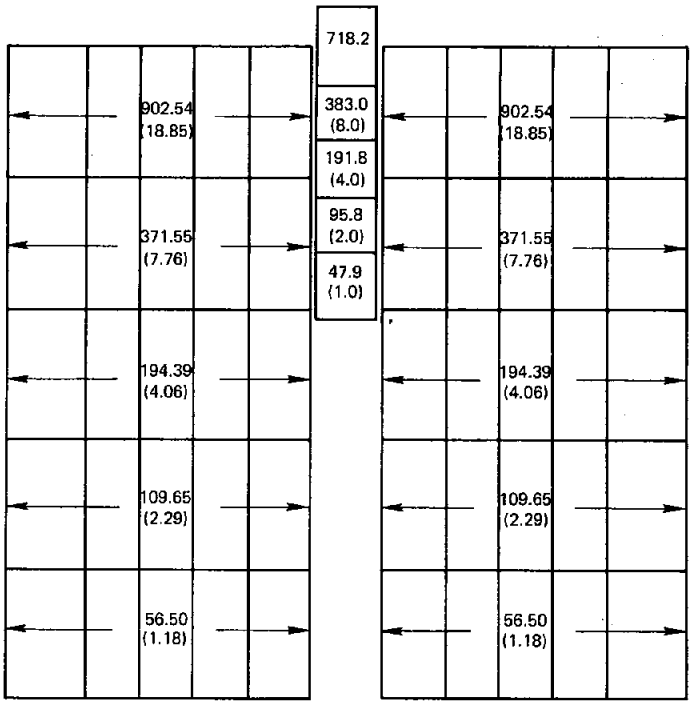

NET FORCE = 18, 309 N, (4116 lbs)
NET MOMENT = 36, 338 N·m, (26, 802 ft-lbs)

Figure A-18. Martin Marietta Case 5 Wind Pressures, Pascals, (lbs/ft^2)

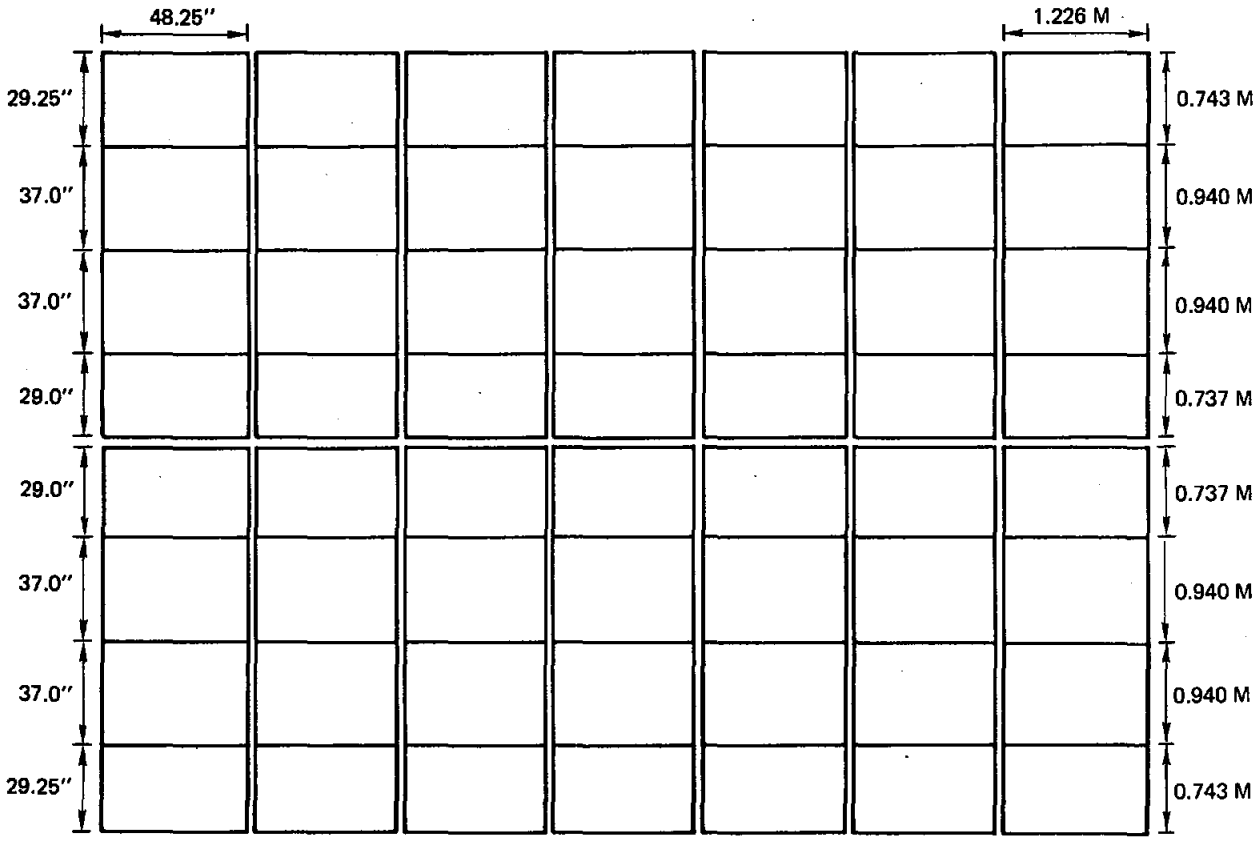

Figure A-19. McDonnell Douglas Heliostat Dimensions

33.52 (0.70)	61.29 (1.28)	75.17 (1.57)	75.17 (1.57)	75.17 (1.57)	61.29 (1.28)	33.52 (0.70)
54.10 (1.13)	82.35 (1.72)	96.72 (2.02)	96.72 (2.02)	96.72 (2.02)	82.35 (1.72)	54.10 (1.13)
73.26 (1.53)	101.98 (2.13)	114.91 (2.40)	114.91 (2.40)	114.91 (2.40)	101.98 (2.13)	73.26 (1.53)
80.44 (1.68)	108.21 (2.26)	122.09 (2.55)	122.09 (2.55)	122.09 (2.55)	108.21 (2.26)	80.44 (1.68)
80.44 (1.68)	108.21 (2.26)	122.09 (2.55)	122.09 (2.55)	122.09 (2.55)	108.21 (2.26)	80.44 (1.68)
73.26 (1.53)	101.98 (2.13)	114.91 (2.40)	114.91 (2.40)	114.91 (2.40)	101.98 (2.13)	73.26 (1.53)
54.10 (1.13)	82.35 (1.72)	96.72 (2.02)	96.72 (2.02)	96.72 (2.02)	82.35 (1.72)	54.10 (1.13)
33.52 (0.70)	61.29 (1.28)	75.17 (1.57)	75.17 (1.57)	75.17 (1.57)	61.29 (1.28)	33.52 (0.70)

NET FORCE = 4964 N, (1164 LBS)
NET MOMENT = 0

Figure A-20. McDonnell Douglas Case 1 Wind Pressures, Pascals, (lbs/ft^2)

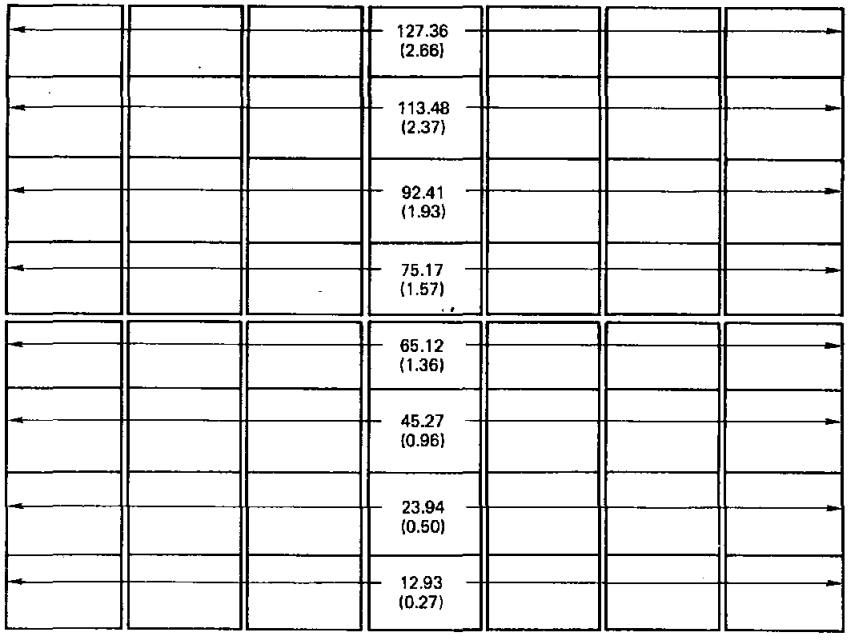

NET FORCE = 3977 N, (894 LBS)
NET MOMENT = 4196 N • M, (3095 FT-LBS)

Figure A-21. McDonnell Douglas Case 2 Wind Pressures, Pascals, (lbs/ft^2)

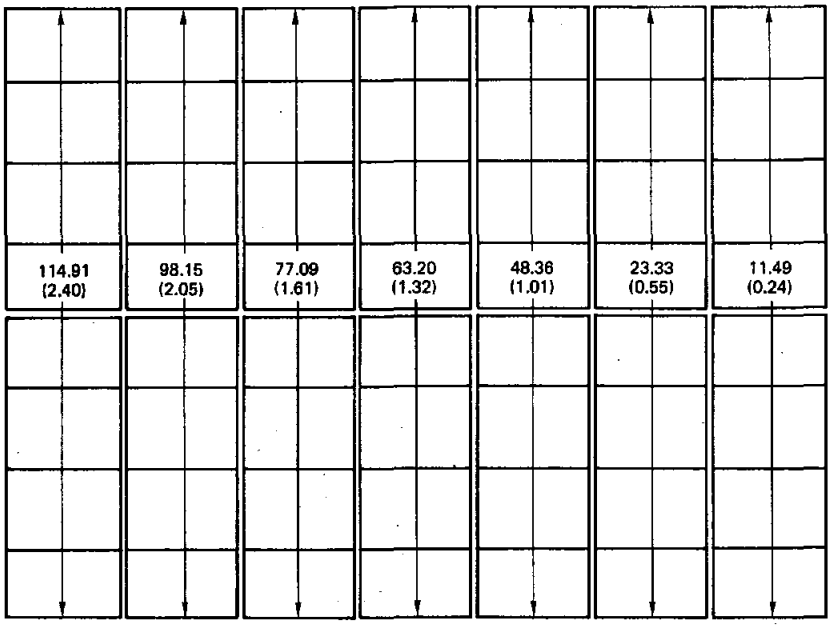

NET FORCE = 3599 N, (809 LBS)
NET MOMENT = 4808 N • M, (3546 FT-LBS)

Figure A-22. McDonnell Douglas Case 3 Wind Pressures, Pascals, (lbs/ft^2)

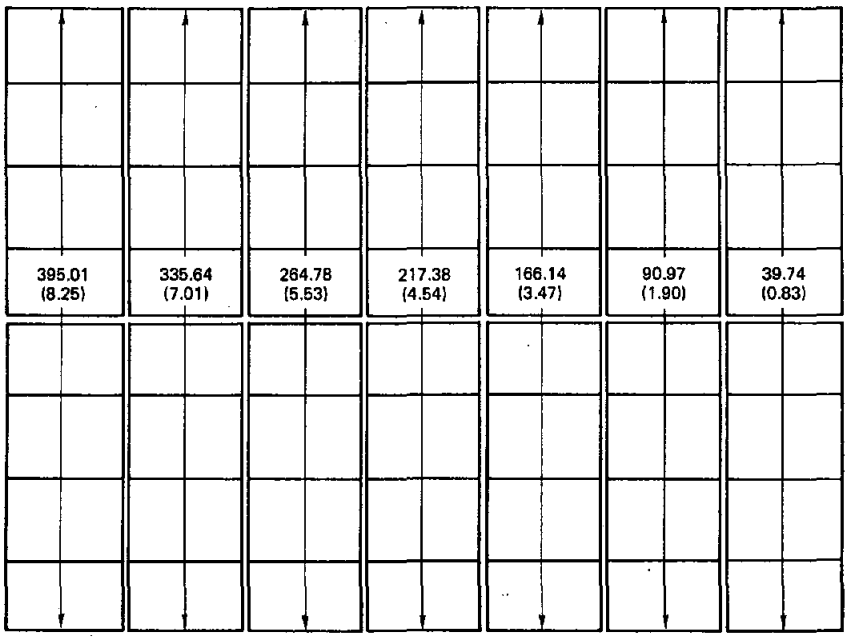

NET FORCE = 12339 N, (2774 LBS)
NET MOMENT = 16487 N • M, (12160 FT-LBS)

Figure A-23. McDonnell Douglas Case 4 Wind Pressures, Pascals, (lbs/ft^2)

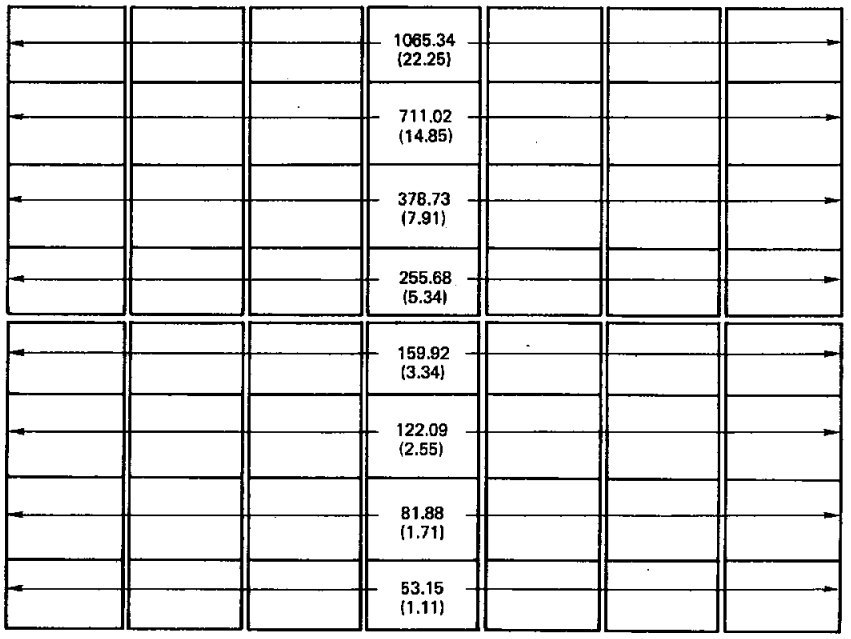

NET FORCE = 20,044 N, (4506 LBS)
NET MOMENT = 32,806 N • M, (24,197 FT-LBS)

Figure A-24. McDonnell Douglas Case 5A Wind Pressures, Pascals, (lbs/ft^2)

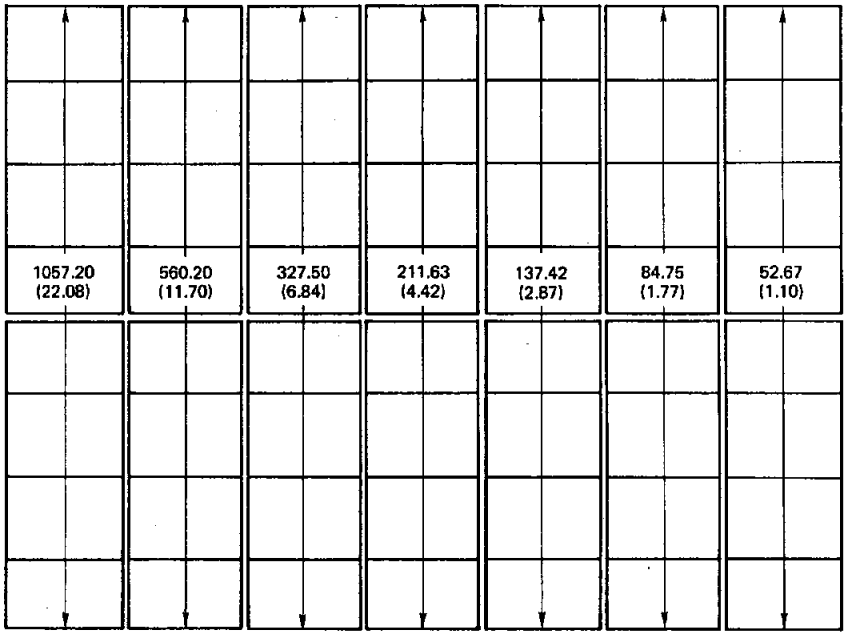

NET FORCE = 19,879 N, (4469 LBS)
NET MOMENT = 41408 N • M, (30541 FT-LBS)

Figure A-25. McDonnell Douglas Case 5B Wind Pressures, Pascals, (lbs/ft^2)

APPENDIX B -- INDIVIDUAL MIRROR MODULE DEFLECTIONS

The following pages list the vector normal to each mirror module from the gravity and operational wind load analyses. Each vector is listed by its i, j and k components in both local and global coordinates.

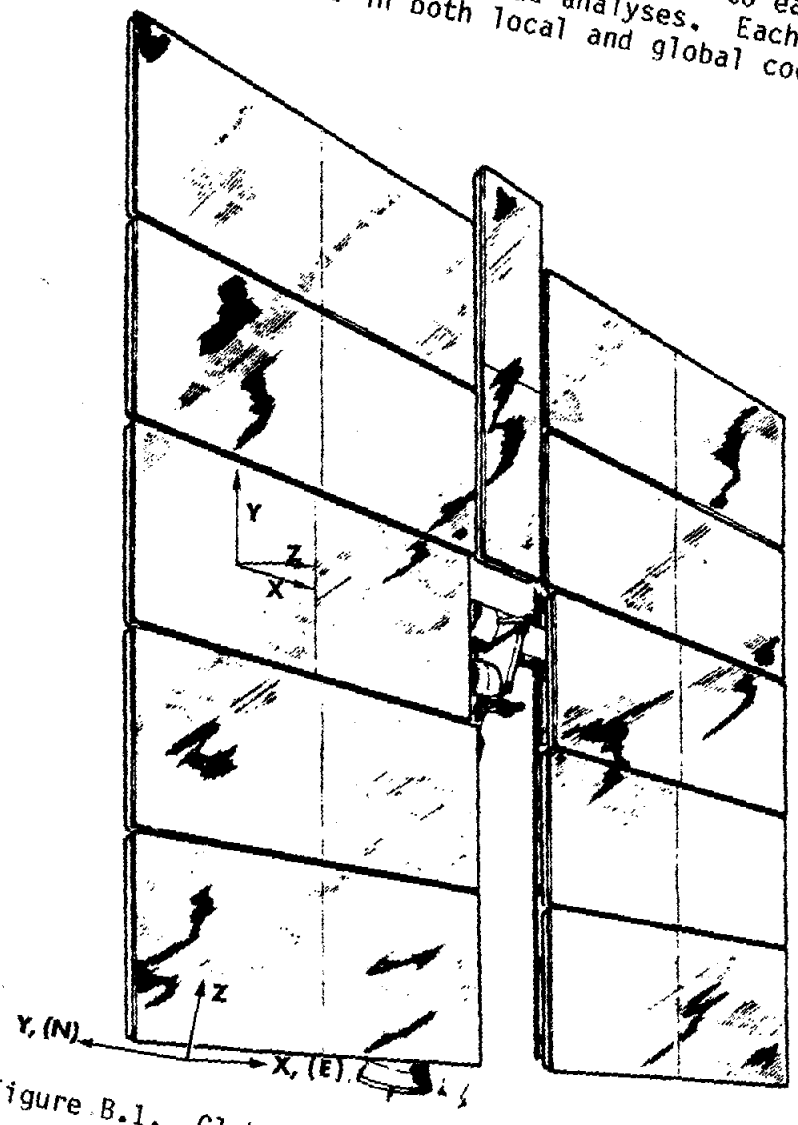

Figure B.1. Global Local Coordinate Convention

In local coordinates, the i component is also the rotation of the module about the y axis, as is the j component the rotation about the x axis, measured in radians. The title for each analysis case shows the elevation angle. Also noted in the title is miscellaneous information pertinent to that analysis. "W/g" and "G ONLY" refer to cases where gravity loading was applied. The McDonnell Douglas and Boeing results had to be averaged over the four possible planes passing through a permutation of the four support points, thre at a time. The average values are those shown and a note of this is made in the caption of those cases. At the end of each case are printed the average rotations and the RMS values for the rotations in local coordinates.

VECTORS NORMAL TO MIRROR SURFACE

	IN LOCAL COORDINATES			IN GLOBAL COORDINATES		
NRT , VERT, W/ G	, ELEVATION ANGLE=	0.	DEGREES FROM VERTICAL			
FACET 1	.00040784	-.00095633	.99999946	.00040784	-.99999954	-.00103966
FACET 2	.00026495	-.00096241	.99999950	.00026495	-.99999954	-.00099821
FACET 3	.00009129	-.00080613	.99999967	.00009129	-.99999968	-.00081128
FACET 4	-.00008995	-.00080628	.99999967	-.00008995	-.99999967	-.00081128
FACET 5	-.00026336	-.00096285	.99999950	-.00026336	-.99999954	-.00099821
FACET 6	-.00040625	-.00095700	.99999946	-.00040625	-.99999954	-.00103966
FACET 7	-.00040784	-.00095633	.99999946	-.00040784	-.99999954	-.00103966
FACET 8	-.00026495	-.00096241	.99999950	-.00026495	-.99999954	-.00099821
FACET 9	-.00009129	-.00080613	.99999967	-.00009129	-.99999968	-.00081128
FACET10	.00008995	-.00080628	.99999967	.00008995	-.99999967	-.00081128
FACET11	.00026336	-.00096285	.99999950	.00026336	-.99999954	-.00099822
FACET12	.00040625	-.00095700	.99999946	.00040625	-.99999954	-.00103966
AVERAGES :	.00000000	-.00090850				
RMS :	.00026500	.00007238				
N = 12						

NRT AT 15D, G ONLY	, ELEVATION ANGLE=	15.	DEGREES FROM VERTICAL			
FACET 1	.00018694	-.00082409	.99999964	.00018694	-.96613679	.25800272
FACET 2	.00004819	-.00079779	.99999968	.00004819	-.96613200	.25804696
FACET 3	-.00011958	-.00071645	.99999974	-.00011958	-.96611101	.25811736
FACET 4	-.00029384	-.00083483	.99999961	-.00029384	-.96614156	.25796407
FACET 5	-.00045985	-.00105437	.99999934	-.00045985	-.96619818	.25770778
FACET 6	-.00059610	-.00101663	.99999931	-.00059610	-.96618845	.25768052
FACET 7	-.00018694	-.00082409	.99999964	-.00018694	-.96613879	.25800272
FACET 8	-.00004819	-.00079779	.99999968	-.00004819	-.96613200	.25804696
FACET 9	.00011958	-.00071646	.99999974	.00011958	-.96611101	.25811736
FACET10	.00029384	-.00083483	.99999961	.00029384	-.96614156	.25796407
FACET11	.00045985	-.00105438	.99999934	.00045985	-.96619818	.25770778
FACET12	.00059610	-.00101663	.99999931	.00059610	-.96618845	.25768052
AVERAGES :	.00000000	-.00087403				
RMS :	.00034271	.00012078				
N = 12						

NRT AT 20D, W/ G	, ELEVATION ANGLE=	20.	DEGREES FROM VERTICAL			
FACET 1	.00011113	-.00077147	.99999970	.00011113	-.93995620	.34128762
FACET 2	-.00002485	-.00073458	.99999973	-.00002485	-.93994361	.34132938
FACET 3	-.00018897	-.00067918	.99999975	-.00018897	-.93992470	.34135760
FACET 4	-.00035916	-.00083610	.99999959	-.00035916	-.93997825	.34116491
FACET 5	-.00052104	-.00107469	.99999929	-.00052104	-.94005964	.34089760
FACET 6	-.00065367	-.00102658	.99999926	-.00065367	-.94004324	.34087625
FACET 7	-.00011112	-.00077147	.99999970	-.00011112	-.93995620	.34128762
FACET 8	.00002485	-.00073458	.99999973	.00002485	-.93994361	.34132938
FACET 9	.00018897	-.00067918	.99999975	.00018897	-.93992470	.34135759
FACET10	.00035916	-.00083610	.99999959	.00035916	-.93997826	.34116490
FACET11	.00052104	-.00107469	.99999929	.00052104	-.94005964	.34089759
FACET12	.00065367	-.00102659	.99999926	.00065367	-.94004324	.34087625
AVERAGES :	.00000000	-.00085377				
RMS :	.00038220	.00014745				
N = 12						

NRT AT 30D, G ONLY	, ELEVATION ANGLE=	30.	DEGREES FROM VERTICAL			
FACET 1	-.00004498	-.00063988	.99999979	-.00004498	-.86634517	.49944438
FACET 2	-.00017070	-.00058304	.99999982	-.00017070	-.86631678	.49947379
FACET 3	-.00032184	-.00058150	.99999978	-.00032184	-.86631601	.49942431
FACET 4	-.00047800	-.00060998	.99999956	-.00047800	-.86643011	.49918527
FACET 5	-.00062602	-.00107820	.99999922	-.00062602	-.86656400	.49891989
FACET 6	-.00074688	-.00101109	.99999921	-.00074688	-.86653051	.49891098
FACET 7	.00004498	-.00063988	.99999979	.00004498	-.86634517	.49944437
FACET 8	.00017070	-.00058304	.99999982	.00017070	-.86631678	.49947378
FACET 9	.00032184	-.00058150	.99999978	.00032184	-.86631601	.49942431
FACET10	.00047800	-.00060999	.99999956	.00047800	-.86643011	.49918527
FACET11	.00062602	-.00107820	.99999922	.00062602	-.86656400	.49891988
FACET12	.00074688	-.00101109	.99999921	.00074688	-.86653051	.49891098
AVERAGES :	.00000000	-.00078395				
RMS :	.00046779	.00020040				
N = 12						

NRT AT 45D, G ONLY , ELEVATION ANGLE= 45. DEGREES FROM VERTICAL

FACET 1	-.00027418	-.00041345	.99999988	-.00027418	-.70739907	.70675590
FACET 2	-.00037871	-.00032967	.99999987	-.00037871	-.70733985	.70675165
FACET 3	-.00050343	-.00040822	.99999979	-.00050343	-.70739538	.70664833
FACET 4	-.00063138	-.00073239	.99999953	-.00063138	-.70762447	.70642270
FACET 5	-.00075182	-.00103213	.99999918	-.00075182	-.70783623	.70620329
FACET 6	-.00084943	-.00093991	.99999920	-.00084943	-.70777108	.70621040
FACET 7	.00027418	-.00041345	.99999988	.00027418	-.70739907	.70675590
FACET 8	.00037872	-.00032967	.99999987	.00037872	-.70733985	.70675165
FACET 9	.00050343	-.00040823	.99999979	.00050343	-.70739538	.70664832
FACET10	.00063138	-.00073240	.99999953	.00063138	-.70762447	.70642269
FACET11	.00075182	-.00103213	.99999918	.00075182	-.70783623	.70620329
FACET12	.00084943	-.00093991	.99999920	.00084943	-.70777109	.70621040
AVERAGES :	.00000000	-.00064263				
RMS :	.00059964	.00027494				

N = 12

NRT AT 60D, G ONLY , ELEVATION ANGLE= 60. DEGREES FROM VERTICAL

FACET 1	-.00048401	-.00015548	.99999987	-.00048401	-.50013464	.86577111
FACET 2	-.00055944	-.00005098	.99999984	-.00055944	-.50004415	.86574439
FACET 3	-.00064832	-.00020389	.99999977	-.00064832	-.50017657	.86568539
FACET 4	-.00073841	-.00059948	.99999955	-.00073841	-.50051908	.86554945
FACET 5	-.00082217	-.00090815	.99999925	-.00082217	-.50078627	.86541224
FACET 6	-.00088915	-.00079772	.99999929	-.00088915	-.50069068	.86542751
FACET 7	.00048401	-.00015548	.99999987	.00048401	-.50013465	.86577111
FACET 8	.00055944	-.00005098	.99999984	.00055944	-.50004415	.86574439
FACET 9	.00064832	-.00020390	.99999977	.00064832	-.50017657	.86568539
FACET10	.00073841	-.00059949	.99999955	.00073841	-.50051909	.86554945
FACET11	.00082217	-.00090815	.99999925	.00082217	-.50078628	.86541224
FACET12	.00088915	-.00079772	.99999929	.00088915	-.50069069	.86542751
AVERAGES :	.00000000	-.00045262				
RMS :	.00070467	.00033157				

N = 12

NRT AT 70D, W/ G , ELEVATION ANGLE= 70. DEGREES FROM VERTICAL

FACET 1	-.00060803	.00002214	.99999981	-.00060803	-.34199934	.93990054
FACET 2	-.00066154	.00013713	.99999977	-.00066154	-.34189128	.93992348
FACET 3	-.00072359	-.00006669	.99999974	-.00072359	-.34207717	.93944402
FACET 4	-.00078546	-.00049147	.99999957	-.00078546	-.34248193	.93937532
FACET 5	-.00084197	-.00079630	.99999933	-.00084197	-.34276831	.93929563
FACET 6	-.00088627	-.00067723	.99999938	-.00088627	-.34265645	.93931055
FACET 7	.00060803	.00002214	.99999981	.00060803	-.34199934	.93990054
FACET 8	.00066154	.00013713	.99999977	.00066154	-.34189128	.93992348
FACET 9	.00072359	-.00006670	.99999974	.00072359	-.34207718	.93944402
FACET10	.00078546	-.00049148	.99999957	.00078546	-.34248194	.93937532
FACET11	.00084197	-.00079630	.99999933	.00084197	-.34276832	.93929563
FACET12	.00088627	-.00067723	.99999938	.00088627	-.34265645	.93931055
AVERAGES :	.00000000	-.00031107				
RMS :	.00075744	.00035978				

N = 12

NRT AT 75D, G ONLY , ELEVATION ANGLE= 75. DEGREES FROM VERTICAL

FACET 1	-.00066114	.00011118	.99999978	-.00066114	-.25871166	.96609913
FACET 2	-.00070271	.00022954	.99999973	-.00070271	-.25859732	.96611689
FACET 3	-.00075022	.00001246	.99999972	-.00075022	-.25880701	.96611975
FACET 4	-.00079685	-.00042875	.99999959	-.00079685	-.25923316	.96569123
FACET 5	-.00083870	-.00072646	.99999938	-.00083870	-.25952068	.96563805
FACET 6	-.00087085	-.00060503	.99999944	-.00087085	-.25940341	.96565083
FACET 7	.00066114	.00011117	.99999978	.00066114	-.25871166	.96609913
FACET 8	.00070271	.00022954	.99999973	.00070271	-.25859732	.96611689
FACET 9	.00075022	.00001245	.99999972	.00075022	-.25880702	.96611975
FACET10	.00079685	-.00042876	.99999959	.00079685	-.25923317	.96569123
FACET11	.00083870	-.00072647	.99999938	.00083870	-.25952069	.96563805
FACET12	.00087085	-.00060503	.99999944	.00087085	-.25940342	.96565083
AVERAGES :	.00000000	-.00023451				
RMS :	.00077357	.00036807				

N = 12

NRT , HORIZ, W/ G	, ELEVATION ANGLE= 90. DEGREES FROM VERTICAL					
FACET 1	-.00079520	.00037209	.99999961	-.00079520	.00037209	.99999961
FACET 2	-.00080010	.00049664	.99999956	-.00080010	.00049664	.99999956
FACET 3	-.00080303	.00022921	.99999965	-.00080303	.00022921	.99999965
FACET 4	-.00080303	-.00022920	.99999965	-.00080303	-.00022920	.99999965
FACET 5	-.00080010	-.00049664	.99999956	-.00080010	-.00049664	.99999956
FACET 6	-.00079520	-.00037208	.99999961	-.00079520	-.00037208	.99999961
FACET 7	.00079520	.00037208	.99999961	.00079520	.00037208	.99999961
FACET 8	.00080010	.00049664	.99999956	.00080010	.00049664	.99999956
FACET 9	.00080303	.00022920	.99999965	.00080303	.00022920	.99999965
FACET10	.00080303	-.00022921	.99999965	.00080303	-.00022921	.99999965
FACET11	.00080010	-.00049664	.99999956	.00080010	-.00049664	.99999956
FACET12	.00079520	-.00037209	.99999961	.00079520	-.00037209	.99999961
AVERAGES :	-.00000000	-.00000000				
RMS :	.00079945	.00038194				
N = 12						

NRT , CASE1, NO G	, ELEVATION ANGLE= 0. DEGREES FROM VERTICAL					
FACET 1	-.00014072	.00062353	.99999980	-.00014072	-.99999981	.00063921
FACET 2	-.00015414	.00068188	.99999976	-.00015414	-.99999977	.00069908
FACET 3	-.00017389	.00061741	.99999979	-.00017389	-.99999981	.00064143
FACET 4	-.00017388	.00045988	.99999988	-.00017388	-.99999989	.00049165
FACET 5	-.00015414	.00039541	.99999991	-.00015414	-.99999992	.00042439
FACET 6	-.00014071	.00045376	.99999989	-.00014071	-.99999990	.00047507
FACET 7	.00014072	.00062353	.99999980	.00014072	-.99999981	.00063921
FACET 8	.00015414	.00068188	.99999976	.00015414	-.99999977	.00069908
FACET 9	.00017389	.00061741	.99999979	.00017389	-.99999981	.00064143
FACET10	.00017388	.00045987	.99999988	.00017388	-.99999989	.00049165
FACET11	.00015414	.00039540	.99999991	.00015414	-.99999992	.00042439
FACET12	.00014071	.00045376	.99999989	.00014071	-.99999990	.00047507
AVERAGES :	-.00000000	.00053864				
RMS :	.00015684	.00010634				
N = 12						

NRT , CASE2, NO G	, ELEVATION ANGLE= 70. DEGREES FROM VERTICAL					
FACET 1	-.00045862	.00095129	.99999944	-.00045862	-.34112607	.94005329
FACET 2	-.00035498	.00098913	.99999945	-.00035498	-.34109049	.94005153
FACET 3	-.00024909	.00082366	.99999963	-.00024909	-.34124604	.93998658
FACET 4	-.00014411	.00067114	.99999976	-.00014411	-.34138940	.93992718
FACET 5	-.00003629	.00066121	.99999978	-.00003629	-.34139874	.93991890
FACET 6	.00007047	.00069665	.99999975	.00007047	-.34136542	.93993187
FACET 7	.00045862	.00095129	.99999944	.00045862	-.34112607	.94005329
FACET 8	.00035498	.00098913	.99999945	.00035498	-.34109050	.94005153
FACET 9	.00024909	.00082366	.99999963	.00024909	-.34124604	.93998658
FACET10	.00014411	.00067114	.99999976	.00014411	-.34138940	.93992717
FACET11	.00003629	.00066120	.99999978	.00003629	-.34139874	.93991890
FACET12	-.00007047	.00069665	.99999975	-.00007047	-.34136543	.93993187
AVERAGES :	.00000000	.00079865				
RMS :	.00026628	.00013277				
N = 12						

NRT , CASE3, NO G	, ELEVATION ANGLE= 0. DEGREES FROM VERTICAL					
FACET 1	-.00065339	.00066926	.99999956	-.00065339	-.99999978	.00093533
FACET 2	-.00064486	.00073213	.99999952	-.00064486	-.99999973	.00097563
FACET 3	-.00062535	.00058648	.99999963	-.00062535	-.99999983	.00085734
FACET 4	-.00062535	.00034692	.99999974	-.00062535	-.99999994	.00071514
FACET 5	-.00064486	.00020127	.99999977	-.00064486	-.99999998	.00067554
FACET 6	-.00065339	.00026414	.99999975	-.00065339	-.99999997	.00070476
FACET 7	-.00029096	.00050120	.99999983	-.00029096	-.99999987	.00057954
FACET 8	-.00027913	.00051130	.99999983	-.00027913	-.99999987	.00058253
FACET 9	-.00025815	.00048861	.99999985	-.00025815	-.99999988	.00055262
FACET10	-.00025815	.00044479	.99999987	-.00025815	-.99999990	.00051427
FACET11	-.00027913	.00042211	.99999987	-.00027913	-.99999991	.00050605
FACET12	-.00029096	.00043220	.99999986	-.00029096	-.99999991	.00052102
AVERAGES :	-.00045864	.00046670				
RMS :	.00018300	.00014691				
N = 12						

VECTORS NORMAL TO MIRROR SURFACE

	IN LOCAL COORDINATES			IN GLOBAL COORDINATES		
MARTIN, VERTICAL	, ELEVATION ANGLE= 0. DEGREES FROM VERTICAL					
FACET 1	.00004156	-.00019968	.99999998	.00004156	-.99999998	-.00020396
FACET 2	.00005124	-.00022752	.99999997	.00005124	-.99999997	-.00023322
FACET 3	.00001921	-.00015804	.99999999	.00001921	-.99999999	-.00015920
FACET 4	-.00003245	-.00019403	.99999998	-.00003245	-.99999998	-.00019673
FACET 5	-.00009005	-.00021145	.99999997	-.00009005	-.99999998	-.00022983
FACET 6	-.00004156	-.00019968	.99999998	-.00004156	-.99999998	-.00020396
FACET 7	-.00005124	-.00022752	.99999997	-.00005124	-.99999997	-.00023322
FACET 8	-.00001921	-.00015804	.99999999	-.00001921	-.99999999	-.00015920
FACET 9	.00003245	-.00019403	.99999998	.00003245	-.99999998	-.00019673
FACET10	.00009005	-.00021145	.99999997	.00009005	-.99999998	-.00022983
FACET11	.00000000	-.00025739	.99999997	.00000000	-.99999997	-.00025739
AVERAGES :	.00000000	-.00020353				
RMS :	.00005024	.00002784				
N = 11						
MARTIN, AT 15 DEGREE	, ELEVATION ANGLE= 15. DEGREES FROM VERTICAL					
FACET 1	-.00008530	-.00015991	.99999998	-.00008530	-.96596720	.25864398
FACET 2	-.00011574	-.00020299	.99999997	-.00011574	-.96597834	.25859334
FACET 3	-.00018742	-.00022983	.99999996	-.00018742	-.96598528	.25853258
FACET 4	-.00027976	-.00032509	.99999991	-.00027976	-.96600991	.25840474
FACET 5	-.00038714	-.00035188	.99999986	-.00038714	-.96601684	.25831368
FACET 6	.00008530	-.00015991	.99999998	.00008530	-.96596720	.25864398
FACET 7	.00011574	-.00020299	.99999997	.00011574	-.96597834	.25859334
FACET 8	.00018742	-.00022983	.99999996	.00018742	-.96598528	.25853258
FACET 9	.00027976	-.00032509	.99999991	.00027976	-.96600991	.25840474
FACET10	.00038713	-.00035188	.99999986	.00038713	-.96601684	.25831368
FACET11	.00000000	-.00011053	.99999999	.00000000	-.96595443	.25871228
AVERAGES :	-.00000000	-.00024090				
RMS :	.00022721	.00008093				
N = 11						
MARTIN, AT 30 DEGREE	, ELEVATION ANGLE= 30. DEGREES FROM VERTICAL					
FACET 1	-.00020593	-.00011006	.99999997	-.00020593	-.86608043	.49979777
FACET 2	-.00027451	-.00016550	.99999995	-.00027451	-.86610814	.49972238
FACET 3	-.00038117	-.00028657	.99999989	-.00038117	-.86616865	.49958695
FACET 4	-.00050819	-.00043475	.99999978	-.00050819	-.86624270	.49942070
FACET 5	-.00065832	-.00046916	.99999967	-.00065832	-.86625989	.49929975
FACET 6	.00020593	-.00011006	.99999997	.00020593	-.86608043	.49979777
FACET 7	.00027451	-.00016550	.99999995	.00027451	-.86610814	.49972238
FACET 8	.00038117	-.00028657	.99999989	.00038117	-.86616865	.49958695
FACET 9	.00050819	-.00043475	.99999978	.00050819	-.86624270	.49942071
FACET10	.00065832	-.00046916	.99999967	.00065832	-.86625989	.49929975
FACET11	.00000000	.00004284	1.00000000	.00000000	-.86600398	.50003710
AVERAGES :	-.00000000	-.00026266				
RMS :	.00041663	.00016636				
N = 11						
MARTIN, AT 45 DEGRE	, ELEVATION ANGLE= 45. DEGREES FROM VERTICAL					
FACET 1	-.00031334	-.00005424	.99999995	-.00031334	-.70714513	.70688189
FACET 2	-.00041580	-.00011846	.99999991	-.00041580	-.70719054	.70680100
FACET 3	-.00055071	-.00032630	.99999980	-.00055071	-.70733747	.70665400
FACET 4	-.00070436	-.00051796	.99999962	-.00070436	-.70747294	.70648828
FACET 5	-.00088770	-.00055779	.99999945	-.00088770	-.70750109	.70636506
FACET 6	.00031334	-.00005423	.99999995	.00031334	-.70714513	.70688189
FACET 7	.00041580	-.00011846	.99999991	.00041580	-.70719054	.70680100
FACET 8	.00055071	-.00032630	.99999980	.00055071	-.70733747	.70665400
FACET 9	.00070436	-.00051796	.99999962	.00070436	-.70747294	.70648828
FACET10	.00088770	-.00055779	.99999945	.00088770	-.70750109	.70636506
FACET11	.00000000	.00019250	.99999998	.00000000	-.70697065	.70724289
AVERAGES :	-.00000000	-.00026882				
RMS :	.00058130	.00024269				
N = 11						

MARTIN,AT 60 DEGREE , ELEVATION ANGLE= 60. DEGREES FROM VERTICAL

FACET 1	-.00039787	.00000705	.99999992	-.00039787	-.49999389	.86622430
FACET 2	-.00052644	-.00006116	.99999986	-.00052644	-.50005296	.86576029
FACET 3	-.00067943	-.00034008	.99999971	-.00067943	-.50029449	.86564526
FACET 4	-.00084810	-.00056088	.99999948	-.00084810	-.50048566	.86551656
FACET 5	-.00105085	-.00060311	.99999927	-.00105085	-.50052222	.86541896
FACET 6	.00039787	.00000705	.99999992	.00039787	-.49999389	.86622430
FACET 7	.00052644	-.00006116	.99999986	.00052644	-.50005296	.86576029
FACET 8	.00067943	-.00034007	.99999971	.00067943	-.50029448	.86564526
FACET 9	.00084809	-.00056088	.99999948	.00084809	-.50048566	.86551656
FACET10	.00105085	-.00060311	.99999927	.00105085	-.50052222	.86541896
FACET11	.00000000	.00032939	.99999995	.00000000	-.49971472	.86619005
AVERAGES :	-.00000000	-.00025336				
RMS :	.00070332	.00030120				
N = 11						

MARTIN,AT 75 DEGREE , ELEVATION ANGLE= 75. DEGREES FROM VERTICAL

FACET 1	-.00045609	.00006718	.99999989	-.00045609	-.25875416	.96604504
FACET 2	-.00060242	-.00000059	.99999982	-.00060242	-.25881962	.96576973
FACET 3	-.00076360	-.00033237	.99999965	-.00076360	-.25914007	.96570995
FACET 4	-.00093640	-.00056794	.99999940	-.00093640	-.25936759	.96564180
FACET 5	-.00114543	-.00060983	.99999916	-.00114543	-.25940805	.96558915
FACET 6	.00045609	.00006718	.99999989	.00045609	-.25875416	.96604504
FACET 7	.00060242	-.00000059	.99999982	.00060242	-.25881962	.96576973
FACET 8	.00076359	-.00033237	.99999965	.00076359	-.25914007	.96570995
FACET 9	.00093640	-.00056794	.99999940	.00093640	-.25936759	.96564180
FACET10	.00114543	-.00060983	.99999916	.00114543	-.25940805	.96558915
FACET11	.00000000	.00044386	.99999990	.00000000	-.25839028	.96604061
AVERAGES :	-.00000000	-.00022211				
RMS :	.00077961	.00034021				
N = 11						

MARTIN,HORIZONTAL , ELEVATION ANGLE= 90. DEGREES FROM VERTICAL

FACET 1	-.00048468	.00012311	.99999987	-.00048468	.00012311	.99999987
FACET 2	-.00063932	.00006015	.99999979	-.00063932	.00006015	.99999979
FACET 3	-.00079823	-.00030323	.99999964	-.00079823	-.00030323	.99999964
FACET 4	-.00096397	-.00053829	.99999939	-.00096397	-.00053829	.99999939
FACET 5	-.00116570	-.00057716	.99999915	-.00116570	-.00057716	.99999915
FACET 6	.00048468	.00012311	.99999987	.00048468	.00012311	.99999987
FACET 7	.00063932	.00006015	.99999979	.00063932	.00006015	.99999979
FACET 8	.00079823	-.00030323	.99999964	.00079823	-.00030323	.99999964
FACET 9	.00096397	-.00053829	.99999939	.00096397	-.00053829	.99999939
FACET10	.00116570	-.00057716	.99999915	.00116570	-.00057716	.99999915
FACET11	.00000000	.00052967	.99999986	.00000000	.00052967	.99999986
AVERAGES :	-.00000000	-.00017647				
RMS :	.00083554	.00035741				
N = 11						

MARTIN,CASE1 , ELEVATION ANGLE= 0. DEGREES FROM VERTICAL

FACET 1	-.00006473	.00025764	.99999996	-.00006473	-.99999997	.00026565
FACET 2	-.00012871	.00024561	.99999996	-.00012871	-.99999997	.00027729
FACET 3	-.00017668	.00016598	.99999997	-.00017668	-.99999999	.00024242
FACET 4	-.00018370	.00012129	.99999998	-.00018370	-.99999999	.00022013
FACET 5	-.00018326	.00011585	.99999998	-.00018326	-.99999999	.00021681
FACET 6	.00006473	.00025764	.99999996	.00006473	-.99999997	.00026565
FACET 7	.00012871	.00024561	.99999996	.00012871	-.99999997	.00027729
FACET 8	.00017668	.00016598	.99999997	.00017668	-.99999999	.00024242
FACET 9	.00018370	.00012129	.99999998	.00018370	-.99999999	.00022013
FACET10	.00018326	.00011585	.99999998	.00018326	-.99999999	.00021681
FACET11	-.00000000	.00027458	.99999996	-.00000000	-.99999996	.00027458
AVERAGES :	-.00000000	.00018976				
RMS :	.00014728	.00006330				
N = 11						

MARTIN,CASE 2 , ELEVATION ANGLE= 70. DEGREES FROM VERTICAL

FACET 1	-.00025939	.00044581	.99999987	-.00025939	-.34160118	.93986890
FACET 2	-.00020020	.00041918	.99999989	-.00020020	-.34162621	.93985140
FACET 3	-.00013616	.00032169	.99999994	-.00013616	-.34171783	.93981204
FACET 4	-.00007879	.00030545	.99999995	-.00007879	-.34173309	.93980047
FACET 5	-.00002465	.00030552	.99999995	-.00002465	-.34173303	.93979741
FACET 6	.00025939	.00044581	.99999987	.00025939	-.34160118	.93986890
FACET 7	.00020020	.00041918	.99999989	.00020020	-.34162621	.93985140
FACET 8	.00013616	.00032169	.99999994	.00013616	-.34171783	.93981204
FACET 9	.00007879	.00030545	.99999995	.00007879	-.34173309	.93980047

FACET10	.00002465	.00030552	.99999995	.00002465	-.34173303	.93979741
FACET11	-.00000000	.00057816	.99999983	-.00000000	-.34147680	.93989020
AVERAGES :	-.00000000	.00037941				
RMS :	.00015534	.00008528				

N = 11

MARTIN,CASE3 , ELEVATION ANGLE= 0. DEGREES FROM VERTICAL

FACET 1	-.00036411	.00019929	.99999991	-.00036411	-.99999998	.00041508
FACET 2	-.00039645	.00017318	.99999991	-.00039645	-.99999999	.00043262
FACET 3	-.00044969	.00002612	.99999990	-.00044969	-1.00000000	.00045045
FACET 4	-.00054398	-.00058603	.99999985	-.00054398	-1.00000000	-.00054821
FACET 5	-.00066120	-.00008621	.99999978	-.00066120	-1.00000000	-.00066679
FACET 6	-.00018038	.00019606	.99999996	-.00018038	-.99999998	.00026642
FACET 7	-.00014695	.00019094	.99999997	-.00014695	-.99999998	.00024094
FACET 8	-.00012972	.00017163	.99999998	-.00012972	-.99999999	.00021514
FACET 9	-.00014505	.00015875	.99999998	-.00014505	-.99999999	.00021503
FACET10	-.00016893	.00015632	.99999997	-.00016893	-.99999999	.00023016
FACET11	-.00018746	.00027573	.99999994	-.00018746	-.99999996	.00033342
AVERAGES :	-.00030672	.00012671				
RMS :	.00017733	.00011114				

N = 11

VECTORS NORMAL TO MIRROR SURFACE

IN LOCAL COORDINATES IN GLOBAL COORDINATES

MDAC ,VERT,W/ G , ELEVATION ANGLE= 0. DEGREES FROM VERTICAL/4 PLANE AVERAGE

FACET 1	-.00016062	-.00065218	.99999971	-.00016062	-.99999979	-.00076025
FACET 2	-.00016630	-.00093410	.99999949	-.00016630	-.99999956	-.00100599
FACET 3	-.00008113	-.00113045	.99999934	-.00008113	-.99999936	-.00114936
FACET 4	.00000000	-.00119732	.99999928	.00000000	-.99999928	-.00119732
FACET 5	.00008113	-.00113045	.99999934	.00008113	-.99999936	-.00114936
FACET 6	.00016630	-.00093410	.99999949	.00016630	-.99999956	-.00100599
FACET 7	.00016062	-.00065218	.99999971	.00016062	-.99999979	-.00076025
FACET 8	.00016086	-.00066565	.99999970	.00016086	-.99999978	-.00077192
FACET 9	.00016661	-.00094749	.99999948	.00016661	-.99999955	-.00101849
FACET10	.00008139	-.00114379	.99999933	.00008139	-.99999935	-.00116250
FACET11	.00000000	-.00121058	.99999927	.00000000	-.99999927	-.00121058
FACET12	-.00008139	-.00114379	.99999933	-.00008139	-.99999935	-.00116250
FACET13	-.00016662	-.00096484	.99999946	-.00016662	-.99999953	-.00103563
FACET14	-.00016086	-.00066565	.99999970	-.00016086	-.99999978	-.00077192
AVERAGES :	-.00000000	-.00095519				
RMS :	.00013109	.00020853				

N = 14

MDAC ,AT 15D,W/ G , ELEVATION ANGLE= 15. DEGREES FROM VERTICAL/4 PLANE AVERAGE

FACET 1	-.00026046	-.00054796	.99999977	-.00026046	-.96606750	.25816981
FACET 2	-.00023964	-.00077708	.99999963	-.00023964	-.96612666	.25799661
FACET 3	-.00010492	-.00089325	.99999959	-.00010492	-.96615663	.25794496
FACET 4	.00000000	-.00091854	.99999958	.00000000	-.96616315	.25793170
FACET 5	.00010492	-.00089325	.99999959	.00010492	-.96615663	.25794496
FACET 6	.00023964	-.00077708	.99999963	.00023964	-.96612666	.25799661
FACET 7	.00026046	-.00054796	.99999977	.00026046	-.96606750	.25816981
FACET 8	.00004914	-.00077494	.99999962	.00004914	-.96612610	.25798089
FACET 9	.00008098	-.00108858	.99999933	.00008098	-.96620700	.25769945
FACET10	.00005166	-.00135043	.99999905	.00005166	-.96627446	.25748777
FACET11	.00000000	-.00145381	.99999894	.00000000	-.96630108	.25741450
FACET12	-.00005166	-.00135044	.99999905	-.00005166	-.96627446	.25748777
FACET13	-.00008099	-.00111447	.99999929	-.00008099	-.96621366	.25767517
FACET14	-.00004914	-.00077494	.99999962	-.00004914	-.96612610	.25798089
AVERAGES :	-.00000000	-.00094734				
RMS :	.00014537	.00027678				

N = 14

MDAC ,AT 30D,W/ G , ELEVATION ANGLE= 30. DEGREES FROM VERTICAL/4 PLANE AVERAGE

FACET 1	-.00034302	-.00042900	.99999982	-.00034302	-.86623982	.49949447
FACET 2	-.00029716	-.00059060	.99999977	-.00029716	-.86632055	.49941225
FACET 3	-.00012181	-.00061932	.99999980	-.00012181	-.86633490	.49945328
FACET 4	-.00000000	-.00060152	.99999982	-.00000000	-.86632601	.49947898
FACET 5	.00012181	-.00061932	.99999980	.00012181	-.86633490	.49945328
FACET 6	.00029716	-.00059060	.99999977	.00029716	-.86632055	.49941225
FACET 7	.00034302	-.00042900	.99999982	.00034302	-.86623982	.49949447
FACET 8	-.00006538	-.00085398	.99999956	-.00006538	-.86645207	.49918659
FACET 9	-.00000960	-.00117893	.99999921	-.00000960	-.86661426	.49891693
FACET10	.00001869	-.00143907	.99999883	.00001869	-.86676898	.49867854
FACET11	.00000000	-.00162217	.99999868	.00000000	-.86683535	.49859450
FACET12	-.00001869	-.00143907	.99999883	-.00001869	-.86676898	.49867854
FACET13	.00000959	-.00121163	.99999917	.00000959	-.86663057	.49888988

FACET14	.00006537	-.00035398	.99999956	.00006537	-.86645207	.49918659

AVERAGES :	-.00000000	-.00089844
RMS :	.00017949	.00040324

N = 14

MDAC ,AT 45D,W/ G , ELEVATION ANGLE= 45. DEGREES FROM VERTICAL/4 PLANE AVERAGE

FACET 1	-.00040351	-.00028342	.99999987	-.00040351	-.70730716	.70675135
FACET 2	-.00033549	-.00036677	.99999988	-.00033549	-.70736608	.70675352
FACET 3	-.00013080	-.00030586	.99999994	-.00013080	-.70732302	.70686294
FACET 4	-.00000000	-.00024599	.99999997	-.00000000	-.70728070	.70693282
FACET 5	.00013080	-.00030586	.99999994	.00013080	-.70732302	.70686294
FACET 6	.00033549	-.00036677	.99999988	.00033549	-.70736608	.70675352
FACET 7	.00040351	-.00028342	.99999987	.00040351	-.70730716	.70675135
FACET 8	-.00017601	-.00087955	.99999953	-.00017601	-.70772844	.70642485
FACET 9	-.00009985	-.00119464	.99999919	-.00009985	-.70795101	.70620956
FACET10	-.00001560	-.00153301	.99999875	-.00001560	-.70818995	.70599097
FACET11	.00000000	-.00168727	.99999858	.00000000	-.70829885	.70591269
FACET12	.00001560	-.00153301	.99999875	.00001560	-.70818995	.70599097
FACET13	.00009985	-.00123204	.99999914	.00009985	-.70797742	.70618472
FACET14	.00017601	-.00087955	.99999953	.00017601	-.70772844	.70642485

AVERAGES :	-.00000000	-.00079265
RMS :	.00021833	.00052919

N = 14

MDAC ,AT 60D,W/ G , ELEVATION ANGLE= 60. DEGREES FROM VERTICAL/4 PLANE AVERAGE

FACET 1	-.00043402	-.00014318	.99999990	-.00043402	-.50012399	.86579652
FACET 2	-.00034891	-.00014209	.99999993	-.00034891	-.50012305	.86583670
FACET 3	-.00013007	.00000388	.99999998	-.00013007	-.49999664	.86602617
FACET 4	-.00000000	.00010135	.99999999	-.00000000	-.49991222	.86607608
FACET 5	.00013007	.00000388	.99999998	.00013007	-.49999664	.86602617
FACET 6	.00034891	-.00014210	.99999993	.00034891	-.50012305	.86583670
FACET 7	.00043402	-.00014318	.99999990	.00043402	-.50012400	.86579652
FACET 8	-.00027358	-.00086581	.99999954	-.00027358	-.50074962	.86554796
FACET 9	-.00018272	-.00114771	.99999925	-.00018272	-.50099362	.86541365
FACET10	-.00004877	-.00148922	.99999881	-.00004877	-.50128915	.86525555
FACET11	.00000000	-.00165318	.99999863	.00000000	-.50143101	.86519763
FACET12	.00004877	-.00148922	.99999881	.00004877	-.50128915	.86525555
FACET13	.00018271	-.00118705	.99999920	.00018271	-.50102766	.86539550
FACET14	.00027357	-.00086581	.99999954	.00027357	-.50074963	.86554795

AVERAGES :	-.00000000	-.00065425
RMS :	.00025004	.00062640

N = 14

MDAC ,AT 75D,W/ G , ELEVATION ANGLE= 75. DEGREES FROM VERTICAL/4 PLANE AVERAGE

FACET 1	-.00043624	.00005279	.99999990	-.00043624	-.25876806	.96603952
FACET 2	-.00033960	.00013797	.99999992	-.00033960	-.25868578	.96602243
FACET 3	-.00012086	.00035927	.99999989	-.00012086	-.25847201	.96604485
FACET 4	-.00000000	.00048791	.99999988	-.00000000	-.25834773	.96605199
FACET 5	.00012087	.00035926	.99999989	.00012087	-.25847201	.96604485
FACET 6	.00033960	.00013796	.99999992	.00033960	-.25868578	.96602243
FACET 7	.00043624	.00005278	.99999990	.00043624	-.25876806	.96603952
FACET 8	-.00035308	-.00074922	.99999963	-.00035308	-.25954267	.96570415
FACET 9	-.00025345	-.00097971	.99999943	-.00025345	-.25976525	.96565084
FACET10	-.00007867	-.00130216	.99999908	-.00007867	-.26007662	.96557424
FACET11	.00000000	-.00146515	.99999893	.00000000	-.26023399	.96554558
FACET12	.00007867	-.00130216	.99999908	.00007867	-.26007662	.96557424
FACET13	.00025345	-.00101842	.99999939	.00025345	-.25980263	.96564185
FACET14	.00035307	-.00074923	.99999963	.00035307	-.25954267	.96570415

AVERAGES :	-.00000000	-.00042761
RMS :	.00027133	.00069693

N = 14

MDAC ,HORIZ,W/ G , ELEVATION ANGLE= 90. DEGREES FROM VERTICAL/4 PLANE AVERAGE

FACET 1	-.00041005	.00013240	.99999990	-.00041005	.00013240	.99999990
FACET 2	-.00030811	.00029641	.99999988	-.00030811	.00029641	.99999988
FACET 3	-.00010373	.00057890	.99999977	-.00010373	.00057890	.99999977
FACET 4	-.00000000	.00073045	.99999973	-.00000000	.00073045	.99999973
FACET 5	.00010373	.00057890	.99999977	.00010373	.00057890	.99999977
FACET 6	.00030811	.00029641	.99999988	.00030811	.00029641	.99999988
FACET 7	.00041005	.00013239	.99999990	.00041005	.00013239	.99999990
FACET 8	-.00040986	-.00069731	.99999966	-.00040986	-.00069731	.99999966
FACET 9	-.00030791	-.00086116	.99999955	-.00030791	-.00086116	.99999955
FACET10	-.00010353	-.00114348	.99999928	-.00010353	-.00114348	.99999928

FACET11	-.CCCCCCCC	-.CC129489	.99999916	-.CCCCCCCC	-.CC129489	.99999916
FACET12	.CC010352	-.CC114348	.99999928	.CC010352	-.CC114348	.99999928
FACET13	.CC030790	-.CC089671	.99999951	.CC030790	-.CC089671	.99999951
FACET14	.CC040985	-.CC069731	.99999966	.CC040985	-.CC069731	.99999966
AVERAGES :	-.CCCCCCCC	-.CC028489				
RMS :	.CC027963	.CC071155				

N = 14

MDAC	,CASE1,W/ G	, ELEVATION ANGLE=	0. DEGREES FROM VERTICAL/4 PLANE AVERAGE			
FACET 1	-.CC023399	-.CC037144	.99999987	-.CC023399	-.99999993	-.CC049010
FACET 2	-.CC021789	-.CC053867	.99999981	-.CC021789	-.99999985	-.CC061332
FACET 3	-.CC009733	-.CC061126	.99999981	-.CC009733	-.99999981	-.CC062302
FACET 4	.CC000000	-.CC061992	.99999981	.CC000000	-.99999981	-.CC061992
FACET 5	.CC009733	-.CC061126	.99999981	.CC009733	-.99999981	-.CC062302
FACET 6	.CC021789	-.CC053867	.99999981	.CC021789	-.99999985	-.CC061332
FACET 7	.CC023399	-.CC037143	.99999987	.CC023399	-.99999993	-.CC049009
FACET 8	.CC008754	-.CC035929	.99999981	.CC008754	-.99999993	-.CC060850
FACET 9	.CC011512	-.CC075576	.99999959	.CC011512	-.99999971	-.CC089594
FACET10	.CC006531	-.CC107579	.99999937	.CC006531	-.99999942	-.CC112181
FACET11	-.CCCCCCCC	-.CC120075	.99999928	-.CCCCCCCC	-.99999928	-.CC120075
FACET12	-.CC006531	-.CC107579	.99999937	-.CC006531	-.99999942	-.CC112181
FACET13	-.CC011512	-.CC078806	.99999956	-.CC011512	-.99999968	-.CC092621
FACET14	-.CC008755	-.CC035929	.99999981	-.CC008755	-.99999993	-.CC060850
AVERAGES :	-.CCCCCCCC	-.CC066267				
RMS :	.CC013984	.CC027345				

N = 14

MDAC	,CASE1,W/OG	, ELEVATION ANGLE=	0. DEGREES FROM VERTICAL/G EFFECTS TAKEN OUT			
FACET 1	-.CCC07337	.CC028C75	.CCCCCC16	-.CC007337	-.CCCCCC14	.CC027015
FACET 2	-.CCCC5159	.CC039543	.CCCCCC32	-.CC005159	-.CCCCCC29	.CC039267
FACET 3	-.CCCC1620	.CC051919	.CCCCCC47	-.CCC01620	-.CCCCCC45	.CC052634
FACET 4	.CCCCCCCC	.CC057740	.CCCCCC53	.CCCCCCCC	-.CCCCCC53	.CC057740
FACET 5	.CCC01621	.CC051919	.CCCCCC47	.CCCC1621	-.CCCCCC45	.CC052634
FACET 6	.CC005160	.CC039543	.CCCCCC32	.CC005160	-.CCCCCC29	.CC039267
FACET 7	.CCCC7337	.CC028C75	.CCCCCC16	.CCCC7337	-.CCCCCC14	.CC027016
FACET 8	-.CCCC7332	.CC030637	.CCCCCC11	-.CCCC7332	-.CCCCCC15	.CC016342
FACET 9	-.CCCC5150	.CC019173	.CCCCCC11	-.CCCC5150	-.CCCCCC16	.CC012255
FACET10	-.CCCC1608	.CC006EC1	.CCCCCCC4	-.CCCC1608	-.CCCCCCC7	.CC004069
FACET11	-.CCCCCCCC	.CCCCC984	.CCCCCCC1	-.CCCCCCCC	-.CCCCCCC1	.CCCCC984
FACET12	.CCCC1608	.CC006EC1	.CCCCCCC4	.CCCC1608	-.CCCCCCC7	.CC004069
FACET13	.CCCC5149	.CC017678	.CCCCCC10	.CCCC5149	-.CCCCCC15	.CC010942
FACET14	.CCCC7331	.CC030637	.CCCCCC11	.CCCC7331	-.CCCCCC15	.CC016342
AVERAGES :	-.CCCCCCCC	.CC029252				
RMS :	.CC004869	.CC017114				

N = 14

MDAC	,CASE2,W/ G	, ELEVATION ANGLE=	70. DEGREES FROM VERTICAL/4 PLANE AVERAGE			
FACET 1	-.CC059087	.CC047444	.99999971	-.CC059087	-.34157427	.93995156
FACET 2	-.CC045334	.CC055407	.99999973	-.CC045334	-.34149943	.93994184
FACET 3	-.CC015C58	.CC083598	.99999957	-.CC015058	-.34123446	.94000695
FACET 4	-.CCCCCCCC	.CC100543	.99999949	-.CCCCCCCC	-.34107518	.94003602
FACET 5	.CC015C58	.CC083597	.99999957	.CC015058	-.34123446	.94000695
FACET 6	.CC045334	.CC055407	.99999973	.CC045334	-.34149944	.93994184
FACET 7	.CC059087	.CC047444	.99999971	.CC059087	-.34157428	.93995156
FACET 8	-.CC039268	-.CC048950	.99999975	-.CC039268	-.34248008	.93946082
FACET 9	-.CC028313	-.CC078667	.99999957	-.CC028313	-.34275927	.93937807
FACET10	-.CC009719	-.CC116e51	.99999922	-.CC009719	-.34311607	.93926696
FACET11	.CCCCCCCC	-.CC135338	.99999908	.CCCCCCCC	-.34329159	.93922888
FACET12	.CC009719	-.CC116652	.99999922	.CC009719	-.34311608	.93926696
FACET13	.CC028312	-.CC083190	.99999952	.CC028312	-.34280175	.93936531
FACET14	.CC039268	-.CC048951	.99999975	.CC039268	-.34248009	.93946082
AVERAGES :	-.CCCCCCCC	-.CC011C68				
RMS :	.CC034250	.CC083CCC				

N = 14

MDAC	,CASE2B,W/O G	, ELEVATION ANGLE=	70. DEGREES FROM VERTICAL/4 PLANE AVERAGE			
FACET 1	-.CC015C58	.CC051590	.99999986	-.CC015058	-.34153531	.93987632
FACET 2	-.CC010688	.CC053782	.99999985	-.CC010688	-.34151471	.93988104
FACET 3	-.CCCC2533	.CC062143	.99999980	-.CCCC2533	-.34143613	.93990863
FACET 4	-.CCCCCCCC	.CC067134	.99999977	-.CCCCCCCC	-.34138921	.93992202
FACET 5	.CCCC2533	.CC062143	.99999980	.CC002533	-.34143613	.93990863
FACET 6	.CC010688	.CC053782	.99999985	.CC010688	-.34151471	.93988104
FACET 7	.CC015058	.CC051590	.99999986	.CC015058	-.34153531	.93987632
FACET 8	-.CC006255	.CC033624	.99999994	-.CC006255	-.34170416	.93981070
FACET 9	-.CC005078	.CC028943	.99999996	-.CC005078	-.34174815	.93979446
FACET10	-.CC002776	.CC024201	.99999997	-.CC002776	-.34179272	.93977710
FACET11	-.CCCCCCCC	.CC022026	.99999998	-.CCCCCCCC	-.34181316	.93976793
FACET12	.CC002776	.CC024201	.99999997	.CC002776	-.34179272	.93977710
FACET13	.CC005078	.CC028354	.99999996	.CC005078	-.34175369	.93979258
FACET14	.CC006255	.CC033624	.99999994	.CC006255	-.34170416	.93981070

AVERAGES :	-.00000000	.00042653				
RMS :	.00007746	.00015649				
N = 14						

MDAC	,CASE3,W/ G	, ELEVATION ANGLE=	0. DEGREES FROM VERTICAL/4 PLANE AVERAGE		
FACET 1	-.00092984	-.00022742	.99999946	-.00092984	-.99999997	-.00096922
FACET 2	-.00089009	-.00053466	.99999940	-.00089009	-.99999985	-.00105636
FACET 3	-.00071341	-.00070172	.99999949	-.00071341	-.99999976	-.00100587
FACET 4	-.00056381	-.00077596	.99999954	-.00056381	-.99999970	-.00096047
FACET 5	-.00050293	-.00078114	.99999956	-.00050293	-.99999970	-.00093324
FACET 6	-.00041427	-.00067360	.99999966	-.00041427	-.99999978	-.00081886
FACET 7	-.00041493	-.00047840	.99999978	-.00041493	-.99999989	-.00066969
FACET 8	-.00064295	-.00066423	.99999952	-.00064295	-.99999978	-.00095652
FACET 9	-.00059178	-.00092092	.99999934	-.00059178	-.99999958	-.00113346
FACET10	-.00058557	-.00114653	.99999914	-.00058557	-.99999934	-.00130593
FACET11	-.00060550	-.00120852	.99999909	-.00060550	-.99999927	-.00135252
FACET12	-.00070032	-.00107231	.99999914	-.00070032	-.99999942	-.00130280
FACET13	-.00078194	-.00081472	.99999926	-.00078194	-.99999966	-.00118212
FACET14	-.00077112	-.00041899	.99999951	-.00077112	-.99999991	-.00091466

AVERAGES :	-.00065060	-.00074422
RMS :	.00015214	.00027048
N = 14		

MDAC	,CASE3,W/O G	, ELEVATION ANGLE=	0. DEGREES FROM VERTICAL/G EFFECTS TAKEN OUT		
FACET 1	-.00076921	.00042477	-.00000025	-.00076921	-.00000018	-.00020897
FACET 2	-.00072380	.00039944	-.00000009	-.00072380	-.00000029	-.00005038
FACET 3	-.00063228	.00042873	.00000015	-.00063228	-.00000040	.00014349
FACET 4	-.00056381	.00042136	.00000026	-.00056381	-.00000042	.00023685
FACET 5	-.00058406	.00034931	.00000022	-.00058406	-.00000034	.00021612
FACET 6	-.00058056	.00026050	.00000017	-.00058056	-.00000022	.00018712
FACET 7	-.00057555	.00017378	.00000005	-.00057555	-.00000010	.00009056
FACET 8	-.00080381	.00000143	-.00000018	-.00080381	0.00000000	-.00018460
FACET 9	-.00075839	.00002657	-.00000014	-.00075839	-.00000003	-.00011497
FACET10	-.00066696	-.00000274	-.00000019	-.00066696	.00000001	-.00014343
FACET11	-.00060550	.00002206	-.00000018	-.00060550	0.00000000	-.00014193
FACET12	-.00061893	.00007148	-.00000019	-.00061893	-.00000007	-.00014030
FACET13	-.00061532	.00015012	-.00000020	-.00061532	-.00000013	-.00014649
FACET14	-.00061026	.00024666	-.00000019	-.00061026	-.00000013	-.00014274

AVERAGES :	-.00065060	.00021096
RMS :	.00007724	.00016638
N = 14		

VECTORS NORMAL TO MIRROR SURFACE

IN LOCAL COORDINATES — IN GLOBAL COORDINATES

BOEING	,VERT,W/ G	, ELEVATION ANGLE=	0. DEGREES FROM VERTICAL/4 PLANE AVERAGE		
FACET 1	.00013300	-.00027154	.99999996	.00013300	-.99999996	-.00030348
FACET 2	.00008166	-.00025618	.99999996	.00008166	-.99999997	-.00027965
FACET 3	.00002784	-.00025516	.99999997	.00002784	-.99999997	-.00025812
FACET 4	-.00002762	-.00025521	.99999997	-.00002762	-.99999997	-.00025814
FACET 5	-.00008143	-.00026630	.99999996	-.00008143	-.99999997	-.00027969
FACET 6	-.00013276	-.00027372	.99999995	-.00013276	-.99999996	-.00030533
FACET 7	-.00013300	-.00027154	.99999996	-.00013300	-.99999996	-.00030348
FACET 8	-.00008166	-.00026618	.99999996	-.00008166	-.99999997	-.00027965
FACET 9	-.00002784	-.00025516	.99999997	-.00002784	-.99999997	-.00025812
FACET10	.00002762	-.00025521	.99999997	.00002762	-.99999997	-.00025814
FACET11	.00008143	-.00026630	.99999996	.00008143	-.99999997	-.00027969
FACET12	.00013276	-.00027372	.99999995	.00013276	-.99999996	-.00030533

AVERAGES :	.00000000	-.00026469
RMS :	.00009142	.00000723
N = 12		

BOEING	AT 15,	, ELEVATION ANGLE=	15. DEGREES FROM VERTICAL/4 PLANE AVERAGE		
FACET 1	-.00000761	-.00021776	.99999997	-.00000761	-.96598216	.25860066
FACET 2	-.00005808	-.00021858	.99999997	-.00005808	-.96598237	.25857809
FACET 3	-.00011091	-.00022989	.99999996	-.00011091	-.96598530	.25855746
FACET 4	-.00016515	-.00027167	.99999994	-.00016515	-.96599610	.25849068
FACET 5	-.00021760	-.00030470	.99999992	-.00021760	-.96600464	.25842469
FACET 6	-.00026757	-.00031797	.99999990	-.00026757	-.96600807	.25838704
FACET 7	.00000761	-.00021776	.99999997	.00000761	-.96598216	.25860066
FACET 8	.00005808	-.00021858	.99999997	.00005808	-.96598237	.25857809
FACET 9	.00011091	-.00022989	.99999996	.00011091	-.96598530	.25855746
FACET10	.00016515	-.00027167	.99999994	.00016515	-.96599610	.25849068
FACET11	.00021760	-.00030470	.99999992	.00021760	-.96600464	.25842469
FACET12	.00026757	-.00031797	.99999990	.00026757	-.96600807	.25838704

AVERAGES :	.00000000	-.00026010
RMS :	.00016429	.00004062
N = 12		

	BOEING	AT 30.	, ELEVATION ANGLE= 30. DEGREES FROM VERTICAL/4 PLANE AVERAGE			
FACET 1	-.00013249	-.00015953	.99999998	-.00013249	-.86610516	.49981741
FACET 2	-.00017944	-.00016560	.99999997	-.00017944	-.86610829	.49978396
FACET 3	-.00022851	-.00019640	.99999995	-.00022851	-.86612359	.49973540
FACET 4	-.00027871	-.00027310	.99999992	-.00027871	-.86616192	.49965115
FACET 5	-.00032710	-.00032386	.99999988	-.00032710	-.86618729	.49958161
FACET 6	-.00037313	-.00034163	.99999986	-.00037313	-.86619617	.49954716
FACET 7	.00013249	-.00015953	.99999998	.00013249	-.86610516	.49981741
FACET 8	.00017944	-.00016560	.99999997	.00017944	-.86610829	.49978396
FACET 9	.00022851	-.00019640	.99999995	.00022851	-.86612359	.49973540
FACET10	.00027871	-.00027310	.99999992	.00027871	-.86616192	.49965115
FACET11	.00032710	-.00032386	.99999988	.00032710	-.86618729	.49958161
FACET12	.00037313	-.00034163	.99999986	.00037313	-.86619617	.49954716
AVERAGES :	.00000000	-.00024339				
RMS :	.00026642	.00007334				

N = 12

	BOEING	,AT 45°,W/	, ELEVATION ANGLE= 45. DEGREES FROM VERTICAL/4 PLANE AVERAGE			
FACET 1	-.00024164	-.00009683	.99999997	-.00024164	-.70717525	.70692189
FACET 2	-.00028242	-.00010784	.99999996	-.00028242	-.70718304	.70689226
FACET 3	-.00032495	-.00015466	.99999994	-.00032495	-.70721615	.70685159
FACET 4	-.00036830	-.00025948	.99999990	-.00036830	-.70729024	.70678766
FACET 5	-.00040991	-.00032380	.99999986	-.00040991	-.70733571	.70673696
FACET 6	-.00044943	-.00034470	.99999984	-.00044943	-.70735048	.70670586
FACET 7	.00024164	-.00009683	.99999997	.00024164	-.70717525	.70692189
FACET 8	.00028242	-.00010784	.99999996	.00028242	-.70718304	.70689226
FACET 9	.00032495	-.00015468	.99999994	.00032495	-.70721615	.70685159
FACET10	.00036830	-.00025948	.99999990	.00036830	-.70729024	.70678766
FACET11	.00040991	-.00032380	.99999986	.00040991	-.70733571	.70673696
FACET12	.00044943	-.00034470	.99999984	.00044943	-.70735048	.70670586
AVERAGES :	.00000000	-.00021456				
RMS :	.00035341	.00009977				

N = 12

	BOEING	AT 60.	, ELEVATION ANGLE= 60. DEGREES FROM VERTICAL/4 PLANE AVVI-GE			
FACET 1	-.00033507	-.00002968	.99999995	-.00033507	-.50002570	.86586901
FACET 2	-.00036701	-.00004472	.99999994	-.00036701	-.50003872	.86585539
FACET 3	-.00040024	-.00010475	.99999992	-.00040024	-.50009071	.86582955
FACET 4	-.00043391	-.00023081	.99999989	-.00043391	-.50019988	.86578609
FACET 5	-.00046604	-.00030451	.99999985	-.00046604	-.50026369	.86574838
FACET 6	-.00049648	-.00032718	.99999983	-.00049648	-.50028332	.86573371
FACET 7	.00033507	-.00002968	.99999995	.00033507	-.50002570	.86586901
FACET 8	.00036701	-.00004472	.99999994	.00036701	-.50003872	.86585539
FACET 9	.00040024	-.00010475	.99999992	.00040024	-.50009071	.86582955
FACET10	.00043391	-.00023081	.99999989	.00043391	-.50019988	.86578609
FACET11	.00046604	-.00030451	.99999985	.00046604	-.50026369	.86574838
FACET12	.00049648	-.00032718	.99999983	.00049648	-.50028332	.86573371
AVERAGES :	.00000000	-.00017361				
RMS :	.00042014	.00011977				

N = 12

	BOEING	AT 75.	, ELEVATION ANGLE= 75. DEGREES FROM VERTICAL/4 PLANE AVVI-GE			
FACET 1	-.00041276	.00004193	.99999992	-.00041276	-.25877854	.96602856
FACET 2	-.00043321	.00002359	.99999992	-.00043321	-.25879626	.96603211
FACET 3	-.00045438	-.00004659	.99999990	-.00045438	-.25886404	.96581193
FACET 4	-.00047555	-.00018711	.99999988	-.00047555	-.25899978	.96579658
FACET 5	-.00049549	-.00026599	.99999984	-.00049549	-.25907596	.96578080
FACET 6	-.00051426	-.00028908	.99999983	-.00051426	-.25909826	.96577624
FACET 7	.00041276	.00004193	.99999992	.00041276	-.25877854	.96602856
FACET 8	.00043321	.00002359	.99999992	.00043321	-.25879626	.96603211
FACET 9	.00045438	-.00004659	.99999990	.00045438	-.25886404	.96581193
FACET10	.00047555	-.00018711	.99999988	.00047555	-.25899978	.96579658
FACET11	.00049549	-.00026599	.99999984	.00049549	-.25907596	.96578080
FACET12	.00051426	-.00028908	.99999983	.00051426	-.25909826	.96577624
AVERAGES :	.00000000	-.00012054				
RMS :	.00046559	.00013331				

N = 12

	BOEING	,HORIZ,W/ G	, ELEVATION ANGLE= 90. DEGREES FROM VERTICAL/4 PLANE AVERAGE			
FACET 1	-.00047473	.00011800	.99999988	-.00047473	.00011800	.99999988
FACET 2	-.00048103	.00009706	.99999988	-.00048103	.00009706	.99999988
FACET 3	-.00048736	.00001980	.99999988	-.00048736	.00001980	.99999988
FACET 4	-.00049322	-.00012836	.99999987	-.00049322	-.00012836	.99999987
FACET 5	-.00049825	-.00020824	.99999985	-.00049825	-.00020824	.99999985
FACET 6	-.00050279	-.00023038	.99999985	-.00050279	-.00023038	.99999985
FACET 7	.00047473	.00011800	.99999988	.00047473	.00011800	.99999988

FACET 8	.00048103	.00009706	.99999988	.00048103	.00009706	.99999988
FACET 9	.00048736	.00001980	.99999988	.00048736	.00001980	.99999988
FACET10	.00049322	-.00012836	.99999987	.00049322	-.00012836	.99999987
FACET11	.00049825	-.00020824	.99999985	.00049825	-.00020824	.99999985
FACET12	.00050279	-.00023038	.99999985	.00050279	-.00023038	.99999985
AVERAGES :	.00000000	-.00005535				
RMS :	.00048966	.00014040				

N = 12

BOEING ,CASE1,W/O G , ELEVATION ANGLE= 0. DEGREES FROM VERTICAL/4 PLANE AVERAGE

FACET 1	-.00007062	.00017770	.99999998	-.00007062	-.99999999	.00019138
FACET 2	-.00008572	.00017341	.99999998	-.00008572	-.99999999	.00019357
FACET 3	-.00009647	.00015622	.99999998	-.00009647	-.99999999	.00018365
FACET 4	-.00009673	.00012055	.99999999	-.00009673	-.99999999	.00015461
FACET 5	-.00008650	.00010334	.99999999	-.00008650	-1.00000000	.00013497
FACET 6	-.00007189	.00009908	.99999999	-.00007189	-1.00000000	.00012269
FACET 7	.00007062	.00017770	.99999998	.00007062	-.99999999	.00019138
FACET 8	.00008572	.00017341	.99999998	.00008572	-.99999999	.00019357
FACET 9	.00009647	.00015622	.99999998	.00009647	-.99999999	.00018365
FACET10	.00009673	.00012055	.99999999	.00009673	-.99999999	.00015461
FACET11	.00008650	.00010334	.99999999	.00008650	-1.00000000	.00013497
FACET12	.00007189	.00009908	.99999999	.00007189	-1.00000000	.00012269
AVERAGES :	.00000000	.00013838				
RMS :	.00008529	.00003210				

N = 12

BOEING ,CASE2,W/ G , ELEVATION ANGLE= 70. DEGREES FROM VERTICAL/4 PLANE AVERAGE

FACET 1	-.00030140	.00031446	.99999991	-.00030140	-.34172463	.93984216
FACET 2	-.00022625	.00030519	.99999993	-.00022625	-.34173334	.93982324
FACET 3	-.00014744	.00027266	.99999995	-.00014744	-.34176391	.93979957
FACET 4	-.00006602	.00023767	.99999997	-.00006602	-.34179680	.93977811
FACET 5	.00001306	.00023318	.99999997	.00001306	-.34180102	.93977353
FACET 6	.00008858	.00023222	.99999997	.00008858	-.34180192	.93977857
FACET 7	.00030140	.00031446	.99999991	.00030140	-.34172463	.93984216
FACET 8	.00022625	.00030519	.99999993	.00022625	-.34173334	.93982324
FACET 9	.00014744	.00027266	.99999995	.00014744	-.34176391	.93979957
FACET10	.00006602	.00023767	.99999997	.00006602	-.34179680	.93977811
FACET11	-.00001306	.00023318	.99999997	-.00001306	-.34180102	.93977353
FACET12	-.00008858	.00023222	.99999997	-.00008858	-.34180192	.93977857
AVERAGES :	-.00000000	.00026590				
RMS :	.00017134	.00003463				

N = 12

BOEING ,CASE3,W/O G , ELEVATION ANGLE= 0. DEGREES FROM VERTICAL/4 PLANE AVERAGE

FACET 1	-.00028654	.00018059	.99999994	-.00028654	-.99999999	.00033886
FACET 2	-.00026954	.00017313	.99999995	-.00026954	-.99999999	.00032048
FACET 3	-.00025761	.00014600	.99999996	-.00025761	-.99999999	.00029614
FACET 4	-.00025784	.00009444	.99999996	-.00025784	-1.00000000	.00027464
FACET 5	-.00027021	.00006728	.99999996	-.00027021	-1.00000000	.00027864
FACET 6	-.00028763	.00005986	.99999996	-.00028763	-1.00000000	.00029401
FACET 7	-.00007206	.00014180	.99999999	-.00007206	-.99999999	.00015934
FACET 8	-.00005461	.00013913	.99999999	-.00005461	-.99999999	.00014969
FACET 9	-.00004221	.00012943	.99999999	-.00004221	-.99999999	.00013620
FACET10	-.00004197	.00011100	.99999999	-.00004197	-.99999999	.00011873
FACET11	-.00005393	.00010128	.99999999	-.00005393	-1.00000000	.00011504
FACET12	-.00007095	.00009863	.99999999	-.00007095	-1.00000000	.00012188
AVERAGES :	-.00016376	.00012021				
RMS :	.00010848	.00003656				

N = 12

REFERENCES

1. S. J. Sackett, "User's Manual for SAP4", Lawrence Livermore Laboratory, UCID-18226, May 1979.

2. B. E. Brown, "Displaying the Results of Three-Dimensional Analysis Using GRAPE, Part 1 Vector Graphics", Lawrence Livermore Laboratory, UCID-18507, October 1979.

3. "Textronics MEG Finite Element Modeling Software Manual", February 1979.

4. W. S. Rorke, Jr., "Second Generation Heliostat Wind Load and Life Cycle Testing", Sandia National Laboratory (No SAN # available yet) November 1981.

5. V. P. Burolla, W. R. Delameter, "Testing and Evaluation of Second Generation Mirror Modules", Sandia National Laboratory (No SAN # available yet) November 1981.

6. D. King, "Beam Quality and Tracking Accuracy Evaluation of Second Generation and Barstow Production Heliostats", Sandia National Laboratory (No SAN # available yet) November 1981 (?).

UNLIMITED RELEASE
INITIAL DISTRIBUTION

U. S. Department of Energy
James Forrestal Building
1000 Independence Avenue, S.W.
Washington, DC 20585
Attn: W. W. Auer
G. W. Braun
K. Cherian
W. Hochheiser
J. E. Rannels

U. S. Department of Energy
1333 Broadway
Oakland, CA 94612
Attn: R. W. Hughey
For: S. D. Elliott
K. A. Rose

University of Houston
Houston Solar Energy Laboratory
4800 Calhoun
Houston, TX 77004
Attn: A. F. Hildebrandt
L. L. Vant-Hull

AMFAC
700 Bishop Street
Honolulu, HI 96801
Attn: G. St. John

ARCO Power Systems
7061 S. University
Suite 300
Littleton, CO 80122
Attn: J. Anderson
F. A. Blake

ARCO
911 Wilshire Boulevard
Los Angeles, CA 90017
Attn: J. H. Caldwell, Jr.

Arizona Public Service Company
P. O. Box 21666, Sta. 5629
Phoenix, AZ 85036
Attn: D. L. Barnes
E. Weber

Battelle/Pacific Northwest Laboratories
P. O. Box 999
Richland, WA 99352
Attn: K. Drumheller
For: R. J. Nesse
R. M. Scheer

Bechtel National, Inc.
P. O. Box 3965
San Francisco, CA 94119
Attn: E. Lam
For: J. B. Darnell
R. L. Lessley

Black & Veatch
P. O. Box 8405
Kansas City, MO 64114
Attn: C. Grosskreutz
For: J. E. Harder
J. Kintigh
S. Levy

Boeing Engineering and Construction
P. O. Box 3707
Seattle, WA 98002
Attn: R. L. Campbell
R. B. GIllette
J. Gintz

Chevron Oil Field Research Company
P. O. Box 446
La Habra, CA 90631
Attn: W. Peake
For: S. Griston
J. Ploeg
W. Stiles

Chevron Research Company
576 Standard Avenue
Richmond, CA 94804
Attn: L. Fraas
J. P. Jarrell

Corning Glass Works
Advanced Products, Bldg. 8-5
Corning, NY 14830
Attn: A. F. Schoemaker

El Paso Electric Company
P. O. Box 982
El Paso, TX 79960
Attn: J. D. Brown
For: M. L. Bonem

Exxon Enterprises
Solar Thermal Systems
P. O. Box 592
Florham Park, NJ 07932
Attn: P. Joy
For: D. Nelson
G. Yenetchi

General Electric
1 River Road
Schenectady, NY 12345
Attn: J. A. Elsner
For: R. N. Griffin
R. Horton

General Motors
GM Technical Center
Detroit, MI 48090
Attn: J. F. Britt

Houston Lighting and Power
P. O. Box 1700
Houston, TX 77001
Attn: J. Ridgway

Jet Propulsion Laboratory
4800 Oak Grove Drive
Pasadena, CA 91109
Attn: W. J. Carley
V. W. Gray
T. O. Thostesen
V. C. Truscello

Los Angeles Water and Power Department
111 North Hope Street
Los Angeles, CA 90051
Attn: R. F. Balingit
W. Engels
J. Kluger
T. Miller
B. M. Tuller

Martin Marietta
P. O. Box 179
Denver, CO 80201
Attn: P. R. Brown
A. E. Hawkins
L. P. Oldham
H. C. Wroton

McDonnell Douglas
5301 Bolsa Avenue
Huntington Beach, CA 92647
Attn: H. Dixon
R. L. Gervais
R. J. Faller
B. K. Knowles
D. A. Steinmeyer
L. Weinstein

Public Service Company of New Mexico
P. O. Box 2267
Albuquerque, NM 87103
Attn: A. Akhil

Southern California Edison
P. O. Box 800
Rosemead, CA 92807
Attn: J. Reeves
K. M. Ross
M. J. Skowronski
P. Skvarna
C. Winarski

Southwestern Public Service Company
P. O. Box 1261
Amarillo, TX 79170
Attn: M. D. Freeman
A. Higgins

Standard Oil of California
555 Market Street
San Francisco, CA 94105
Attn: S. Kleespies

U. S. Gypsum
101 S. Wacker Drive
Chicago, IL 60606
Attn: Ray McCleary

Washington Water & Power
E 1411 Mission Street
Spokane, WA 99216
Attn: A. Meyers

Westinghouse
P. O. Box 10864
Pittsburgh, PA 15236
Attn: J. J. Buggy
R. W. Devlin
W. G. Parker

Winsmith
172 Eaton
Springville, NY 14141
Attn: R. S. Bhise
W. H. Heller

G. E. Branvold, 4710; Attn: J. F. Banas, 4716
J. A. Leonard, 4717
J. V. Otts, 4713
D. G. Schueler, 4720
T. B. Lane, 5520
R. G. Kepler, 5810; Attn: L. A. Harrah, 5811
J. G. Curro, 5813
F. P. Gerstle, 5814
J. N. Sweet, 5824; Attn: R. B. Pettit, 5824
E. P. Roth, 5824
T. B. Cook, 8000; Attn: A. N. Blackwell, 8200
B. F. Murphey, 8300
C. S. Hoyle, 8122; Attn: V. D. Dunder, 8122
R. J. Gallagher, 8124
D. M. Schuster, 8310; Attn: R. E. Stoltz, 8312
For: M. D. Skibo, 8312
A. J. West, 8314
W. R. Even, 8315
R. L. Rinne, 8320
L. Gutierrez, 8400; Attn: R. A. Baroody, 8410
R. C. Wayne, 8430
D. E. Gregson, 8440
C. M. Tapp, 8460
C. S. Selvage, 8450
T. D. Brumleve, 8451
C. T. Yokomizo, 8451
H. F. Norris, Jr., 8451
W. S. Rorke, Jr., 8452
A. C. Skinrood, 8452
D. N. Tanner, 8452
V. P. Burolla, 8453
W. R. Delameter, 8453
C. L. Mavis, 8453 (5)
S. S. White, 8453
W. G. Wilson, 8453
Publications Division 8265, for TIC (27)
Publications Division 8265/Technical Library Processes Division, 3141 (3)
Technical Library Processes Division, 3141 (3)
M. A. Pound, 8214, for Central Technical Files (3)